

## AN ABSTRACT OF THE THESIS OF

Mohamed B. Al-Fageeh for the degree of Master of Science in Biochemistry and Biophysics presented on February 12, 2003.

Title: Functional Analysis of Novel  $\beta$ -catenin Mutants

Abstract approved Redacted for privacy

Roderick H. Dashwood

$\beta$ -catenin is a multi functional protein that is involved in cell-cell adhesion and cell signaling. In non-stimulated cells,  $\beta$ -catenin is tightly down-regulated by GSK-3 $\beta$ -dependent phosphorylation at Ser and Thr residues, followed by rapid ubiquitination and proteasomal degradation. It is well established that mutations within the regulatory GSK-3 $\beta$  region lead to stabilized  $\beta$ -catenin and constitutive  $\beta$ -catenin/TCF-dependent gene activation. Furthermore, it has been shown that amino acids adjacent to codon 33, namely 32 and 34 of  $\beta$ -catenin, are hotspots for substitution mutations in carcinogen-induced animal tumors. Thus, a major hypothesis of this thesis was that substitution mutations at codon 32 of  $\beta$ -catenin interfere with phosphorylation and ubiquitination of  $\beta$ -catenin.

Site-directed mutagenesis was used to create defined  $\beta$ -catenin mutants, namely D32G, D32N, and D32Y. The signaling potential of various  $\beta$ -catenin was analyzed in a gene reporter assay by co-transfection with a *hTcf* cDNA with a reporter plasmid containing a Tcf-dependent promoter (TOPFlash). There was a significant enhancement of the reporter gene activity with all  $\beta$ -catenin mutants compared to WT  $\beta$ -catenin after 48 hours of transfection. Protein analysis by Western blotting showed massive accumulation of mutant  $\beta$ -catenin. Antibody specific for phosphorylated  $\beta$ -catenin showed that the accumulated D32G and

D32N  $\beta$ -catenin proteins were strongly phosphorylated both *in vivo* and *in vitro*, whereas D32Y  $\beta$ -catenin exhibited significantly attenuated phosphorylation *in vivo*. Further studies showed, however, that none of the mutants was sufficiently ubiquitinated. In addition, inhibition of the proteasome activity by ALLN was associated with accumulation of cytosolic  $\beta$ -catenin, which was transcriptionally inactive. This suppression of  $\beta$ -catenin transcriptional capacity was independent of ALLN-associated apoptosis in the transfected cells. Furthermore, exogenous  $\beta$ -catenin mediated modest cell survival and rendered cells sensitive to apoptotic stimuli.

Thus, although codon 32 of  $\beta$ -catenin is not a direct target for phosphorylation, results from this thesis suggested that it affects the phosphorylation and ubiquitination of the adjacent Ser-33 residue of  $\beta$ -catenin, which is a direct target of GSK-3 $\beta$ . In addition, these results showed for the first time that the phosphorylation step of  $\beta$ -catenin is not enough to regulate transcriptional activity, and that  $\beta$ -catenin still needs to be ubiquitinated for successful down-regulation.

©Copyright by Mohamed B. Al-Fageeh

February 12, 2003

All Right Reserved

**Functional Analysis of Novel  $\beta$ -catenin Mutants**

**by**

**Mohamed B. Al-Fageeh**

**A THESIS**

**Submitted to**

**Oregon State University**

**In partial fulfillment of**

**the requirement for the**

**degree of**

**Master of Science**

**Presented February 12, 2003**

**Commencement June 2003**



Master of Science thesis of Mohamed B. Al-Fageeh presented on February 12, 2003.

APPROVED:

Redacted for privacy

---

Major Professor, representing Biochemistry and Biophysics

Redacted for privacy

---

Head of the Department of Biochemistry and Biophysics

Redacted for privacy

---

Dean of the Graduate School

I understand that my thesis will become part of the permanent collection of Oregon State University libraries. My signature below authorizes release of my thesis to any reader upon request.

Redacted for privacy

---

Mohamed B. Al-Fageeh, Author

## ACKNOWLEDGMENTS

I wish to express my sincere gratitude to my advisor, Dr. Roderick H. Dashwood, for all the help, support and endurance throughout my research in his laboratory. In addition, I would like to thank Dr. Andrew Buermeyer, Dr. Chrissa Kioussi and Dr. Jeffrey Widrick for being on my thesis committee and for reviewing this manuscript.

Gratitude also goes to Dr. Qingjie Li for helping with molecular cloning techniques, Dr. G. Dario Diaz for helping with flow cytometry analysis and Mohaiza Dashwood for assisting in cell culture techniques.

The author would also like to thank Dr. Hans Clevers for providing WT  $\beta$ -catenin construct and  $\alpha$ ABC antibody, Dr. Akira Kikuchi for providing rAxin construct and Dr. Marc van de Wetering for providing Tcf-4 construct.

Finally, I would like to express my heartfelt appreciation to my wife and daughter for their endless support during good and bad times. Without them, I could not have completed this thesis.

## TABLE OF CONTENTS

	<u>Page</u>
1 CHAPTER 1: INTRODUCTION .....	1
2 CHAPTER 2: LITERATURE REVIEW .....	4
2.1 EPIDEMIOLOGY AND ETIOLOGY OF HCRC.....	4
2.2 GENETIC MODEL OF HCRC .....	5
2.3 GENETIC INSTABILITY IN HCRC.....	6
2.4 COLORECTAL CANCER MAJOR GENES.....	8
2.4.1 <i>APC</i> (Adenomatous Polyposis Coli ).....	8
2.4.2 <i>K-ras</i> oncogene (Kirsten rat sarcoma 2 viral oncogene homolog) ....	9
2.4.3 <i>SMAD4/DPC4</i> .....	10
2.4.4 <i>DCC</i> (Deleted in Colorectal Cancer) .....	10
2.4.5 <i>P53</i> (the guardian of the genome).....	10
2.4.6 DNA mismatch repair (MMR) genes.....	11
2.5 MAJOR HEREDITARY HCRC SYNDROMES .....	11
2.5.1 Familial Adenomatous Polyposis (FAP).....	11
2.5.2 Attenuated FAP (AFAP).....	12
2.5.3 Hereditary Nonpolyposis Colorectal Cancer (HNPCC) .....	12
2.5.4 Familial Colorectal Cancer (FCC) .....	13
2.5.5 Juvenile polyposis .....	13
2.6 SPORADIC COLORECTAL CANCER .....	13
2.7 CANONICAL WNT SIGNALING PATHWAY .....	14
2.7.1 Wnt signaling pathway proteins.....	15
2.7.2 Model for Wnt signaling .....	23
2.7.3 Target genes of Wnt signaling pathway.....	24
2.8 $\beta$ -CATENIN AND COLORECTAL CANCER .....	24

## TABLE OF CONTENTS (Continued)

	<u>Page</u>
2.8.1 Discovery and structure of $\beta$ -catenin .....	25
2.8.2 $\beta$ -catenin in cell-cell adhesion .....	27
2.8.3 $\beta$ -catenin in cell junctions and signaling.....	32
2.8.4 $\beta$ -catenin phosphorylation.....	33
2.8.5 The nuclear activities of $\beta$ -catenin .....	36
2.8.6 $\beta$ -catenin and apoptosis.....	37
2.8.7 Mechanisms of abnormal accumulation of $\beta$ -catenin .....	39
2.8.8 Mutations of human $\beta$ -catenin gene ( <i>CTNNB1</i> ) .....	40
2.8.9 $\beta$ -catenin mutations in experimentally-induced animal tumors.....	41
 3 CHAPTER 3: MATERIALS AND METHODS. ....	 46
3.1 PLASMID CONSTRUCTION .....	46
3.1.1 Site-directed mutagenesis.....	46
3.1.2 Prokaryotic expression vectors .....	50
3.2 CELL CULTURE .....	52
3.3 TRANSIENT TRANSFECTION .....	53
3.4 REPORTER GENE ASSAY.....	53
3.5 SDS-PAGE ANALYSIS.....	54
3.6 $\beta$ -CATENIN PHOSPHORYLATION ANALYSIS .....	55
3.7 PURIFICATION OF GST TAGGED PROTEINS.....	55
3.8 <i>IN VITRO</i> PHOSPHORYLATION ASSAY.....	56
3.9 MYC-TAG $\beta$ -CATENIN IMMUNOPRECIPITATION .....	57
3.10 CELL CYCLE ANALYSIS.....	58
3.11 CASPASE-3 ACTIVITY .....	59

## TABLE OF CONTENTS (Continued)

	<u>Page</u>
4 CHAPTER 4: RESULTS .....	60
4.1 ANALYSIS OF THE TRANSACTIVATION POTENTIAL OF WT AND MUTANT $\beta$ -CATENIN IN REPORTER ASSAYS .....	60
4.2 ANALYSIS OF THE PHOSPHORYLATION STATUS OF WT AND MUTANT $\beta$ -CATENIN BY WESTERN BLOTTING .....	63
4.3 THE UBIQUITINATION STATUS OF WT AND MUTANT $\beta$ -CATENIN.....	66
4.4 ANALYSIS OF THE UBIQUITINATION STATUS OF EXOGENOUS WT AND MUTANT $\beta$ -CATENIN BY WESTERN BLOTTING. ....	69
4.5 IMMUNOPRECIPITATION OF EXOGENOUS WT AND MUTANT $\beta$ -CATENIN.....	69
4.6 COMPARISON BETWEEN D32Y, S33Y AND D45 $\beta$ -CATENIN TRANSACTIVATION AND PROTEIN ACCUMULATION .....	71
4.7 THE EFFECTS OF THE PROTEASOMES INHIBITOR ALLN ON $\beta$ -CATENIN TRANSACTIVATION.....	73
4.8 ANALYSIS OF THE EFFECTS OF OVER-EXPRESSION OF $\beta$ -CATENIN ON CELL CYCLE AND APOPTOSIS.....	76
5 CHAPTER 5: DISCUSSION.....	83
6 CHAPTER 6: CONCLUSIONS .....	91
REFERENCES.....	93

## LIST OF FIGURES

<u>Figure</u>	<u>Page</u>
1: The multi-step model of colorectal cancer.....	7
2: The Canonical Wnt signaling pathway .....	25
3: The primary structure of $\beta$ -catenin. ....	28
4: Molecular architecture of E-cadherin-mediated cell-cell adhesion .....	30
5: Putative sequential cleavage sites in $\beta$ -catenin for caspase-3.....	39
6: Overall distribution of <i>CTNNB1</i> mutations reported in human cancers .....	42
7: Overall distribution of $\beta$ -catenin mutations reported in HCRC.....	42
8: $\beta$ -catenin mutation spectrum in experimentally-induced animal tumors,.....	45
9: PCR-Based Site-Directed Mutagenesis by ‘Overlap Extension’.....	49
10: Transactivation potential of $\beta$ -catenin in HEK-293 cells. ....	62
11: Phosphorylation status of $\beta$ -catenin. ....	64
Figure 12: <i>In vitro</i> phosphorylation of $\beta$ -catenin by GSK-3 $\beta$ . ....	66
Figure 13: Effects of ALLN on $\beta$ -catenin transactivation and stability.....	68
14: Effects of ALLN on total and exogenous $\beta$ -catenin .....	70
15: Immunoprecipitation of $\beta$ -catenin .....	71
16: D32Y, S33Y and $\Delta$ 45 $\beta$ -catenin are functionally equivalent in reporter assays.....	72
17: Apoptotic morphology of HEK-293 cells treated with ALLN or STS.....	75

## LIST OF FIGURES (Continued)

<u>Figure</u>	<u>Page</u>
18: ALLN induces apoptosis in HEK-293 cells.....	76
19: ALLN decreases the transactivation capacity of $\beta$ -catenin. ....	77
20: Inhibition of caspase-3 by Z-VAD-FMK.....	79
21: Effect of constitutive $\beta$ -catenin over-expression on cell cycle kinetics and apoptosis.....	80
22: Effects of $\beta$ -catenin over-expression on c-jun activation. ....	81
23: Anti-apoptosis effect of various $\beta$ -catenin in HEK-293 cells.....	81
24: Anti-caspase-3 effects of $\beta$ -catenins over-expression. ....	82
25: $\beta$ -catenin mutation spectrum in carcinogen-induced rat colon tumors.....	84

## LIST OF TABLES

<u>Table</u>	<u>Page</u>
1: Mutation spectra of human <i>CTNNB1</i> .....	43
2: $\beta$ -catenin mutations in experimentally-induced animal tumors.....	44
3: $\beta$ -catenin mutation variety in experimentally-induced animal tumors .....	45
4: The primers used for site-directed mutagenesis.....	48
5: The primers used for subcloning $\beta$ -catenin, <i>rAxin</i> and <i>GSK-3<math>\beta</math></i> .....	52



## LIST OF ABBREVIATIONS

1-HA	1-hydroxyanthraquinone
A	Adenosine
ACF	Aberrant Crypt Foci
ACS	The American Cancer Society
AFAP	Attenuated Familial Adenomatous Polyposis
Ala	Alanine
ALLN	N-Ac-Leu-Leu-norleucinal
AOM	Azoxymethane
APC	Adenomatous Polyposis coli
Arg	Arginine
Asn	Asparagine
ATP	Adenosine triphosphate
bp	base pair
C	Cytosine
cDNA	complementary deoxyribonucleic acid
CIN	Chromosomal instability
CK	Casein kinase
CRC	Colorectal cancer
Cys	Cysteine
DCC	Deleted in Colorectal Cancer
DEN	Diethylnitrosamine
dkk-1	Dickkopf-1
DMH	1,2-dimethylhydrazine
DMSO	Dimethyl Sulfoxide
DNA	Deoxyribonucleic acid

dNTP	deoxynucleotide triphosphate
DPC4	Deleted in Pancreatic Carcinoma 4
Dsh	Dishevelled
FAP	Familial Adenomatous Polyposis
FCC	Familial Colorectal Cancer
Frat-1	Frequently rearranged in advanced T-cell lymphomas 1
Fz	Frizzled
G	Guanine
Glu	Glutamate
Gly	Glycine
GSK	Glycogen synthase kinase
GST	Glutathione S-Transferase
HCC	Hepatocellular carcinomas
HCRC	Human colorectal cancer
HDAC	Histone deacetylase
HNPCC	Hereditary Non-Polyposis Colorectal Cancer
Ile	Isoleucine
IQ	2-amino-3-methylimidazo[4,5-f]quinoline
JMD	Juxtamembrane domain
K-ras	Kirsten rat sarcoma 2 viral oncogene homolog
LEF	Lymphoid enhancer factor
Leu	Leucine
LOH	Loss of Heterozygosity
LRP	Low-density lipoprotein Receptor-related Protein
Lys	Lysine
MAM	Methylazoxymethanol acetate
MCR	Mutation Cluster Region
Met	Methionine

MLH1	human MutL Homolog –1
MLH3	human MutL Homolog –3
MMR	Mismatch repair
MNNG	N-methyl-N'-nitro-N-nitrosoguanidine
MNUR	N-methylnitrosourethane
MSH2	MSH2 human MutS Homolog –2
MSH3	human MutS Homolog –3
MSH6	human MutS Homolog –6
MSI	Microsatellite instability
NES	Nuclear export signals
NLS	Nuclear localization signal
NNK	Nitrosamine 4-methylnitrosamino-1-(3-pyridyl)-1-butanone
NSAIDs	Nonsteroidal anti-inflammatory drugs
P53	Protein 53
PAGE	Polyacrylamide gel electrophoresis
PARP	Poly (ADP-ribose) polymerase
PCR	Polymerase chain reaction
Phe	Phenylalanine
PhIP	2-amino-1-methyl-6-phenylimidazo[4,5- <i>b</i> ]pyridine
PP2A	Protein phosphatase 2A
Pro	Proline
PY	Phosphotyrosine
p $\beta$ -catenin	Phosphorylated $\beta$ -catenin
q	Long arm of the chromosome
RER	Replication errors
RNA	Ribonucleic acid
RT-PCR	Reverse transcription polymerase chain reaction
SAMP	Serine-alanine-methionine-proline

Ser	Serine
SMAD4	Human homologs of Drosophila Mad 4
Src	Avian sarcoma viral oncogene
STS	Staurosporine
T	Thymidine
TBP	TATA box-binding protein
TCF	T-cell transcription factors
TG	Transgenic
TGF $\beta$	Transforming growth factor $\beta$
Thr	Threonine
Tyr	Tyrosine
Val	Valine
VHL	Von Hippel-Lindau
Wnt	Wingless type
WT	Wild-type

Dedicated to my wife and my daughter, whose support was precious.

## Functional Analysis of Novel $\beta$ -catenin Mutants

### 1 CHAPTER 1: INTRODUCTION

Cancer is a major health concern in western communities. In the United States, over 17 million cancer cases have been diagnosed since 1990 and around 1,334,100 new cases are expected this year. Approximately, 556,500 Americans are expected to die of cancer in year 2003. Cancer accounts for 25 % of all deaths; therefore, it is ranked the second fatal disease next to cardiovascular diseases (1).

Cancer, which is characterized by uncontrolled, abnormal proliferation of cells, is now a general term for more than 100 diseases. Tumorigenesis is a multi-step process that occurs due to several genetic alterations that facilitate the progression of normal cell to malignant derivatives. These genetic hits typically target the genes responsible for determination of the cell fates such as: cell differentiation, growth, survival and death. Even minimal subversions of the genes controlling these processes might lead to cancer. The mutations predisposing to cancer can be inherited (germline) or, in most cases, acquired (sporadic). Unlike, germline mutations which are present in every single cell of the body, sporadic mutations are not inherited; they are induced randomly by certain carcinogens at specific organs and passed to the defected cell descendents only (2).

Cancerous cells are self-sufficient in growth signals and have resistance to growth inhibitors and apoptosis. In addition, malignant tumors are able to promote angiogenesis, the process of development of new capillary blood vessels, allowing constant supply of oxygen and nutrients for the rapidly growing cells. In the later stages of tumorigenesis, cancer cells metastasize. They detach from their origin and travel to remote sites at which they form secondary tumors (2).

Cancers of the colon and rectum (Colorectal cancer, CRC or HCRC) are epithelial-derived tumors (adenocarcinomas or adenomas) considered amongst the major causes of malignancy-related mortality worldwide. Hence, HCRC has been a favorable subject for extensive research during the last decade. HCRC is caused by inactivation mutations (inherited and/or acquired) in the gatekeeper and / or caretaker genes. Examples of the gatekeeper and the caretaker gene defects are the Familial Adenomatous Polyposis (FAP) and Hereditary Non-Polyposis Colorectal Cancer (HNPCC), respectively. FAP patients harbor germline mutations which, inactivate one adenomatous polyposis coli (*APC*) allele, resulting in the development of numerous polyps in the colon in early stages of life. The probability that polyps will develop into malignant tumors increases as other sporadic mutations inactivate the second *APC* allele. In contrast, HNPCC patients harbor mutations in the DNA repair machinery genes (MMR), which lead to an increase in the rate of other acquired mutations (3).

It is well established that *APC* is a tumor suppressor gene involved in many biological processes including the regulation of the Wnt signaling pathway. *APC* down-regulates the key mediator protein of Wnt signaling pathway,  $\beta$ -catenin (4). Mutations in the *APC* gene lead to abnormal accumulation of cytosolic  $\beta$ -catenin, which eventually migrates to the nucleus and transactivates genes critical for cell growth. Alternatively, it also has been shown that sporadic colorectal tumors with WT *APC* harbor mutations in the N-terminal region of  $\beta$ -catenin, which render it unresponsive to *APC*-mediated degradation (5). The molecular analysis of WT and mutant  $\beta$ -catenin has identified critical Serine and Threonine residues, namely, Ser-33, Ser-37, Thr-41 and Ser-45. The phosphorylation of these residues by GSK-3 $\beta$  is obligatory for consequent ubiquitination and proteasomal degradation of  $\beta$ -catenin (6). The cumulative knowledge from numerous mutational analysis studies in human tumors, cancer cell lines as well as animal models has revealed that these

residues and their surrounding ones are hotspots for substitution and deletion mutations (7).

Although this thesis focuses on the genetic events in HCRC and the  $\beta$ -catenin signaling pathway, it is important to mention that one to two-thirds of HCRC are attributed to diet. Therefore, much attention has been focused on investigating the gene-environment interactions and their roles in HCRC tumorigenesis (8). Interestingly, the pattern of  $\beta$ -catenin mutations in human colon tumors is different from that observed in chemically-induced animal tumors. In HCRC, most of the mutations substitute or delete codon 45. In contrary, colorectal tumors from animals treated with dietary carcinogens harbor mutations that tend to cluster around Ser-33. Dietary factors, such as Chlorophyllin and Indole-3-carbinol, shift the spectrum of gene mutations to include Thr-41 and Ser-45 mutations (9).

The aim of this thesis was to investigate the molecular mechanisms of  $\beta$ -catenin accumulation associated with substitution mutations of the amino acids surrounding the critical N-terminal Serine and Threonine residues. Specifically, the goal was to provide a functional analysis of mutations at codon 32 of *Ctnnb1*, a major mutation hotspot in murine colon tumors.



## 2 CHAPTER 2: LITERATURE REVIEW

### 2.1 EPIDEMIOLOGY AND ETIOLOGY OF HCRC

HCRC is considered the third most common cause of cancer related-death and infirmity in western countries. In the United States, the American Cancer Society (ACS) estimated that 147, 500 new cases of HCRC will be diagnosed and 57,100 Americans are expected to die of HCRC in year 2003, making it the second deadliest cancer among nonsmokers, only next to prostate cancer in men and breast cancer in woman. Nonetheless, it is noteworthy that the overall HCRC death rates declined by 1.7% per year from 1992 to 1998. This decline was likely achieved via (noticeable) improvements in early detection and prevention techniques. The lifetime HCRC risk is approximately 6%, although, 90% of all HCRC occur after age 50. The incidence and mortality of HCRC are unrelated to gender type in early life; nonetheless, men are more vulnerable to the disease after age 50 (1). In contrast, HCRC incidence and mortality are markedly influenced by race and ethnicity. Both are higher in blacks and Asian islanders compared to Native American Indians and Hispanics (1). It is fortunate that HCRC is a curable disease if diagnosed early with adequate screening protocols (10, 11).

Globally, the incident and mortality of HCRC vary in different geographic regions of the world and are shifted by changing of residency and lifestyle. For instance, the HCRC mortality rates significantly increased among Japanese emigrants to the United States compared to Japanese in Japan (12).

Several studies of the inherited tumors and their germ line mutations have shown that genetic factors markedly increase the risk of developing HCRC. It was estimated that 25% of HCRC patient have family history with inherited mutations that account for 5~6% of all HCRC incidents (13). Even though the family history increased the susceptibility to HCRC, many case-control and epidemiology studies

have revealed that HCRC is a multifactorial disease. The susceptibility to HCRC is markedly influenced by the environmental risk factors such as diet and life style. Increased risk of colorectal neoplasia was seen with high meat and alcohol consumption and smoking. These factors elevate the possibility of acquiring somatic mutations (14, 15) . In contrast; contrary associations exist with healthy life style practices such as fruits and vegetables consumption and physical activities. Additionally, nonsteroidal anti-inflammatory drugs (NSAIDs) and hormone replacement therapy have been shown to decrease the risk of HCRC (16-18). These findings were extensively deliberated by many *in vivo* and *in vitro* studies, with much attention focused on the possible role of dietary carcinogens and anti-carcinogens (9, 15, 19-28).

## 2.2 GENETIC MODEL OF HCRC

Resembling other types of malignancies, HCRC is a polygenic disease that requires multiple genetic “hits” to arise and progress in a step-wise manner. For a normal epithelium tissue to be transformed to adenoma and then to carcinoma, at least seven independent genetic events ought to occur, each providing clonal selection advantage. One mutation occurs in the oncogene *K-ras* and other mutations inactivate the tumor suppressor genes *APC*, *DCC*, *SMAD4* and *P53* (29-31). Molecular analysis of different histopathological stages of the adenoma-carcinoma sequence has shown that each stage of tumor progression was associated with specific genetic defects. Therefore, Fearon and Vogelstein identified the genes responsible for colon tumorigenesis and proposed a model of HCRC progression (Figure 1). Their model suggested that mutations in the *APC* gene activate the neoplastic progression, resulting in small adenomas. These small benign tumors evolve with time to mature malignancies (carcinomas) as mutations accumulate in other genes (*K-ras*, *DCC*, TGF $\beta$ -related genes, and *p53*). The whole process of

tumor evolution is accelerated by defects in the caretaker genes (30, 32). Furthermore, Kinzler and Vogelstein suggested that bi-allelic inactivation of tumor suppressor genes (the gatekeepers), such as *p53*, *RBI*, *VHL*, or *APC*, is the rate-limiting event of cancer evolution. Additional inactivation of the caretaker genes leads to genetic instability, which consecutively results in increased mutation rates in all genes (mutator phenotype). Therefore, the caretaker genes are considered indirect suppressors (33, 34). Interestingly, an alternative pathway to the adenoma–carcinoma sequence has been proposed recently. The new heterogeneous pathway suggested that up to 70 % of all HCRC cases, which retain WT *APC* gene, arise through epigenetic silencing of the genes of cell proliferation, cell cycle and DNA repair machinery (35, 36).

### 2.3 GENETIC INSTABILITY IN HCRC

Molecular and Cytogenetic analyses of HCRC tumors have revealed different alterations in the cellular genome structure called “genetic instability” including chromosomal and microsatellite instabilities. The chromosomal instabilities arise due to aberrant mitotic recombination or chromosome segregation that causes loss or gain of large segments of chromosomal material in up to 85% of HCRC tumors. The most frequently observed losses involve chromosomal regions 5q, 17p, and 18q. These chromosomal segments are known to include important tumor suppressor genes including *APC* on 5q, *TP53* on 17p, and *DPC4* and *DCC* on 18q. (37-39). Loss of heterozygosity (LOH), a consequence of CIN, was observed at high frequencies centered around *APC* in 5q, *P53* in 17p, and *SMAD4* in chromosome 18q (29, 34). Rare losses of chromosome 17p were observed in adenomas and total losses were observed in 75% of carcinomas. These observations supported the notion that *p53* inactivation takes place at a later stage of the tumorigenesis pathway (40).

Microsatellites are short (1-6 bp), repetitive units of DNA tracts widely spread throughout the coding and non-coding regions of the genome. Slippage of DNA polymerase during the replication of these regions creates mismatch regions with a loop-like structure, which are corrected immediately by MMR machinery. Of all HCRC cases, 15 % are sporadic MIN tumors occurred mainly due to defects in the DNA mismatch repair genes (MMR) (29, 41).

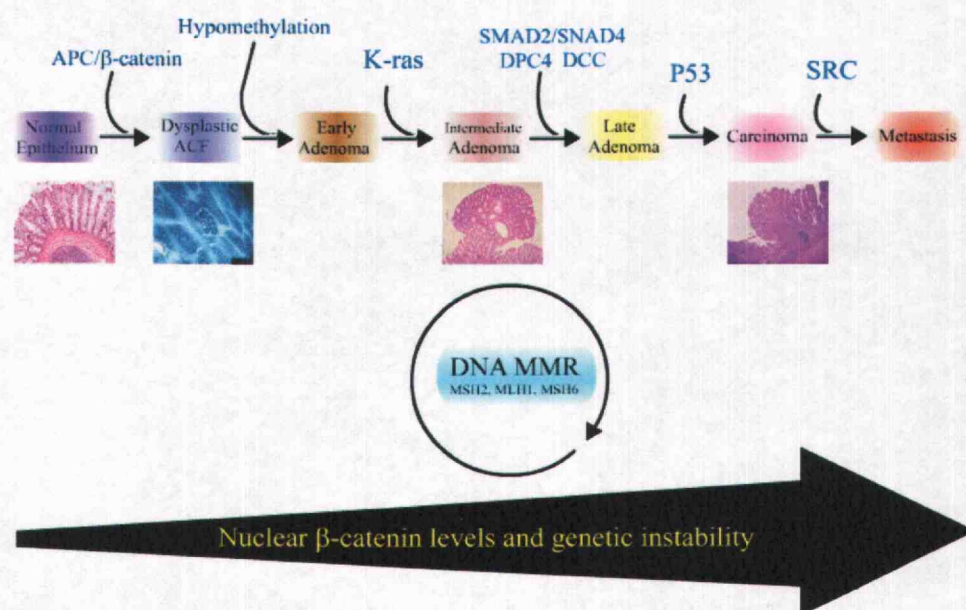


Figure 1: The multi-step model of colorectal cancer.

The top line indicates the adenoma-carcinoma sequence. Mutations in *APC* or  $\beta$ -catenin initiate the neoplastic process, resulting in adenomas, which progress to carcinomas as mutations in other genes accumulate. The process is accelerated by mutations in the caretaker genes, which lead to genetic instability. Insert figures indicate the histopathology of colorectal cancer.

Modified from Fodde *et al*, Fearon *et al*, and Kinzler *et al* (29, 30, 42).

## 2.4 COLORECTAL CANCER MAJOR GENES

The major HCRC genes are those genes necessary and sufficient for the disease causation. HCRC major genes are classified into three types: "gatekeeper" genes (tumor suppressor genes); "caretaker" genes (DNA damage response genes); and "landscaper" genes (genes that control the cellular microenvironment) (33). The gatekeeper genes are accountable for maintaining a steady cell population and ensure that cells respond appropriately to circumstances that require collaborate cell growth such as that after tissue damage. Inactivating mutation in the gatekeeper genes lead, in many situations, to an increase in cell division rate compared to cell death and thus to a net abnormal increase in cell number (42). In contrast, mutations in the caretaker genes do not lead directly to cancer. However, inactivation of caretaker genes might lead to genetic instability that in turn results in increased mutation rates for all other genes. Therefore, the probability of developing mutations at the gatekeeper genes is increased by the presence of mutations in a caretaker gene (33, 38).

### 2.4.1 *APC* (Adenomatous Polyposis Coli )

*APC*, referred to as the "gatekeeper" gene of colorectal cancer, is located on chromosome 5q21. *APC* is a large gene of 15 exons, and encodes a 312 kDa protein that is important in cell-cell adhesion, signal transduction, cell migration, apoptosis and chromosomal segregation during mitosis (29, 43, 44). *APC* was identified after rigorous molecular studies of germ line mutations in FAP patients and sporadic mutations in HCRC tumors (45). Mutations in the *APC* gene are amongst the early genetic hits that play pivotal role in the development of colon tumorigenesis. Mutational analysis of both inherited and sporadic colorectal tumors have shown that the majority of human carcinomas and adenomas have mutations in the *APC*

gene, mostly, insertions, deletions, and nonsense mutations that lead to frame shifts or premature stop codons in the mRNA transcript. The end product is nonfunctional or truncated APC protein (46). Approximately, 90 % of all mutations observed in familial and sporadic HCRC are located between codons 1286 and 1513 at exon 15, in a region named the “mutation cluster region” (MCR) (47, 48). Notably, germ line mutations of *APC* do not necessarily lead to (though they markedly increase the risk of) developing HCRC. Additional genetic alterations are seemingly required for definite disease development (42). Moreover, mutations in *APC* were coupled to disruption of normal tissue morphology (dysplasia) (49). In addition, it has been shown recently that 50 % reduction in the expression of one *APC* allele may indeed be sufficient to lead to FAP through so-called “haploinsufficiency” (50). The APC function as a  $\beta$ -catenin-mediated degradation protein will be discussed in greater detailed below (see Canonical Wnt signaling pathway genes).

#### 2.4.2 *K-ras* oncogene (Kirsten rat sarcoma 2 viral oncogene homolog)

The *K-ras* proto-oncogene resides on chromosome 12p12, and encodes a 21-kDa protein (p21<sup>ras</sup>) involved in the G-protein signal transduction pathway and in modulating cellular proliferation and differentiation. Over a third of HCRC have mutated *K-ras* gene, preferentially at hotspot codon 12, that lead to the development of the tumor (51, 52). The observation that only a third of human cancers have *K-ras* mutations and these mutations are more common in the rectum than in the colon tumors indicated that other unidentified oncogenes might be involved in the development of HCRC. Other pathogenic pathways might be expected to promote *APC*-dependent tumorigenesis in the absence of activation of *K-ras* (29, 36, 53). *K-ras* mutations were associated with small nondysplastic lesions, and with the putative pre-neoplastic lesions called Aberrant Crypt Foci

(ACF), which are postulated to be an early events of adenoma to carcinoma sequence and precede the maturity of HCRC (Figure 1) (54).

#### 2.4.3 *SMAD4/DPC4*

The *SMAD4* gene (*DPC4* in human) is located on chromosome 18q22. *DPC4* is a downstream mediator of TGF $\beta$  signaling pathway. TGF- $\beta$  is a potent suppressor of cell growth. Many evidences point to the role of *SMAD4* as a tumor suppressor gene in the majority of pancreatic cancers, and at least a subset of colorectal cancers (55).

#### 2.4.4 *DCC* (Deleted in Colorectal Cancer)

The *DCC* gene resides on chromosome 18q21.1, and codes for the axonal chemoattractant netrin-1 receptor. The exact function of *DCC* is yet to be discovered, however, it was hypothesized that *DCC* may function as a tumor suppressor protein, possibly through induction of apoptosis (56).

#### 2.4.5 *P53* (the guardian of the genome)

*p53* or *TP53* is a tumor suppressor gene located at chromosome 17p13 and is one of the most frequently mutated genes in human cancers. The *p53* gene is mutated in up to 70 % of HCRC (36, 53). The normal functions of *p53* include regulation of G1 and G2 cell-cycle checkpoints in response to DNA damage and apoptosis induced by certain stimuli, such as DNA-damaging agents and hypoxia (40).

#### 2.4.6 DNA mismatch repair (MMR) genes

MMR genes classified as caretaker genes include *hMSH2* on chromosome 2p16; *hMLH1* on chromosome 3p21; *hPMS1* and *hPMS2* on chromosomes 2q31 and 7q11, respectively; *hMSH6* on chromosome 2p16; and *hMSH3* on chromosome 5q11.2-q13.2. Their main function is to maintain the fidelity of DNA replication. Mutations in these genes lead to HNPCC which is characterized by MSI (57-59).

### 2.5 MAJOR HEREDITARY HCRC SYNDROMES

The inherited HCRC tumors are classified, according to their genetic instability status, into tumors with chromosomal instability and tumors with microsatellite instability. FAP and HNPCC syndromes are examples of hereditary HCRC with chromosomal instability and microsatellite instability, respectively.

#### 2.5.1 Familial Adenomatous Polyposis (FAP)

FAP is well-characterized aggressive autosomal dominant disorder that accounts for 1% of all HCRC cases. The incidence of FAP in the population is approximately 1 in 8000 (48). FAP patients harbor heterozygous germ line mutations in *APC*, thus, the probability of the offspring to inherit the affected *APC* allele is 50%. Individuals who inherit the mutant *APC* allele have 90 % risk to develop HCRC. FAP patients develop abundant numbers of colonic and rectum adenomatous polyps by the first ten years of life and develop HCRC by age 40 (60). A strong correlation between the type of *APC* mutation and degree of severity of polyposis phenotype has been observed. FAP patients diagnosed with severe



polyposis phenotype (more than 5000 colorectal polyps) usually harbor *APC* mutations between codons 1250 and 1464 or at codon 233 in exon 6 and at codons 486 and 499 in exon 11. In addition, mutations in codons 1309 and 1310 tend to cause a predominantly severe phenotype with an earlier initiation of the disease (4).

### 2.5.2 Attenuated FAP (AFAP)

Attenuated FAP (AFAP) is a less severe variant of FAP. Patients with AFAP develop smaller number of tumors and at older age than those with classic FAP. In addition, the risk of manifesting polyps is lower compared with the risk of polyposis among carriers of FAP-predisposing mutations (61, 62).

### 2.5.3 Hereditary Nonpolyposis Colorectal Cancer (HNPCC)

HNPCC is an autosomal dominant condition caused by mutation of one of several DNA mismatch repair genes and accounts for 3% to 5% of all colorectal cancer. Unlike FAP, HNPCC patients develop HCRC without developing unusual numbers of adenomatous polyps. Furthermore, individuals with germ line DNA MMR gene mutations have an estimated 70% lifetime risk of developing colorectal cancer by age 44 (63, 64).

#### 2.5.4 Familial Colorectal Cancer (FCC)

FCC accounts for 15% of all HCRC cases. FCC patients have a family history, which does not fit the criteria of FAP neither HNPCC, or may not appear to follow a recognizable pattern of inheritance (65).

#### 2.5.5 Juvenile polyposis

Familial juvenile polyposis is an autosomal dominant syndrome characterized by the appearance of numerous polyps throughout the colon. Unlike other polyposis syndromes, these polyps are predominately juvenile in histology and originate from abnormal proliferating stromal cells (hamartoma) rather than epithelial cells (66).

### 2.6 SPORADIC COLORECTAL CANCER

Sporadic tumors account for about 75% of all HCRC incidence. Similar to the inherited HCRC, sporadic tumors originate from colorectal adenomas and develop to carcinoma over a long period of time in a multi-step behavior, nonetheless, family history is omitted (30). It is believed that environmental and dietary factors trigger somatic mutations that provide growth advantages and enhance tumor progression. Apparently, these mutations target genes that are critical for cell growth, apoptosis and DNA MMR machinery (67, 68). Throughout sporadic HCRC progression, mutations of the *APC*, *K-ras*, *DCC* and *P53* genes are the major genetic alterations respectively(4). Somatic mutation that inactivate the WT *APC* allele is rate-limiting in the majority of sporadic HCRC (4). Mutated APC protein fails to negatively regulate the Canonical Wnt signaling pathway and leads

to a constitutive  $\beta$ -catenin-mediated activation of cell cycle, cell proliferation and differentiation genes (42). Additionally, epigenetic mechanisms such as abnormal methylation of the promoters of the proto-oncogenes and tumor suppressor genes may alter gene activities. Hypermethylation and hypomethylation are associated with gene silencing and over-transcription respectively (69, 70). *APC* promoter 1A hypermethylation has been reported in colorectal and other types of cancer (4). Finally, sporadic HCRC is characterized by genetic instabilities, loss of heterozygosity (LOH), and increased replication errors (RER) (71, 72).

## 2.7 CANONICAL WNT SIGNALING PATHWAY

In biological systems, signaling pathways are the most efficient way of transmitting and amplifying extra cellular signals through plasma membrane into the nucleus. Typically, signal transduction pathways are initiated by extra-cellular stimuli such as hormones, growth factors, and cytokines. These ligands bind explicitly to and activate their receptors at the cell surface. Signals from these receptors are then amplified within the target cell, resulting in the expression of target genes and subsequent biological responses. An example of a transduction pathway is the Wnt signaling pathway (Figure 2). It is a highly conserved pathway critical for proper development of the multi-cellular organisms. Wnt signaling is essential for cell proliferation, differentiation and epithelial-mesenchymal interactions. In addition, inappropriate activation of Wnt signaling plays a fundamental role in the initiation and progression of colorectal and several other cancers (73).

## 2.7.1 Wnt signaling pathway proteins

### 2.7.1.1 Wnt (Wnt ligands)

Wnt signaling proteins are a group of about 100 secreted glycoproteins that are highly conserved between *Drosophila*, *C. elegans*, and vertebrates. At least 16 members are originated in vertebrates, involved in a variety of developmental processes. The *Drosophila* *wg* gene is the best-characterized Wnt gene that provided a prototype to elucidate other Wnt genes (74). A comprehensive list and updates of Wnt genes can be reviewed on Wnt web page at <http://www.stanford.edu/~rnusse/Wntwindow.html>.

Credits are given to extensive epistasis studies in *Drosophila* and functional and mutational studies in mouse that elucidated the highlights of the genetic pathway of Wnt signaling (75, 76). In *Drosophila*, phenotypic mutational studies of *wg* gene have helped uncovering five other Wnt genes: *Porcupine* (*porc*), *Dishevelled* (*dsh*), *Armadillo* (*arm*; the *Drosophila* homolog of  $\beta$ -catenin), *Pangolin* (*pan*, also called *Tcf*) and *Zeste-white 3* (*zw3* also called *GSK*). Embryos that are mutant in *wg*, *porc*, *dsh*, *arm* and *pan*, *Tcf* showed defects in embryonic segment polarity, however, *zw3* mutant showed opposite phenotype (77). Wnt signaling pathway plays a key role in dorsal axis development in vertebrates. Microinjection of Wnt RNAs into ventral-vegetal blastomeres of *Xenopus* embryos resulted into generation of a secondary dorsal-ventral axis (78). In contrast, inhibition of Wnt signaling by injection of *Axin* mRNA in *Xenopus* embryos suppresses the formation of the primary axis (79).

The correlation between Wnt genes and cancer was studied broadly, however, the result were variable and inconclusive (7). Wnt ligands can promote neoplastic transformation and tumor formation *in vivo* and *in vitro*, most likely through  $\beta$ -catenin up-regulation (80-82). In addition, changes in the level of mRNA

expression of Wnt proteins have been reported in HCRC. For instance, *Wnt-2* mRNA, which is absent in normal colonic mucosa, was detected in colon tumors (83).

#### 2.7.1.2 Fz (Frizzled)

To initiate Wnt signaling cascade, Wnt proteins bind and form heterotrimeric complex with one of nine seven-pass trans-membrane receptors encoded by the Frizzled genes together with the low-density lipoprotein receptor-related protein 5 or 6 (LRP5 or LRP6). It has been shown recently that the binding affinities of Frizzled receptors to different classes of Wnt proteins are variable. The specificity of Wnt proteins to Frizzled receptors has been investigated in *Xenopus* embryos and 293T cells using a novel set of Wnt-Fz fusion constructs. In 293T cells, Wnt signaling pathway was activated when different Wnt-Fz fusion proteins were co-expressed with LRP6, but not LRP5. Interestingly, Wnt signaling pathway was activated to the same extent by different Wnt protein classes fused to the same Frizzled receptor. However, Wnt activations were variable when different Wnt protein classes were fused to different Frizzled receptors (84). In addition, it has been postulated that *Fz-1* and *Fz-2* receptors may be implicated in HCRC metastasis (83). Furthermore, micro array analysis and *Xenopus* axis duplication assays revealed a role of *Fz-10* in human carcinogenesis through up-regulation of the Canonical Wnt signaling pathway (85).

#### 2.7.1.3 Frat-1 (frequently rearranged in advanced T-cell lymphomas 1)

*Frat-1* was first identified as a proto-oncogene involved in the progression of mouse T cell lymphomas (86). *Frat-1* is an intronless gene located on

chromosome 10q24.1 and encodes a 233 amino-acid protein (87). *Frat-1* has been linked to Canonical Wnt signaling pathway after the discovery that *GBP*, *Frat-1* *Xenopus* homolog, binds and inhibit GSK-3 $\beta$  when expressed in *Xenopus* embryos (88). Upon Wnt signaling, Dishevelled recruits Frat-1, which degenerates the Dishevelled-Axin-GSK ternary complex, and inhibits the Axin-dependent phosphorylation of  $\beta$ -catenin (89). Furthermore, *Frat-1* contains a nuclear export sequence (NES) that facilitates GSK-3 $\beta$  nuclear transport. Thus, the access of GSK-3 $\beta$  to its cytosolic substrates including  $\beta$ -catenin is dynamically regulated (90). *Frat-1* mRNA levels were high in several cancers cell lines tested including gastric cancer cell line TMK1; pancreatic cancer cell lines TMK1, esophageal cancer cell lines TE2, TE3, TE4; a cervical cancer cell line SKG-IIIa, and breast cancer cell lines MCF-7 and T-47D (91).

#### 2.7.1.4 Dsh (Dishevelled)

Dishevelled belongs to a family of eukaryotic signaling phosphoproteins that contain a conserved 85-residue (DIX domain). Genetic analysis in *Drosophila* positioned *Dishevelled* downstream of *Frizzled* and upstream of  *$\beta$ -catenin* (92). Dishevelled associates with and is phosphorylated by Casein kinase I and II upon activation of Wnt signaling pathway (93, 94). In the absence of Wnt stimuli, Dishevelled binds to Frat-1 and to Axin of  $\beta$ -catenin destruction complex, however, it seems that this interaction does not appear to have an essential role in  $\beta$ -catenin regulation. Nevertheless, when Wnt signaling pathway is activated, a possible post-translational modifications of Dishevelled and /or other members of  $\beta$ -catenin destruction complex may permit the interaction between Frat-1 and GSK-3 $\beta$  and lead to dissociation  $\beta$ -catenin destruction complex (89).

#### 2.7.1.5 PP2A (Protein phosphatase 2A)

PP2A is a Serine/Threonine phosphatase that is involved in various cellular processes. The protein is a heterotrimeric one composed of a regulatory subunit "A", a catalytic subunit "C", and variable regulatory subunit "B". PP2A binds directly to Axin through its C subunit and interacts with APC through its B subunit and promotes their dephosphorylation (95, 96). Microinjection assays in *Xenopus laevis* revealed that *PP2A-C* is an essential positive constituent of Wnt signaling that can act both downstream or parallel to  $\beta$ -catenin (97). Alterations in PP2A subunits are associated with human malignancies (98, 99).

#### 2.7.1.6 GSK-3 $\beta$ (Glycogen synthase kinase-3 $\beta$ )

The unusual Serine/Threonine kinase, *zeste white-3/shaggy* in *Drosophila*, is a major regulator of several signaling pathways including Wnt signaling pathway. The mammalian homology GSK-3 was discovered more than two decades ago as a 51 kDa kinase that regulates the glycogen synthase functions. Subsequent biochemical analysis of GSK-3 isolated from rabbit skeletal muscle revealed two GSK-3 isoforms: GSK-3 $\alpha$  and GSK-3 $\beta$ . (100, 101). Examples of GSK-3 functions are illustrated in Insulin and Wnt signaling pathways in which, GSK-3 phosphorylation inhibits glycogen synthase activity and targets  $\beta$ -catenin for proteasomal degradation respectively. Upon Insulin or Wnt stimulation, GSK-3 activity is reduced, thereby increases the metabolism of glucose to glycogen and stabilizes  $\beta$ -catenin respectively (102, 103). GSK-3 phosphorylates a wide range of substrates. In addition to  $\beta$ -catenin, APC and Axin, GSK-3 phosphorylates ATP-citrate lyase, protein phosphatase 1, cAMP-dependent protein kinase, eIF2B,

inhibitor-2, c-Jun, c-Myc, Myb, CREB, Tau, and I $\kappa$ B. Therefore, GSK-3 plays important role in controlling transcription, translation, cytoskeleton, cell cycle, and glycogen metabolism processes (103). Epistasis studies in *Drosophila* have located *GSK-3 $\beta$*  downstream of *Disheveled* and upstream of  *$\beta$ -catenin* in the Canonical Wnt signaling pathway (104). GSK-3 $\beta$  exerts negative regulation on Canonical Wnt signaling pathway via phosphorylation of  $\beta$ -catenin at certain residues, namely Thr-41, Ser-37, and Ser-33 sequentially. Nonetheless, GSK-3 $\beta$  phosphorylation of  $\beta$ -catenin requires a preceding priming event at Ser-45 by Casein kinase I $\epsilon$  (CKI $\epsilon$ ). Axin facilitates this process by binding and scaffolding both CKI $\epsilon$  and  $\beta$ -catenin. However, inhibition of GSK-3 $\beta$  *in vivo* decreased Ser-45 phosphorylation, indicating that GSK-3 $\beta$  kinase activity is essential for the priming event (105). Studies in *Drosophila* have shown that, upon Wnt signaling, the kinase activity of GSK-3 $\beta$  is regulated (rather than the protein level) (106). The GSK-3 $\beta$  activity is regulated by several mechanisms. Unlike Insulin pathway, in which GSK-3 $\beta$  is inhibited by protein kinase B-dependent phosphorylation at Ser-21 in GSK-3 $\alpha$  and Ser-9 in GSK-3 $\beta$ , Wnt signaling inhibits GSK-3 $\beta$  through its binding to Frat-1 (GBP) and Dishevelled. This binding inhibits GSK-3 catalytic activity and facilitates the dissociating of  $\beta$ -catenin destruction complex (89, 107). Molecular analysis of several colon cancer cell lines has revealed inverse correlation between GSK-3 $\beta$  activity and differentiation status. For instance, treatment of the low differentiated colon cancer cell line LIM2537 with sodium butyrate, a potent differentiation inducer, led to marked reduction in the GSK-3 $\beta$  activity accompanied by  $\beta$ -catenin stabilization and sequestering to cell periphery (108).



#### 2.7.1.7 Adenomatous polyposis coli (APC)

*APC* was mentioned above as the main gene of HCRC, in which mutations (germline or somatic) are common in inherited and sporadic colorectal tumors. The first clue that linked *APC* to the Canonical Wnt signaling pathway came from the observation that  $\beta$ -catenin binds APC (109). When Wnt signaling is active, APC forms a complex with  $\beta$ -catenin, Axin and GSK-3 $\beta$ .  $\beta$ -catenin binds to 15- and 20-amino-acid repeats, whereas Axin binds to SAMP (Ser-Ala-Met-Pro) repeats in APC. This complex facilitates the phosphorylation and the subsequent ubiquitination and degradation of  $\beta$ -catenin (29). APC contains nuclear localization signals (NLS) and nuclear export signals (NES) which indicates a possible role of APC in the regulation of  $\beta$ -catenin nuclear trafficking (110). However, a new controversial study argued that  $\beta$ -catenin may transduce Wnt signaling through exporting TCF from the nucleus or activating it in the cytoplasm rather than migrating to the nucleus (111).

#### 2.7.1.8 Axin

Axin is a tumor suppressor gene critical for Wnt signaling pathway. Axin negatively regulates the Canonical Wnt signaling pathway by interacting with PP2A, GSK-3 $\beta$ , APC and  $\beta$ -catenin. This interaction enhances the phosphorylation of  $\beta$ -catenin and APC by the GSK-3 $\beta$ ; however, the precise mechanism of this process is still to be elucidated. (112). Moreover, Conductin, a homolog of Axin, can also bind to  $\beta$ -catenin and APC, however, in spite of this resemblance, Conductin failed to correct Axin mutations in hepatocellular carcinomas (HCC), suggesting distinct functions of Axin and Conductin (7). Recent studies have shown that Axin and CK1 $\epsilon$  form a complex that induces  $\beta$ -catenin phosphorylation

at Ser-45, an essential priming site for GSK-3 $\beta$  *in vivo* (113). Furthermore, inactivation mutations in *Axin* have been reported to associate with human neoplasms including breast cancer, neuroblastoma, HCRC, HCC and other tumors (114). In HCRC, *Axin2* mutations were reported in 11 of 45 colorectal tumors with defective MMR genes (115).

#### 2.7.1.9 Casein kinases (CK)

Several Casein kinases are involved in the regulation of Canonical Wnt signaling pathway including Casein kinase I (CKI  $\alpha$ ,  $\beta$ ,  $\gamma$ ,  $\delta$  or  $\epsilon$ ) and Casein kinase II (CKII). Both CKI and CKII are Serine/Threonine kinases first isolated by expression cloning in *Xenopus* embryos. Their functions mimicked the developmental properties of Wnt signaling. CKI and CKII action were associated with hyper-phosphorylation of Dishevelled (94, 116, 117). Additionally, CKII and GSK-3 $\beta$  play significant role in strengthen cell-cell adhesions by phosphorylating the cytoplasmic domain of E-cadherin and thereby enhancing the binding affinity of  $\beta$ -catenin to E-cadherin *in vitro* (118). Furthermore, CKI $\epsilon$  forms a ternary complex with Axin and Dishevelled and stimulates the Axin-mediated phosphorylation of APC, therefore, it positively regulates the Canonical Wnt signaling pathway (119, 120). It has been reported by two independent research groups that CKI $\epsilon$  as well as CKI $\alpha$  are priming kinases for GSK-3 $\beta$ . Both were capable to phosphorylate  $\beta$ -catenin at Ser-45. Phospho-Ser45- $\beta$ -catenin is a better substrate for GSK-3 $\beta$  than non-phosphorylated  $\beta$ -catenin (121, 122). Additionally, latest studies have shown that Diversin, an ankyrin repeat protein, was essential for efficient CKI $\epsilon$  –dependent phosphorylation of  $\beta$ -catenin by GSK-3 $\beta$ . It interacts with CKI $\epsilon$  and Axin/Conductin and recruits CKI $\epsilon$  to the  $\beta$ -catenin degradation complex (123).

#### 2.7.1.10 $\beta$ -TrCp (slimb in *Drosophila*)

$\beta$ -TrCp, a component of an E3 ubiquitin ligase, is an F-box/WD40-repeat protein that is essential for proper development and Canonical Wnt signaling pathway (124). The F-box interacts with the ubiquitin complex, whereas the WD40 repeats mediate the interaction of the N-terminus of  $\beta$ -catenin. The interaction between WD40 domain and  $\beta$ -catenin required preceding phosphorylation of codons 33,37,41 and 45 (125).

#### 2.7.1.11 TCF/ LEF transcription factors

The T-cell transcription factors (Tcf) and the Lymphoid enhancer factor (LEF) (Pangolin in *Drosophila*) together comprise a group of transcription factors characterized by harboring high mobility group (HMG) domain proteins that recognize the same DNA consensus motif (CCTTTGATC). LEF/TCF transcription factor superfamily includes several interrelated transcription factors, i.e. LEF-1, TCF-1, TCF-3, and TCF-4 that require other co-factors to activate gene transcription (7). Transient reporter gene assays have shown that  $\beta$ -catenin is a co-factor capable to bind, through its armadillo repeat region, to XTcf-3 and together transactivate appropriate reporter genes (126).

## 2.7.2 Model for Wnt signaling

### 2.7.2.1 Passive mode

In the absence of Wnt signaling, the cytosolic pool of  $\beta$ -catenin is tightly down-regulated. Firstly, Diversin recruits CKI $\epsilon$  to a multi-protein complex composed of  $\beta$ -catenin, Axin, APC, and GSK-3 $\beta$  (123). Secondly, CKI $\alpha$  or/and CKI $\epsilon$  phosphorylate  $\beta$ -catenin at Ser-45. This priming phosphorylation enables GSK-3 $\beta$  to phosphorylate  $\beta$ -catenin at Thr-41, Ser-37 and Ser-33 consecutively (121, 122). Thirdly, phosphorylated  $\beta$ -catenin is targeted for ubiquitination by  $\beta$ -TrCP. Finally, the poly ubiquitinated  $\beta$ -catenin is recognized by proteasomes and subsequently degraded (Figure 2) (127). There are several proposed mechanisms to inhibit Wnt signaling pathway. As an example, Dickkopf-1 (dkk-1), a cysteine-rich secreted protein, is an extra-cellular Wnt inhibitor that interacts with Wnt co-receptor low-density-lipoprotein-receptor-related co-receptor (LRP) (128). Alternatively, over-expression of dominant negative regulators such as Dishevelled, Axin, GSK-3 $\beta$ , APC and dominant negative forms of TCF could provide a way to suppress Wnt signaling (126, 129-131). Of course, mutations affecting various members also can inhibit this pathway.

### 2.7.2.2 Active state

Wnt proteins bind and activate the transmembrane Frizzled family receptors and initiate the Wnt signaling cascade through phosphorylation and activation of the Dishevelled protein by CKI and CKII (93, 94). The active Dishevelled recruits Frat-1 to Dvl-GSK-Axin ternary complex. Subsequently, Frat-1 facilitates the

degeneration of the complex (89). Thus,  $\beta$ -catenin is no longer recruited to its destruction complex and therefore not phosphorylated and no longer recognized by  $\beta$ -TrCP.  $\beta$ -catenin translocates into the nucleus, binds to TCF/LEF transcription factors and transactivates Wnt signaling responsive genes (132-134).

### 2.7.3 Target genes of Wnt signaling pathway

The list of Wnt signaling target genes is growing rapidly. Wnt signaling responsive genes include proliferation-related genes such as *cyclin D1*, *c-myc*, *c-jun* and *fra-1* (135). A comprehensive list of up-to-date Wnt signaling target genes can be reviewed at Wnt signaling target genes web page <http://www.stanford.edu/~rnusse/pathways/targets.html>

## 2.8 $\beta$ -CATENIN AND COLORECTAL CANCER

$\beta$ -catenin is a multi-functioning protein that is involved in maintaining cell-cell architecture as well as cell signaling.  $\beta$ -catenin binds to the cytosolic tail of adhesion molecules, called cadherins, at the cellular membrane and links them to actin cytoskeleton. Thus,  $\beta$ -catenin has dual roles in cell adhesion and Wnt signaling.  $\beta$ -catenin not bound to cadherin proteins in the Adherin junctions on the plasma membrane is destroyed in the cytoplasm (see above).

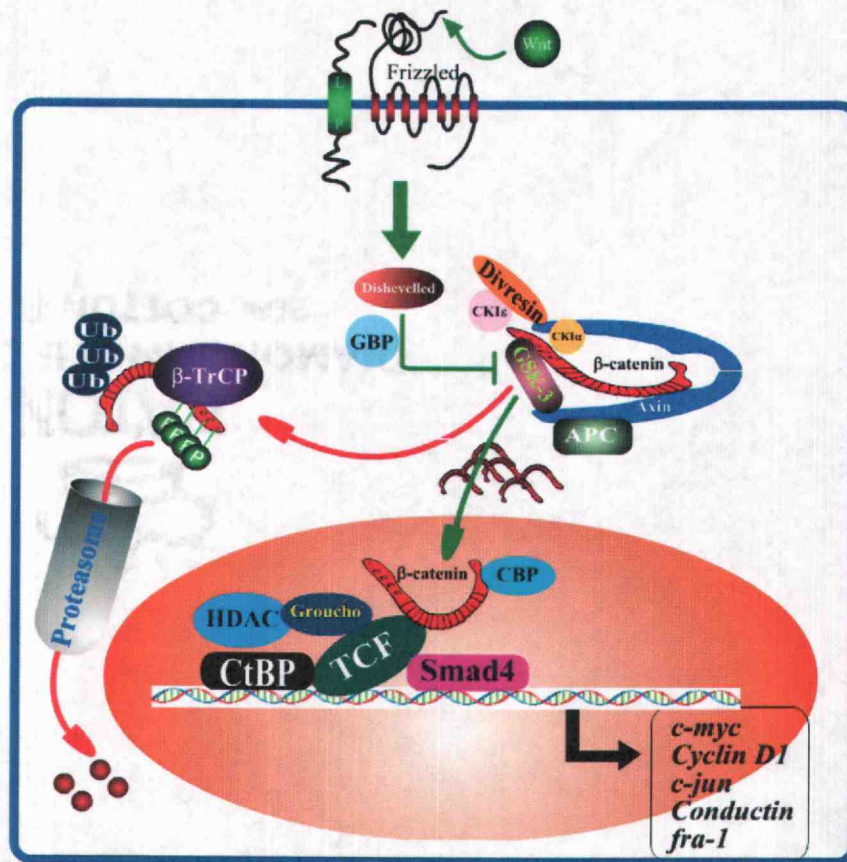


Figure 2: The Canonical Wnt signaling pathway.

When cells are not stimulated (e.g. by Wnt ligands),  $\beta$ -catenin is continuously phosphorylated, ubiquitinated and degraded by proteasomes (red arrows). However, upon Wnt stimulation, GSK-3 $\beta$  is inhibited and the non-phosphorylated accumulated  $\beta$ -catenin migrates into the nucleus, at which it binds TCF transcription factors and together transactivate Wnt signaling target genes (green arrows). Modified after Huelsken *et al* (136).

### 2.8.1 Discovery and structure of $\beta$ -catenin

$\beta$ -catenin was first discovered as a 92 kDa protein associated with the carboxy terminus of E-cadherin in *Xenopus laevis* at the cell membrane. Sequence analysis of  $\beta$ -catenin cDNA revealed close homology to the mammalian

*plakoglobin* and to the *Drosophila* segment polarity gene *Armadillo* (137). Studies in *Drosophila*, *Xenopus* and *C. elegans* have shown that  $\beta$ -catenin is involved in many developmental processes including segment polarity, axis formation and mesoderm induction respectively (138). The human  $\beta$ -catenin protein is encoded by 23.2 kb gene named *CTNNB1* identified by analysis of cDNA and genomic clones. The *CTNNB1* gene comprises 16 exons ranging from 61 to 790 bp in size. Intronic regions vary in size between 84 bp and 6700 bp with 50 % of all introns smaller than 550 bp. The complete human  $\beta$ -catenin mRNA size is 3362 bp composed of 2346 bp of coding sequence, 214 bp and 802 bp of 5'UTR and 3'UTR, respectively. The transcription initiation site resides 214 nucleotides upstream of the ATG initiation codon at exon 2. The 5'-flanking region is GC-rich and contains a TATA box and potential binding sites for common transcription factors, such as NF $\kappa$ B, SP1 and AP2. However, it lacks a CCAAT box (139). The *CTNNB1* locus was mapped by in situ fluorescence analysis on 3p22-p21.3 (140).

In contrast, rat  $\beta$ -catenin protein is encoded by 9082 bp gene *Ctnnb1*. Work by this author and colleagues showed that rat *Ctnnb1* comprises 14 exons and 13 introns (141). Exons vary in size from 61 to 356 bp, while introns range in size from 76 to 2524 bp. The transcription initiation site is located 157 bp upstream of the ATG start codon at exon 1. The complete rat  $\beta$ -catenin mRNA size is 2650 bp composed of 2343 bp of coding sequence, 157 bp and 147 bp of 5'UTR and 3'UTR respectively. Surprisingly, the GSK-3 $\beta$  regulatory region of rat  $\beta$ -catenin is located at exon 2, in contrast to human *CTNNB1* which is located at exon 3 (141).

Mouse  $\beta$ -catenin *Catnb1* coding region is similar in size to human and rat, however, the 5'UTR and 3'UTR are 97 bp and 147 bp respectively. The coding region of *Ctnnb1* harbors 89 % and 95 % homology to *CTNNB* and *Catnb1*, respectively (141). *CTNNB1*, *Ctnnb1*, and *Catnb1* encode the same size  $\beta$ -catenin protein, however rat and mouse  $\beta$ -catenin have Pro-706 instead of Ala-706 (141).

The primary structure of human  $\beta$ -catenin protein comprises three domains. The amino-terminal domain consists of 130 amino acids including the putative sites for phosphorylation by CKI and GSK-3 $\beta$  (Ser-33, Ser-37, Thr-41 and Ser-45). The armadillo (arm) repeat domain consists of 12 imperfect repeats of 42 amino acids that facilitate  $\beta$ -catenin binding to other proteins such as APC, E-cadherin, Axin and TCF/LEF. The carboxy-terminal domain comprises 100 amino acids that function as a transactivation domain (Figure 3) (138).

The three-dimensional structure of the armadillo repeat region of the murine  $\beta$ -catenin has been solved by Huber and others. Each 42 amino acid arm repeat region consists of 3  $\alpha$ -helices connected with a short loop re-orienting the polypeptide by 90° to form a compact unit that is resistance to proteolysis. However, inconsistencies in the structural pattern have been observed, for example, the first helix in the seventh repeat was replaced by a loop. The other variation is a 22 amino acid insertion in repeat 10. The 12 amino acids repeats region form a super-helix contains positively charged grooves that assist the interaction with acidic regions of cadherins, APC, and the TCF/LEF family transcription factors (142).

### 2.8.2 $\beta$ -catenin in cell-cell adhesion

$\alpha$ ,  $\beta$  and  $\gamma$ -catenins, structurally related molecules, were originally described as mediators of a cell-cell adhesion complex that connects the cytoplasmic domain of the transmembrane glycoprotein Uvomorulin (E-cadherin) to the cytoskeletal structures (143, 144). The Cadherins are a superfamily of transmembrane glycoproteins that mediate homophilic  $\text{Ca}^{2+}$ -dependent cell-cell adhesion, cytoskeletal anchoring and cell signaling (145). The Cadherins proteins are classified into classical cadherins, desmosomal cadherins and protocadherins



(146). The cell-cell adhesion junctions are formed through the homophilic interactions between the extra-cellular domains of the cadherins, located on neighboring cell membranes. The catenin proteins ensure the stability of cell adhesion junctions by linking and anchoring the intracellular domain of the cadherins to the actin cytoskeleton (146). E-cadherin is a prototype of the classical cadherins which is responsible for the integrity of epithelial cells. Removal of  $\text{Ca}^{2+}$  abolishes E-cadherin adhesive activity, render cadherins susceptibility to proteolytic degradation and induces a dramatic reversible conformational change in the entire extra-cellular region (146).

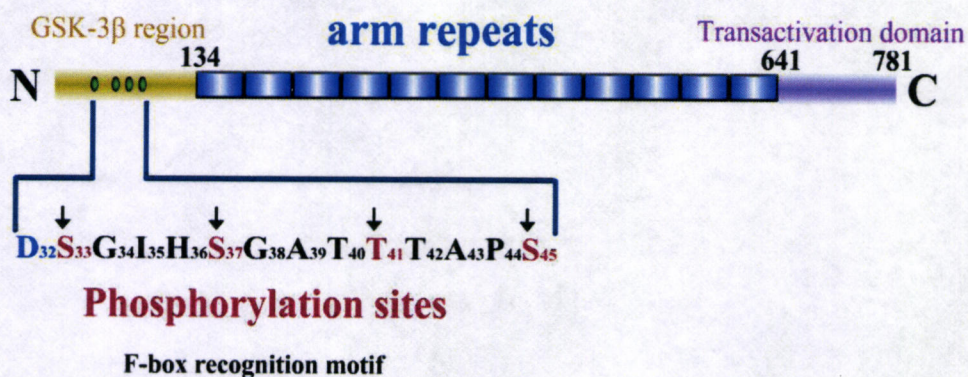


Figure 3: The primary structure of β-catenin.

The β-catenin protein is composed of three domains. The N-terminal domain harbors the GSK-3β and CKI phosphorylation sites and the F-box recognition motif that regulate β-catenin stability. The core armadillo repeat (called arm) region facilitates the binding of β-catenin to other members of Wnt signaling and cell adhesion, such as APC, TCF/LEF and E-cadherin. The C-terminal harbors the transactivation domain.

### 2.8.2.1 Architecture of the E-cadherin-mediated cell-cell adhesion junction

The three-dimensional structure of two N-terminal extra-cellular domains of E-cadherin was determined by magnetic resonance spectroscopy in the presence of calcium ions.  $\text{Ca}^{2+}$  facilitates the dimerization of two E-cadherin molecules within one cell through homophilic contacts on cad1 repeat. A dimer can then interact with similar dimers on neighbouring cells to form a zipper-like structure (Figure 4) (143).

The observation that cadherins proteins are resistance to non-ionic detergent extraction that successfully solubilized other membrane proteins led to the conclusion that cadherins are tightly connected to the cytoskeleton (144). On the cytosolic side of cellular membrane, the carboxy-terminal of E-cadherin is connected to cytoskeletal structures through  $\alpha$  and  $\beta$  or  $\gamma$ -catenin (plakoglobin). The biochemical analysis of recombinant cadherin and catenin proteins in protein-protein interaction experiments have revealed that  $\beta$ -catenin directly binds, with high affinity, to both the cytoplasmic domain of E-cadherin and to  $\alpha$ -catenin, however  $\alpha$ -catenin can not bind directly to the cytosolic domain of E-cadherin. On the other hand,  $\gamma$ -catenin can substitute for  $\beta$ -catenin but binds with less affinity to E-cadherin (145).



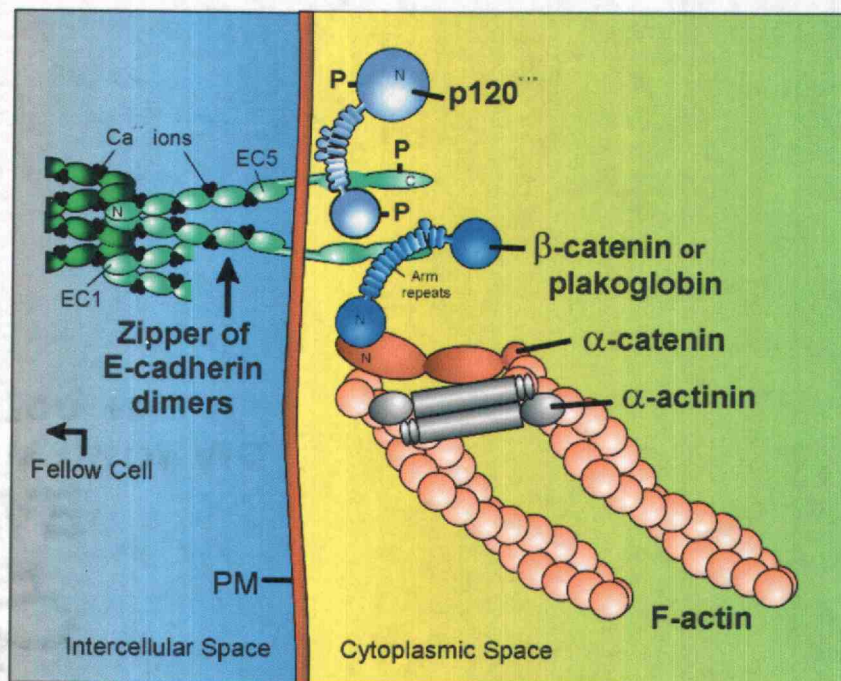


Figure 4: Molecular architecture of E-cadherin-mediated cell-cell adhesion  
 On the extra-cellular side of the cell, E-cadherin mediates cell-cell contacts by forming a zipper-like structure. On the cytoplasmic side of the cell, the carboxy terminal of E-cadherin binds to  $\beta$ -catenin which connects the cell junction molecules to the cytoskeleton by binding to  $\alpha$ -catenin.  
 Adapted from Nollet *et al* (146).

The role of  $\beta$ -catenin in cell-cell adhesion was established after several mutation analysis experiments of *Armadillo* in *Drosophila* embryos. Results have shown that Adherens junctions assembly was abolished in the absence of *Armadillo* (147). Crystal structure of the E-cadherin cytoplasmic domain complexed with  $\beta$ -catenin has shown that, the interaction extends over the entire armadillo repeat region of  $\beta$ -catenin and the phosphorylation of E-cadherin results in interactions with a hydrophobic region of  $\beta$ -catenin (148).

The binding of E-cadherin to  $\beta$ -catenin is controlled by the tyrosine phosphorylation of  $\beta$ -catenin. Phosphorylation of Tyr-86 and Tyr-654 residues of  $\beta$ -catenin by tyrosine kinase *Src* is critical for the dissociation of the adherence junction (149).  $\alpha$ -catenin binds to  $\beta$ -catenin at its N-terminal region (31-amino acid sequence in the first armadillo repeat) through formation of a four-helix bundle, and connects the cadherin- $\beta$ -catenin complex to the actin cytoskeleton (150).  $\gamma$ -catenin demonstrates high homology to  $\beta$ -catenin, however, its role in cell adhesion is not fully understood (144). Additionally, members of p120<sup>cm</sup> (p120) superfamily including  $\delta$ -catenin, an Armadillo protein, were found to bind to another conserved cytoplasmic domain of E-cadherin, however, little is known about their function (146). The p120 binds to the juxtamembrane domain (JMD) of cadherins. Recent study has shown that p120 was found to be mutated in SW48 HCRC cell line resulting in poor differentiation, however, restoring the normal levels of p120 have led to increased levels of E-cadherin and subsequently the reversion to normal epithelial morphology (151).

#### 2.8.2.2 Cell adhesion and oncogenesis

It was assumed that the disruption of epithelial cell-cell adhesion in the above pathway might lead to increased cell motility, impaired growth suppression, and eventually uncontrolled cell proliferation and cancer metastasis (152). Inactivation mutations (missense mutations and in-frame deletions) in the human E-cadherin gene, which are associated with marked reduction of the hemophilic cell-cell adhesion, have been reported in gastric and breast cancer (146). On the other hand mutations, which inactivate cell adhesion aspects of catenins, have been reported. For example, in-frame deletion of  $\beta$ -catenin (nucleotides 82 to 402) in

human gastric cancer cell line HSC-39 completely abolished E-cadherin-mediated cell-cell adhesion, in spite of high expression of E-cadherin at the cell membrane (153).

### 2.8.3 $\beta$ -catenin in cell junctions and signaling

The role of  $\beta$ -catenin in cell signaling was first found after several comparative studies of signaling pathways in *Drosophila* and *Xenopus*. Mutational and epistasis experiments in *Drosophila* have ultimately led to the discovery that the *Armadillo* gene, which is a crucial mediator for wingless-mediated cell signaling during normal development. Afterward, the discovery of the homology between  $\beta$ -catenin and the *Drosophila* segment polarity gene *Armadillo* have led to work on the signaling role of  $\beta$ -catenin in human cells (154). These findings have led to a new classification of the sub-cellular localization of  $\beta$ -catenin: as a part of the cell-cell adhesion complex (membrane-bound), cytoplasmic (free or bound to its destruction complex) and nuclear. As discussed above, the membrane-bound  $\beta$ -catenin is primarily in contact with E-cadherin and  $\alpha$ -catenin at cell adhesion junctions. This contact is regulated by the tyrosine phosphorylation on  $\beta$ -catenin and E-cadherin. Upon the tyrosine phosphorylation of the adhesion complex, E-cadherin- $\beta$ -catenin complex is subsequently ubiquitinated by HAKAI and endocytosed. Eventually, this pool of  $\beta$ -catenin will be degraded through the proteasomal pathway (155). On the contrary, the cytosolic  $\beta$ -catenin is transcriptionally active; therefore, the protein level is regulated by efficient degradation machinery (see Wnt signaling model above).

## 2.8.4 $\beta$ -catenin phosphorylation

### 2.8.4.1 Tyrosine phosphorylation of $\beta$ -catenin

The tyrosine phosphorylation of  $\beta$ -catenin at cell-cell adhesion complexes is regulated by tyrosine kinases (TKs) and protein-tyrosine phosphatases (PTPs), in a process that increases the dynamics of adhesion complexes and elevates the PY- $\beta$ -catenin in the cytosol (149). Stimulation of tyrosine phosphorylation of the adhesion complex by transfection of the cytoplasmic TK, such as Rous sarcoma virus (*v-src*) gene, caused unstable cell-cell adhesion and stimulated the spreading of chick embryonic fibroblasts cells (156). Although both Tyr-86 and Tyr-654 phosphorylation by *c-src* have been observed *in vitro*, site-directed mutagenesis experiments have revealed that only Tyr-654 phosphorylation was relevant for cell adhesion complex dissociation (149). Interestingly, Tyr-654 residue is located in the 12th and last armadillo repeat of  $\beta$ -catenin, a region involved in the binding of TATA box-binding protein (TBP) (157). Phosphorylation of Tyr-654 residue increased the binding of PY- $\beta$ -catenin to TBP both *in vitro* and *in vivo*, and was associated with higher stimulation of Tcf-4- $\beta$ -catenin transcriptional activity. These data suggested that when  $\beta$ -catenin is not phosphorylated at Tyr-654, it harbors a compact conformation structure, in which the C-terminus is folded and bound to the armadillo repeat regions. This folding provides binding selection for high affinity ligands (E-cadherin) over those of low binding affinity (TPB) and has no effects on Tcf-4 which mainly associates to repeats 3-8. Consequently, phosphorylation of Tyr-654 would expose the C-terminal, allowing for better chance for low affinity proteins to bind to the armadillo repeat region (158). In addition, the transactivation potential of the free cytosolic PY- $\beta$ -catenin has been investigated in several HCRC cell lines. HCT-15 colon carcinoma and NIH 3T3

fibroblasts cell lines treated with pervanadate, a PTPase inhibitor, showed translocation of  $\beta$ -catenin from the cell periphery to the cytosol. Nonetheless, the binding affinity of PY- $\beta$ -catenin to LEF-1 remained unchanged compared to non-phosphorylated  $\beta$ -catenin (159).

#### 2.8.4.2 Serine / Threonine phosphorylation of $\beta$ -catenin

Although it was well established that both the Serine/Threonine kinase GSK-3 $\beta$  and  $\beta$ -catenin are necessary for appropriate development in *Xenopus*, the direct interaction between these two proteins remained uncertain. It was then discovered by Yost and colleagues that GSK-3 phosphorylates  $\beta$ -catenin at a consensus sequence at its N-terminal including Ser-33; Ser-37; Thr-41 and Ser-45(160). The later phosphorylation has been shown more recently to require as a priming phosphorylation by CKI (161, 162). A yeast two-hybrid assay has revealed that rAxin directly interacts with the armadillo repeats 2-7 of  $\beta$ -catenin. This interaction enhanced the GSK-3 $\beta$ -dependent phosphorylation of  $\beta$ -catenin (163). Additionally, Axin directly binds and stimulates the GSK-3 $\beta$ -dependent phosphorylation of APC. Surprisingly,  $\beta$ -catenin stimulated the phosphorylation of APC in the presence of Axin *in vitro* (164). Additionally, recent study has shown that Diversin recruits CKI $\epsilon$  to the  $\beta$ -catenin degradation complex. CKI $\epsilon$ / CKI $\alpha$  then induces  $\beta$ -catenin phosphorylation at Ser-45. This step is followed by successive sequential phosphorylation of Thr-41, Ser-37 and Ser-33 of  $\beta$ -catenin by GSK-3 $\beta$ (161, 162).

#### 2.8.4.3 Serine / Threonine dephosphorylation of $\beta$ -catenin

An alternative mechanism of activating Wnt signaling without the need of Wnt proteins has recently been proposed. Dephosphorylation of the p $\beta$ -catenin can stabilize and increase the cytosolic levels of  $\beta$ -catenin. Sadot and colleagues have found that p $\beta$ -catenin can indeed be de-phosphorylated at Ser-37 and Ser-33 by an unknown phosphatase. Kinetic studies showed that the rate of the dephosphorylation process was equivalent to that of the GSK-3 $\beta$ -mediated phosphorylation of  $\beta$ -catenin. The p $\beta$ -catenin accumulates predominantly in the nucleus and forms a complex with LEF/TCF. However, the p $\beta$ -catenin-LEF/TCF complex fails to form a ternary complex with the DNA binding site of LEF/TCF (165). Concurring studies have shown that activation of Wnt signaling leads to accumulation of  $\beta$ -catenin, which was de-phosphorylated at Ser-37 and Thr-41 (166).

#### 2.8.4.4 $\beta$ -catenin ubiquitination and degradation

It is now obvious that  $\beta$ -catenin is degraded through the ubiquitin/proteasome pathway. When C57MG, LTK<sup>-</sup>, Neuro2A and human breast epithelial cell lines were treated with proteasomal inhibitor ALLN (N-Ac-Leu-Leu-norleucinal) or lactacystin, a highly specific inhibitor of proteasomal activity,  $\beta$ -catenin protein levels were increased dramatically. The elevation in  $\beta$ -catenin proteins was accompanied by the appearance of one or more higher molecular weight bands after western blotting analysis. These bands represent the (poly) ubiquitinated  $\beta$ -catenin (6, 125). Substitution mutations in the GSK-3 $\beta$  consensus phosphorylation motif have completely eradicated the ubiquitination of  $\beta$ -catenin (6). The poly-ubiquitination of  $\beta$ -catenin is mediated by  $\beta$ -TrCp, an F-box protein



and a component of an SCF-ubiquitin ligase, in a process that required a prior phosphorylation of  $\beta$ -catenin by GSK-3 $\beta$ . The process of ubiquitination typically occurs in a multi-step manner. The activation enzyme (E1) mediates the ATP-dependent transfer of ubiquitin groups into the ubiquitin-conjugating enzyme (E2). The ubiquitin ligase (E3) transfers the ubiquitin group from the E2 to lysine residues in the target protein. This process is repeated several times to generate poly-ubiquitinated proteins (167). Substitution mutations in the GSK-3 $\beta$  region, namely S33A, S37A, T41A and S45A, abolished  $\beta$ -catenin recognition by  $\beta$ -TrCp (168). It is noteworthy that the poly-ubiquitinated  $\beta$ -catenin is not stable in the absence of ubiquitin-conjugating enzymes inhibitors (155). In accord, the de-ubiquitinating enzyme, Fam, was found to bind to and stabilize  $\beta$ -catenin indicating that  $\beta$ -catenin is undergoing rapid de-ubiquitination (169).

#### 2.8.5 The nuclear activities of $\beta$ -catenin

Accumulated  $\beta$ -catenin in the cytosol find its way to the nucleus, and it binds to TCF/LEF transcription factors and transactivates genes controlling cell fates. It was surprising to find that  $\beta$ -catenin lacks the nuclear localization sequence (NLS), although it is mainly localized at the nucleus upon Wnt signaling activation. The findings that  $\beta$ -catenin shares the same nuclear pore components with importin- $\beta$ / $\beta$ -karyopherin suggested that  $\beta$ -catenin may be transported independently to the nucleus through a direct interaction with nuclear pore apparatus in a similar way to importin- $\beta$ / $\beta$ -karyopherin (170). An alternative mechanism of  $\beta$ -catenin transportation could be through TCF, which may bind to  $\beta$ -catenin in the cytoplasm and carry it into the nucleus (138). In contrast, some recent studies showed that  $\beta$ -catenin is shuttled from the nucleus to the cytosol, by APC, which harbors two nuclear export sequences at its N-terminus (171).

In the absence of nuclear  $\beta$ -catenin, TCF and its co-repressor partners repress Wnt signaling target genes. These co-repressors include Groucho (Grg/TLE) family and CtBP. Groucho interacts with histone deacetylase-1 (HDAC-1) (172). Once in the nucleus,  $\beta$ -catenin binds to TCF/LEF transcription factors and several other activators. These include TATA box-binding protein (TBP) (see Tyrosine phosphorylation of  $\beta$ -catenin), TIP49, P300 and CREB-binding protein (CBP). TIP49, which harbors similarities to ATPase and helicase RuvB, interacts with both  $\beta$ -catenin and TBP and is believed to bridge  $\beta$ -catenin and the basal transcription machinery (173).

#### 2.8.6 $\beta$ -catenin and apoptosis

Apoptosis (programmed cell death) is a genetically regulated process that is essential for appropriate development, differentiation, tissue homeostasis and defense against pathogens. Apoptosis is induced by an array of different signals including radiation, growth factor withdrawal, and cytotoxic agents like chemotherapeutic drugs. Apoptosis is associated with the deregulation of oncogenes and tumor suppressor genes. Apoptotic cells are morphologically characterized by cytoplasmic shrinkage, nuclear condensation, DNA fragmentation and membrane blebbing (174). Apoptosis is normally initiated by mitochondrial damage, which leads to the release of cytochrome c into the cytosol. Cytochrome c and the apoptotic protease-activating factor-1 (Apaf-1) recruits and activates procaspase-9 in an ATP-dependent manner. The active caspase-9 consequently activates other downstream caspases that in turn cleave target proteins and induce apoptosis (175).

Apoptosis plays a critical role in regulating cell-cell adhesion dynamics through processing of the linker protein  $\beta$ -catenin. Immunoblotting analysis of

apoptotic HUVEC, NIH3T3 and MDCK cells has shown that apoptosis was associated with caspase-3-dependent degradation of  $\beta$ -catenin and plakoglobin, but not of  $\alpha$ -catenin under the same conditions. Caspase-3 (also known as CPP32, apopain and Yama), an effector caspase, is activated during apoptotic signaling events by upstream proteases including caspase-6 and caspase-8 (174).

The caspase-3-dependent degradation of  $\beta$ -catenin generates fragments that lacked  $\alpha$ -catenin binding site, thereby, dismantling the association between E-cadherin complex and the cytoskeleton. Furthermore, proteolytic degradation of  $\beta$ -catenin was inhibited by overexpressing Bcl-2, an anti-apoptotic protein that prevents apoptosis and inhibits activation of the caspases (176, 177). A similar degradation phenomenon of  $\beta$ -catenin was observed in colon cancer cell lines undergoing apoptosis: WiDr, DLD-1, and a rat hepatoma cell line McA-RH7777 (178). Edman degradation sequencing and mass spectrometry analysis of apoptosis-cleaved  $\beta$ -catenin domains showed five possible caspase-3 cleavage sites (DXXD): Asp-32, Asp-83, Asp-115, Asp-751 and Asp-764. *In vitro* time course cleavage of  $\beta$ -catenin by recombinant caspase-3 showed that  $\beta$ -catenin was first cleaved at the C-terminus (Asp-764) followed by cleavage at the N-terminus Asp-32, Asp-83, Asp-115, respectively (Figure 5). Lastly,  $\beta$ -catenin is further truncated at a second C-terminal cleavage site (Asp-751). Reporter gene assay of  $\beta$ -catenin cleaved products co-transfected with hTcf-4 showed marked decrease in the transcriptional activity of all truncated  $\beta$ -catenins (179).

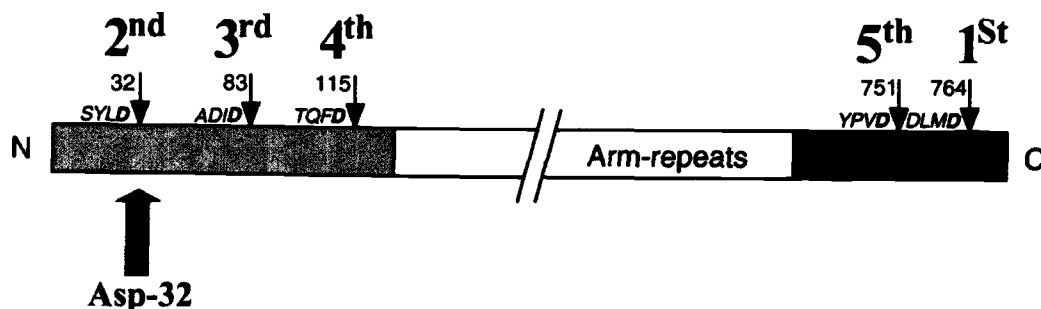


Figure 5: Putative sequential cleavage sites in  $\beta$ -catenin for caspase-3. Modified after Steinhusen *et al* (179).

The effect of  $\beta$ -catenin on apoptosis has been studied. Over-expression of  $\beta$ -catenin in the NIH 3T3 fibroblast cells, human colon carcinomas SW480, HCT116, DLD1 and SW48 induced apoptosis independent of its transactivating function (180). Controversially, activation of Wnt signaling in Rat-1 cells with Wnt-1 led to inhibition of drug-induced apoptosis. However, inhibition of  $\beta$ -catenin/Tcf transcription activity in SW480 cells by constitutive expression of dominant negative Tcf-4 (DN-Tcf-4) mediated cells killing. The same spontaneous apoptosis was observed when the transcriptional activity of  $\beta$ -catenin was inhibited by forced expression of DN-Tcf-4 in HT-29 cells (181).

#### 2.8.7 Mechanisms of abnormal accumulation of $\beta$ -catenin

Morin and others have shown that the abnormal activation of  $\beta$ -catenin is due to defects in *APC* or  *$\beta$ -catenin* genes. As mentioned previously, approximately 85 % of all HCRC tumors harbor *APC* mutations, associated with the elevation of  $\beta$ -catenin protein levels. Additionally, point mutations affecting  $\beta$ -catenin N-terminal residues were found in about 50% of all HCRC tumors that retained WT

*APC* (182). Mutations that inactivate several members of  $\beta$ -catenin destruction complex including *APC*, *Axin* and *Conductin* have been reported in numerous tumors and cancer cell lines. These mutations are associated with stabilizing of cellular  $\beta$ -catenin (183).

#### 2.8.8 Mutations of human $\beta$ -catenin gene (*CTNNB1*)

Substitution mutations targeted to specific Serine and Threonine residues at the regulatory N-terminal domain of  $\beta$ -catenin abrogate the phosphorylation-dependent interaction of  $\beta$ -catenin with  $\beta$ -TrCp and eventually lead to abnormal buildup of  $\beta$ -catenin in the cytosol (5). It has been reported that the GSK-3 $\beta$  region of  $\beta$ -catenin is a hotspot for missense and in-frame deletion mutations in a wide variety of human cancers as well as in chemically and genetically-induced animal tumors. Notably, mutational screening of exon 3 of *CTNNB1* from 202 sporadic colorectal tumors revealed that the overall  $\beta$ -catenin mutations frequency is quite low and not seen in invasive cancers. Moreover, it appears that  *$\beta$ -catenin* mutations are exclusive to tumors harboring *APC* mutations (24). Polakis has surveyed all mutations affecting  $\beta$ -catenin amino acid sequence between Ser-29 and Lys-49 that were observed in human tumors and reported in the literature before October, 2000 (7). The survey was of  $\beta$ -catenin mutations reported in several cancer types including colorectal, desmoid, endometrial, gastric, hepatocellular, hepatoblastoma, medulloblastoma, ovaria, uterine, endometrial, and prostate cancer (see reference (7) for citations). Codons for the GSK-3 $\beta$  phosphorylation sites (33, 37, 41, and 45) were the dominant mutational hotspots (Figure 6); 24 % of all mutations reported in the literature were observed at Ser-45. This now makes sense after the discovery that codon 45 is an obligatory priming site, and that its phosphorylation precedes (and is required for) the successful phosphorylation of other Ser/ Thr residues at the

GSK-3 $\beta$  region of  $\beta$ -catenin *in vivo*. The other hotspots of mutations are Thr-41, Ser-37 and Ser-33, which account for 18%, 12% and 9%, respectively. Surprisingly, Asp-32, which is not a direct target for phosphorylation by GSK-3 $\beta$ , accounted for 14 % of all mutations observed. However this percentage is decreased to 5% if only HCRC mutations are considered (Figure 7). In this case, mutations at codon 45 now become the dominant genetic alteration, and accounted for 55 % of all  $\beta$ -catenin mutations.

#### 2.8.9 $\beta$ -catenin mutations in experimentally-induced animal tumors

In contrast to human CRC, which is mainly due to activation mutations in the *APC* gene, *Apc* mutations are very rare in rat colon tumors. Only 15 to 59 % of F344 rat colon tumors induced by heterocyclic amine (HCAs) dietary carcinogens, such as 2-amino-1-methyl-6-phenylimidazo[4,5-*b*]pyridine (PhIP) and 2-amino-3-methylimidazo[4,5-*f*]quinoline (IQ), harbored *APC* mutations (184, 185). In addition, Dashwood and colleagues demonstrated that the incidence of mutations in the *Apc* and *Cttnb1* genes is 100% in rat tumors induced by PhIP and IQ and occur in a mutually exclusive manner (28). Several *in vivo* studies have shown that tumor induction by HCAs in animal models including male F344 rats and male ICR mice lead to elevation in  $\beta$ -catenin mutations. These mutations sequestered around codon 33 of the GSK-3 $\beta$  region of  $\beta$ -catenin and targeted other critical Ser/Thr residues important for  $\beta$ -catenin degradation (Table 2 and 3) Furthermore, the most intriguing observation is that, the mutation pattern of  $\beta$ -catenin in animal models is shifted toward the N-terminal of  $\beta$ -catenin when tumors are induced with certain carcinogens (Figure 8). Moreover, codon 32 and 34 were major hotspots, presumably due to the presence of two CTGGA sequences in this region (186).



A major goal of this thesis was to test the hypothesis that, like direct substitutions of Ser/Thr residues, substitutions of amino acids adjacent to Ser-33 could stabilize  $\beta$ -catenin. As a corollary, the specific nature of the substitution could affect phosphorylation and/or ubiquitination of  $\beta$ -catenin.

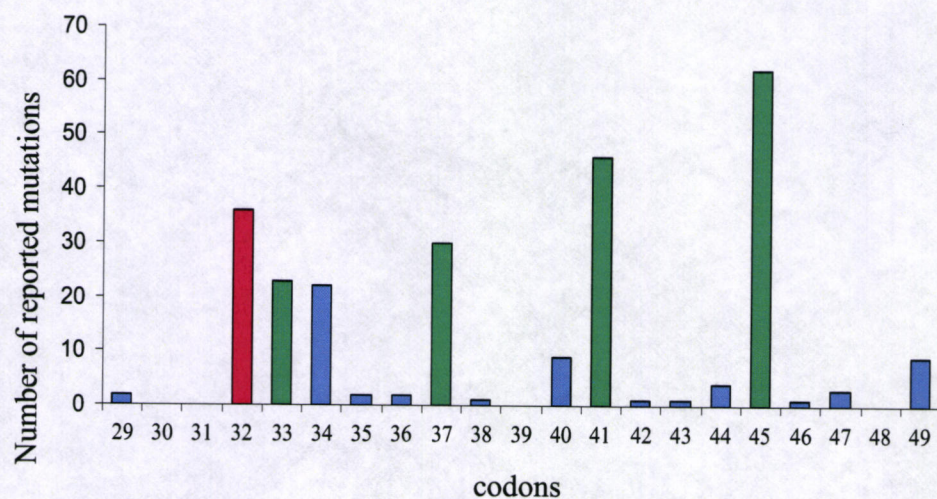


Figure 6: Overall distribution of *CTNNB1* mutations reported in human cancers

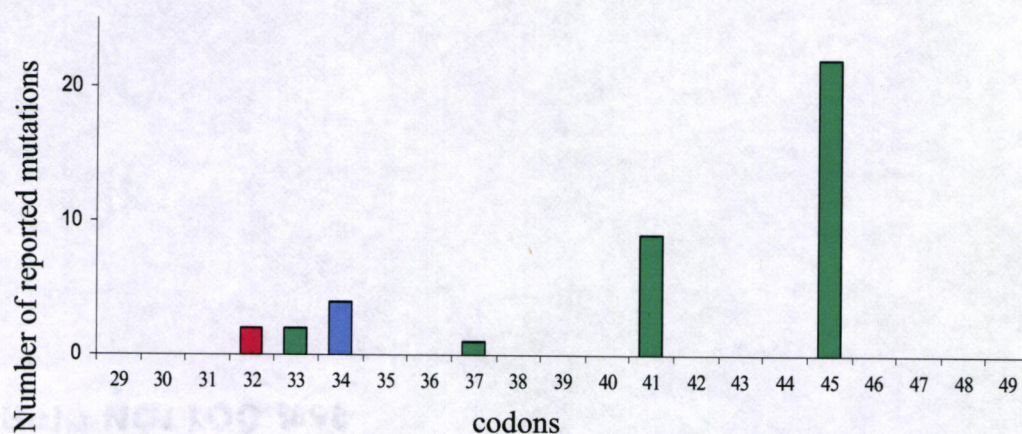


Figure 7: Overall distribution of  $\beta$ -catenin mutations reported in HCRC.

Table 1: Mutation spectra of human *CTNNB1*.

Codon	WT	Substitution mutations				
32	GAC (Asp)	<u>T</u> AC (Tyr)	AAC (Asn)	G <u>G</u> C (Gly)	G <u>T</u> C (Val)	G <u>C</u> C (Ala)
33	TCT (Ser)	T <u>G</u> T (Cys)	T <u>T</u> T (Phe)	<u>C</u> CT (Pro)	<u>C</u> TT (Leu)	
34	GGA (Gly)	G <u>T</u> A (Val)	G <u>A</u> A (Glu)	<u>A</u> GA (Arg)		
35	ATC (Ile)	A <u>G</u> C (Ser)				
36	CAT (His)	<u>C</u> CT (Pro)	<u>T</u> AT (Tyr)			
37	TCT (Ser)	T <u>A</u> (Tyr)	<u>G</u> CT (Ala)	T <u>T</u> T (Phe)	T <u>G</u> T (Cys)	
38	GGT (Gly)	G <u>A</u> T (Asp)				
40	ACT (Thr)	A <u>T</u> T (Ile)				
41	ACC (Thr)	<u>G</u> CC (Ala)	A <u>T</u> C (Ile)			
42	ACA (Thr)	A <u>T</u> A (Ile)				
43	GCT (Ala)	G <u>T</u> T (Val)				
44	CCT (Pro)	<u>T</u> CT (Ser)				
45	TCT (Ser)	T <u>T</u> T (Phe)	<u>C</u> CT (Pro)	T <u>A</u> T (Tyr)	T <u>G</u> T (Cys)	
46	CTG (Ile)	<u>G</u> TG (Val)				
47	AGT (Ser)	A <u>A</u> T (Asn)				
49	AAA (Lys)	A <u>G</u> A (Arg)				

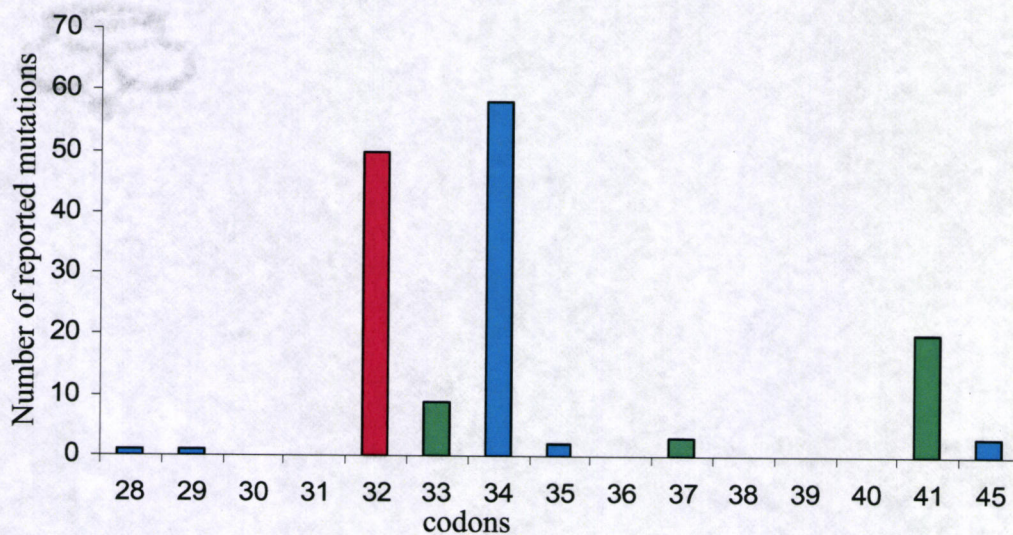


Table 2:  $\beta$ -catenin mutations in experimentally-induced animal tumors.

Animal	Carcinogen	Cancer	codons															Ref
			28	29	30	31	32	33	34	35	36	37	38	39	40	41	45	
F344 rat	IQ & PhIP	CRC	-	-	-	-	3	-	3	1	-	2	-	-	-	-	-	(28)
TG-mice	-	HCC	-	-	-	-	3	3	4	-	-	3	-	-	-	2	1	(187)
F344 rat	1-HA & MAM	CRC	-	-	-	-	3	-	13	-	-	-	-	-	-	2	-	(188)
B6C3F1 mice	DEN	HCC	-	-	-	-	-	-	-	-	-	-	-	-	-	7	-	(23)
F344 rat	DEN	HCC	-	-	-	-	-	2	3	-	-	-	-	-	-	-	-	(26)
ICR mice	AOM	CRC	-	-	-	-	-	3	4	-	-	1	-	-	-	1	-	(189)
F344 rat	AOM	CRC	-	-	-	-	9	3	9	-	-	-	-	-	-	5	-	(190)
F344 rat	AOM	CRC	1	1	-	-	4	1	4	1	-	-	-	-	-	1	-	(191)
F344 rat	IQ & DMH	CRC	-	-	-	-	21	2	10	-	-	-	-	-	-	6	3	(9)
F344 rat	NNK	HCC	-	-	-	-	-	1	-	-	2	2	-	-	-	-	-	(192)
TG-mice	DEN	HCC	-	-	-	-	-	-	-	-	-	-	-	-	-	-	4	(22)
F344 rat	1-HA & MAM	CRC	-	-	-	-	8	-	13	-	-	-	-	-	-	5	-	(193)
F344 rat	PhIP	CRC	-	-	-	-	2	-	2	-	-	-	-	-	-	-	-	(194)

Table 3:  $\beta$ -catenin mutation variety in experimentally-induced animal tumors.

CODON	WT	Substitution mutations			
32	GAT (Asp)	<u>A</u> AT (Asn)	GGT (Gly)		
33	TCT (Ser)	<u>G</u> CT (Ala)	TTT (Phe)	<u>C</u> CT (Pro)	TAT (Tyr)
34	GGA (Gly)	GT <u>A</u> (Val)	GAA (Glu)	<u>A</u> GA (Arg)	
35	ATC (Ile)	AGC (Ser)			
36	CAC (His)	<u>G</u> AC (Asp)			
37	TCT (Ser)	<u>G</u> CT (Ala)	TTT (Phe)	TGT (Cys)	<u>C</u> CT (Pro)
41	ACC (Thr)	<u>G</u> CC (Ala)	ATC (Ile)		
45	<u>C</u> CT (Pro)				

Figure 8:  $\beta$ -catenin mutation spectrum in experimentally-induced animal tumors, Showing codon 32 and 34 as major “hotspots”.

### 3 CHAPTER 3: MATERIALS AND METHODS

#### 3.1 PLASMID CONSTRUCTION

##### 3.1.1 Site-directed mutagenesis

Myc-tagged h $\beta$ -catenin plasmids were constructed that harbor substitution mutations at codon 32, namely D32G, D32N and D32Y, using PCR-based site-directed mutagenesis by overlap extension (195, 196). Briefly, as shown in Figure 9, two sets of primer pairs (a “left” and a “right” pair) were used, each of which amplifies approximately one-half of the region that includes codon 32 of a construct containing myc-tagged human WT  $\beta$ -catenin cDNA (provided by Dr. Hans Clevers, Utrecht, The Netherlands). The inner primers, namely bR32G/bF32G, bR32N/bF32N or bR32Y/bF32Y are a complement of each other and contain the desired mutation. The forward primer, bF5, and the reverse primer, bR2, are the outside primers. A comprehensive list of primers used is shown in Table 4.

The first round of PCR involved six reactions, and was conducted using the following sets of primers: bF5 + bR32G, bF5 + bR32N, bF5 + bR32Y, bR2 + bF32G, bR2 + bF32N and bR2 + bF32Y for PCR reactions one to six respectively. The PCR was conducted using the following conditions: pre-heat at 94° C for 3 min, amplification for 30 cycles in which each cycle consists of denaturation step at 94° C for 30 sec, annealing at 55C° for 30 sec, polymerization at 72C° for 30 sec, followed by a final extension at 72° C for 7 min. The PCR templates (160 bp) from reactions 1, 2 and 3 were mixed to the PCR templates (198 bp) from reactions 4, 5 and 6 respectively and purified using Wizard ® PCR Preps DNA purification System (Promega). The DNA mixture was denatured, and then renatured under



non-stringent conditions, allowing overhangs to anneal. Using the outside primers, the second PCR round started with only one cycle to achieve full extension (pre-heat at 94° C for 30 sec , annealing at 42° C for 30 sec and extension at 65° C for 60 sec), followed by 18 cycles at higher stringency (pre-heat at 94° C for 30 sec, annealing at 55° C for 60 sec and polymerization at 72° C for 60 sec). All PCR reactions were conducted using Takara DNA polymerase kit (Takara Biomedicals). The PCR reaction volume was 50 µl and contained 50 pg of myc-hβ-catenin plasmid DNA, 200 µM dNTPs, 400 nM of appropriate primers, 0.2 µl of 5 units/ml *Taq* DNA polymerase and 5µl of 10X PCR buffer. A geneAmp PCR system 9700 thermal cycler (PE applied Biosystems) was used to run all PCR reactions.

The 339 bp PCR product from the second PCR round was purified and was subjected to *Bam*HI/*Xho*I double digestion for 3 hours. The digested products (269 bp) were purified, quantitated using a Shimadzu UV-2401 PC spectrophotometer and analyzed on 1 % Agarose gel after staining with ethidium bromide.

Separately, 2 µg of the myc-hβ-catenin construct were subjected to *Bam*HI/*Xho*I double digestion for 3 hours and a large fragment of about 7 kb that contains hβ-catenin cDNA that lacks the first 269 bp, was excised and purified from 1% agarose gel after ethidium bromide staining. The 269 bp inserts generated from the site directed mutagenesis experiment were ligated to the large fragment in 1:3 molar ratio of vector to insert respectively. Five µl of the ligation reaction were transformed into One Shot® Top 10 competent cells (Invitrogen) according to the supplier instruction manual. The transformed cells were plated onto agar plates containing 100 µg/ml Ampicillin and were incubated overnight at 37° C. Bacterial colonies were screened by growing 10~40 single colonies in 6 ml of LB media contain 150 µg/ml Ampicillin for 6~8 hours. Bacteria from one ml of LB culture was harvested by centrifuging at 5000 rpm for 10 minutes and the bacterial pellet was resuspended in 100 µl ice-cold PBS. Two µl of the bacterial suspension was used as a PCR template using the outside primers. The PCR products were purified

and then subjected to *HinfI* digestion. The WT sequence harbors three *HinfI* recognition sites that generate four DNA fragments, 7 bp, 18 bp, 148 bp and 163 bp, whereas, introducing mutation at codon 32 abolished one of the *HinfI* recognition motifs. Thus, digesting mutants with *HinfI* generated only three fragments, 18 bp, 155 bp and 163 bp. The *HinfI* digested PCR products were analyzed on 4% agarose gel. The plasmid DNA from the positive clones was isolated with Qiafilter plasmid maxi prep kit (Qiagen) and submitted for sequencing. S33Y and  $\Delta 45$  h $\beta$ -catenin constructs were made previously by using site-directed mutagenesis and fragment switching as described elsewhere (197).

Table 4: The primers used for site-directed mutagenesis.

Primer	Sequence (5' $\rightarrow$ 3')	Description
BF5	GATCGCCGCCATGGAGCAG	Sense outside primer
BR2	TGAGCTCGAGTCATTGCATAC	Antisense outside primer
BF32G	CTTACCTGGGCTCTGGAATCC	Sense inner primer, D32G
BF32N	CTTACCTGAACTCTGGAATCC	Sense inner primer, D32N
BF32Y	CTTACCTGTACTCTGGAATCC	Sense inner primer, D32Y
BR32G	GGATTCCAGAGCCCAGGTAAG	Antisense inner primer, D32G
BR32N	GGATTCCAGAGTTCAGGTAAG	Antisense inner primer, D32N
BR32Y	GGATTCCAGAGTACAGGTAAG	Antisense inner primer, D32Y

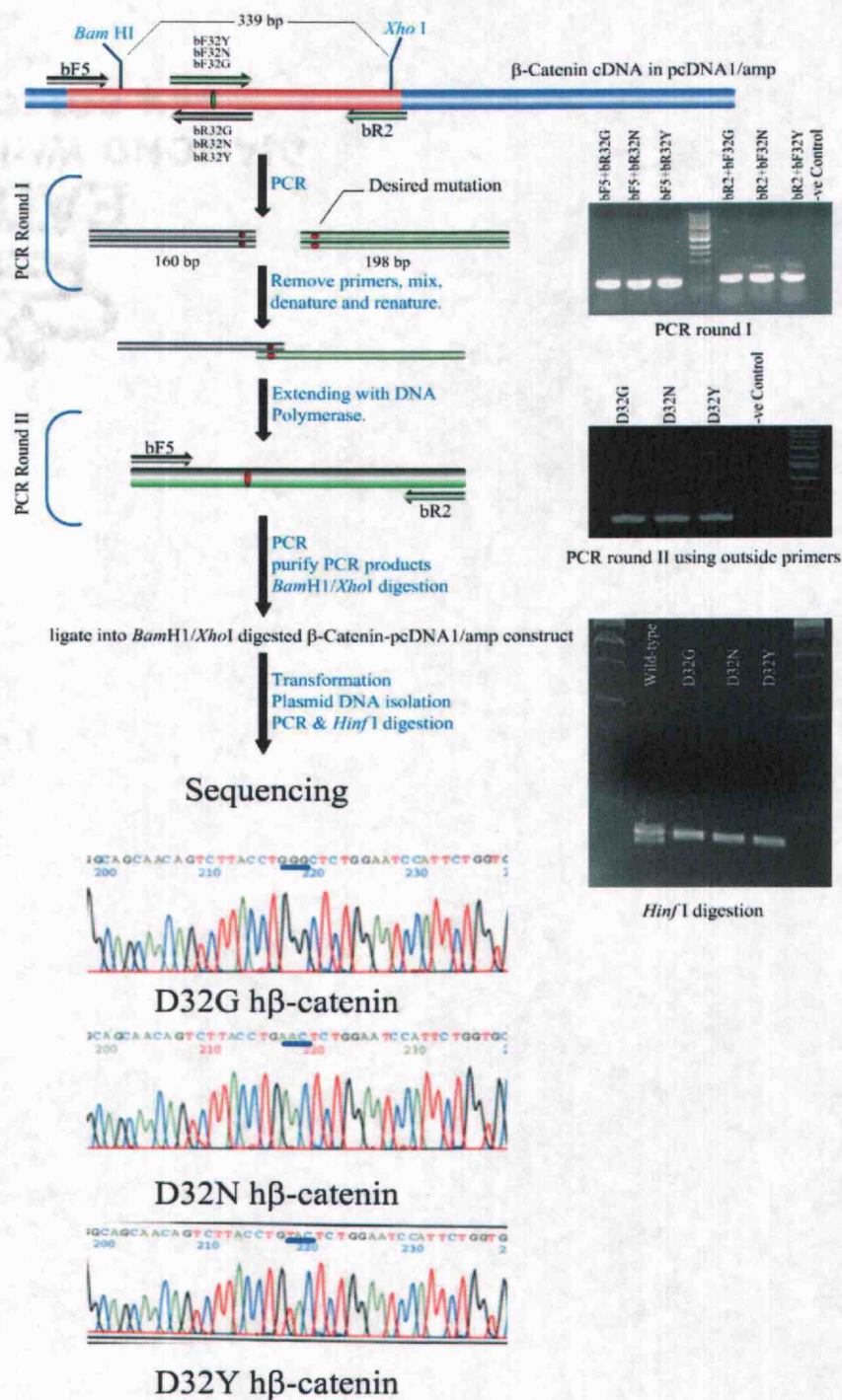


Figure 9: PCR-Based Site-Directed Mutagenesis by 'Overlap Extension'.

### 3.1.2 Prokaryotic expression vectors

WT, D32G, D32N, D32Y, S33Y and  $\Delta 45$  h $\beta$ -catenin cDNAs were subcloned into a GST-gene fusion expression vector, pGEX-5x-2 (Amersham Pharmacia Biotech). One set of primers were designed to amplify the full length h $\beta$ -catenin cDNA using various pcDNAI/amp constructs previously made as templates. The antisense primers were engineered to contain a *Not* I restriction site. A comprehensive summary of all primers used is shown in Table 5. The PCR reaction volumes were 50  $\mu$ l and contained 200  $\mu$ M dNTPs, 400 nM of appropriate primers, 50 pg of appropriate h $\beta$ -catenin construct, 1  $\mu$ l of 2.5 units/ml native *pfu* DNA polymerase (Startagene) and 5  $\mu$ l of 10X PCR buffer. The amplification reactions were initiated by a pre-heating step at 94° C for 2 min and cycling conditions were: 94° C for 45 sec, annealing at 55° C for 45 sec and polymerization at 72° C for 3 min, followed by 72° C for 10 min. The size of PCR products was 2349 bp that contain *Not*I restriction site at their 3' end. The PCR products were digested with *Not*I for 3 hours, purified and quantitated spectrophotometrically.

Simultaneously, 2~4  $\mu$ g of the pGEX-5x-2 vector was subjected to overnight *Sma*I digestion to create 5' blunt ends followed by *Not*I digestion. The DNA purification was conducted after each digestion cycle due to incompatible reaction buffer systems. five-fold molar excess of the digested PCR products were ligated overnight to the linearized vector at 16° C. Approximately, 2~5  $\mu$ l of the ligation reactions were transformed into One Shot® Top 10 competent cells. Single colonies (10~40) were screened by PCR using pGEX5' and pGEX3' primers (supplied with pGEX-5x-2 expression vector), which are pGEX-5x-2 specific and amplify 172 bp which flanks the insert region. Plasmid DNA from the positive colonies was purified and was submitted for sequencing using pGEX5' primer.

For *rAxin* cloning, one pair of primers (Table 5) was designed to amplify the region between 298~506 of rat Axin cDNA using pMALC-2 construct as a

template (generous gift from Dr. Akira Kikuchi). The forward and reverse primers contain *EcoRI* and *NotI* restriction sites, respectively. The PCR products were purified and digested with *EcoRI* and *NotI*. Meanwhile, pGEX-5x-2 expression construct was doubly digested with *EcoRI/NotI* and purified. Ligation was performed in 1:5 molar ratio of vector to insert overnight, followed by transformation. The bacterial colonies were screened by PCR using pGEX3' and pGEX5' primers. Plasmid DNA was isolated from the positive colonies and submitted for sequencing.

For hGSK-3 $\beta$  cloning, WT hGSK-3 $\beta$  cDNA was synthesized from HEK-293 cells. Cells were seeded into T-75 flasks and grown to confluency. The cell monolayer was washed twice with pre-warmed PBS and trypsinized with 0.25% trypsin, 0.03% EDTA. The cells were counted and  $5\sim7 \times 10^6$  cells were used for mRNA isolation using Micro-FastTrack™ 2.0 mRNA Isolation Kit (Invitrogen) according to the supplier instruction manual. cDNAs were synthesized from 2  $\mu$ l mRNA by using oligo (dT) primer and Thermoscript RT-PCR system (Gibco BRL). GSK-3 $\beta$  forward and reverse primers were designed to contain *EcoRI* and *NotI* restriction sites, respectively (Table 5). PCR was conducted in a final volume of 50  $\mu$ l including 200  $\mu$ M dNTPs, 400 nM of appropriate primers, 2  $\mu$ l cDNA solution, 1  $\mu$ l of 2.5 units/ml native *pfu* DNA polymerase and 5  $\mu$ l of 10X PCR buffer. The PCR products were purified and digested with *EcoRI* and *NotI*. The pGEX-5x-2 vector was digested with *EcoRI* and *NotI* and purified. Five molar excess of the digested PCR products were ligated to the linearized pGEX-5X-2 overnight at 16° C followed by bacterial transformation. The bacterial colonies were screened by PCR using pGEX3' and pGEX5' primers. Plasmid DNA was isolated from the positive colonies and submitted for sequencing.



Table 5: The primers used for subcloning *β-catenin*, *rAxin* and *GSK-3β*.

Primer	Sequence (5' → 3')	Description
hβC-SubCF	GCTACTCAAGCTGATTTGA TGGAG	Sense primer for hβ-catenin cDNA subcloning.
hβC-SubCR	TCACGATGGCGGCCGCTTT ACAGGTCAGTATCAAACCA G	Antisense primer for hβ-catenin subcloning, with <i>Not</i> I restriction site.
GSK-3β-F	GCTGCGATGCGAATTCTCA TGTCAGGGCGGCCCAGAAC CAC	Sense primer for <i>GSK-3β</i> subcloning, with <i>Eco</i> R I restriction site
GSK-3β-R	CAGCTCTCGAGCGGCCGC TCAGGTGGAGTTGGAAGCT GATGC	Antisense primer for GSK-3β cDNAs subcloning, with <i>Not</i> I restriction site
rAxin-For	CTGGATCCCGGAATTCCAT GCAGAGTCCCAAATGAAT GTCCAG	Sense primer for <i>rAxin</i> subcloning, with <i>Eco</i> R I restriction site
rAxin-Rev	GCGACTCGATGCGGCCGC TCAGTCCACCTTTTCCACCT TGCC	Antisense primer for rAxin subcloning, with <i>Not</i> I restriction site

### 3.2 CELL CULTURE

The Human embryonic kidney 293 (HEK-293) cells were purchased from the American Type Culture Collection (ATCC) and maintained in minimum essential media (MEM) (Gibco-BRL, Life Technologies) supplemented with 10% horse serum, 2mM L-Glutamine and 1mM sodium pyruvate at 37° C under 5% CO<sub>2</sub>.

### 3.3 TRANSIENT TRANSFECTION

All transfection experiments were performed in triplicate using the Effectene transfection reagent kit (Qiagen). HEK-293 cells were seeded at a density of  $1 \times 10^6$  on 60 mm poly-D-lysine-coated plates (Becton Dickinson) and grown overnight to 50~70% confluency. Prior to transfection, cells were washed with pre-warmed PBS and 4 ml of fresh media were added to each plate. A combined 2  $\mu\text{g}$ , or unless indicated otherwise of appropriate plasmid DNA were dissolved in 150  $\mu\text{l}$  of the DNA-condensation buffer (buffer EC). Enhancer buffer (16  $\mu\text{l}$ ) was added for 5 minutes followed 25  $\mu\text{l}$  of Effectene reagent. The centrifuge tubes were vortexed briefly and incubated at room temperature for 15 minutes. One ml of fresh media was added to each tube and mixed by pipetting. The transfection mixture was then added drop-wise to the cells and evenly distributed by gentle agitation. A pSV- $\beta$ -galactosidase vector (Promega) was included in all transfection experiments as a transfection efficiency control.

### 3.4 REPORTER GENE ASSAY

HEK-293 cells were transfected in triplicate with combined plasmid DNAs as follows: 0.5  $\mu\text{g}$  of WT or mutant h $\beta$ -catenin, 0.5  $\mu\text{g}$  of  $\beta$ -catenin reporter Gene (TOPFlash) (provided by Dr. Hans Clevers), 0.5  $\mu\text{g}$  of hTcf-4 construct (kind gift from Dr. Marc van de Wetering, Utrecht, The Netherlands) and 0.1  $\mu\text{g}$  of pSV- $\beta$ -galactosidase vector as an internal control. pcDNA1/amp plasmid DNA (Invitrogen) was added to complete the DNA quantity to 2  $\mu\text{g}$ . The transfected cells were incubated at humidified 37° C under 5% CO<sub>2</sub> for indicated time periods. At the time of harvesting, cells were washed twice with PBS and lysed for 15 minutes with the Reporter Lysis Buffer (RLB) (Promega) and harvested by scraping. The

lysates were cleared by centrifugation at 14,000 rpm for 5 minutes at 4° C. Cell lysates were either analyzed immediately or stored at -80 C for later analysis. The luciferase and  $\beta$ -galactosidase activities were measured using an Orion Microplate Luminometer (Berthold Detection systems) with the Bright-Glo Luciferase (Promega) and Galacto-Star (Tropix) assay systems, respectively. Luciferase activity was normalized to  $\beta$ -galactosidase activity and results were optimized as mean  $\pm$  SD.

### 3.5 SDS-PAGE ANALYSIS

Protein concentrations for total cell lysates were determined as described elsewhere (198). Protein (15~20  $\mu$ g) was subjected to SDS-PAGE using a 4~12% Bis-Tris Gel (Novex). The gels were run at 150 Volts for 1.5 hours. The protein was then transferred onto nitrocellulose membrane (Invitrogen) at 35 Volts for 1.5 hours. The nitrocellulose membranes were stained with either Coomassie Brilliant Blue R-250 (Fisher Biotech) or Amido Black staining solution (Sigma) for one minute to confirm protein equal loading and successful transfer. The nitrocellulose membrane was blocked with 2% of BSA in PBS for one hour and washed three times every five minutes with PBS-T. The membrane was first incubated overnight at 4° C with the indicated primary antibody, then washed every five minutes for 30 minutes with PBS-T and incubated with secondary antibody conjugated with horseradish peroxidase (Bio-Rad) for one hour. Finally, the membrane was developed for one minute using ECL reagents (Amersham). Membrane developing and Imaging analysis were by an AlphaImnotech photodocumentation system.

### 3.6 $\beta$ -CATENIN PHOSPHORYLATION ANALYSIS

Four different commercial anti- $\beta$ -catenin antibodies were used which recognize different phosphorylation status of  $\beta$ -catenin: (i) anti- $\beta$ -catenin monoclonal antibody (Transduction labs), which recognizes total  $\beta$ -catenin regardless of phosphorylation status; (ii) anti-p $\beta$ -catenin-41/45 (Cell Signaling Technology), a monoclonal antibody specific for either pThr-41, pSer-45, or both; (iii) anti-p $\beta$ -catenin 33/ 37/41 (Cell Signaling Technology), a monoclonal antibody that recognizes pSer-33, pSer-37, or pThr-41; (iv) anti-de-phospho- $\beta$ -catenin ( $\alpha$ ABC or  $\alpha$ -active  $\beta$ -catenin), a monoclonal antibody that recognizes  $\beta$ -catenin when it is non-phosphorylated at both Ser-37 and Thr-41 (provided by Dr. Hans Clevers). The optimal dilutions of these antibodies were: 1:500, 1:1000, 1:1000 and 1:100, respectively.

### 3.7 PURIFICATION OF GST TAGGED PROTEINS

*E. coli* strain BL21 was transformed with the appropriate prokaryotic expression plasmids and plated on agar plates containing 150  $\mu$ g/ml Ampicillin. The next day, single colonies were picked up to start 6 ml 2X YTA cultures containing 150  $\mu$ g/ml Ampicillin. The starter cultures were continuously shaken at 240 rpm overnight at 37 C. Approximately 5 ml of each starter culture were seeded into 300 ml of fresh 2X YTA culture containing 150  $\mu$ g/ml Ampicillin and were shaken at 300 rpm at 37 C. The bacterial growth was monitored closely and when the O.D. A600 of each culture was 0.4~0.6, the expression of GST-tagged proteins was induced by adding isopropyl- $\beta$ -D-thiogalactopyranoside (IPTG) to a final concentration of 1  $\mu$ M. After 3 hours, cells were collected by centrifugation for 10 min at 5000 rpm and the cell pellet was resuspended in 20 ml lysis buffer (10 mM

DTT/1mM PMSF/0.2mg/ml lysozyme) and incubated on ice for 30 min. Subsequently, 2.25 ml of 10% Triton X-100 in STE buffer (10 mM Tris-HCl, pH 8, 1 mM EDTA and 150 mM NaCl) were added followed by adding 225  $\mu$ l 1M MgCl<sub>2</sub> and 5  $\mu$ l DNase I and incubated for 30 min on ice. In the meantime, 50 % slurry of Glutathione Sepharose 4B was prepared by washing 2 ml of Glutathione Sepharose<sup>TM</sup> 4B (Amersham Pharmacia Biotech) with 50 ml ice-cold PBS twice. Glutathione Sepharose beads in PBS were spun down at 2500 rpm for 1 minute and the supernatant was removed carefully. The beads were resuspended in appropriate volume of PBS to give ~ 50 % slurry. Approximately 2 ml Glutathione Sepharose solution were added to the cell lysate and rocked gently at 4° C for 2 hours. The cell lysate/Glutathione Sepharose beads mixture was spun down at 2500 for one minute and the supernatant was removed. The beads pellet was washed carefully at least five times with ice-cold PBS followed by one time wash with PBS/10mMDTT/ 1% Triton X-100. The GST-tagged proteins were eluted by washing beads with 500  $\mu$ l elution buffer (50 mM Tris pH 9, 5 mM Glutathione). The eluted proteins were analyzed by SDS-PAGE followed by silver or coomassie blue staining and were quantitated by Bio-Rad Protein Assay (Bio-Rad) according to supplier instruction manual.

### 3.8 *IN VITRO* PHOSPHORYLATION ASSAY

A 30  $\mu$ l kinase reaction mixture was prepared freshly by combining 400 ng GST-rAxin, 400 ng of GST-GSK-3 $\beta$  and 200 ng of GST-WT or mutant  $\beta$ -catenin. The kinase reaction was initiated by adding 3  $\mu$ l of 10X kinase buffer (200 mM Tris-HCl pH 7.5, 100  $\mu$ M MgCl<sub>2</sub>, 50 mM DTT and 200  $\mu$ M ATP) and incubated at 30° C for four hours. The reaction was stopped by adding 7.5  $\mu$ l SDS sample buffer and was heated at 75° C for 10 minutes. kinase reaction cocktail (15  $\mu$ l ) was

analyzed on SDS-PAGE followed by immunoblotting with anti-p $\beta$ -catenin-33/37/41 antibodies.

### 3.9 MYC-TAG $\beta$ -CATENIN IMMUNOPRECIPITATION

WT or mutant myc-tag  $\beta$ -catenin plasmid DNA (2  $\mu$ g) were transfected into HEK-293 cells for 48 hours, and 20 hours before harvesting 100  $\mu$ M ALLN were added to induce accumulation of ubiquitinated  $\beta$ -catenin. After 48 hours, cells were washed twice with PBS and harvested by adding 500  $\mu$ l of ice-cold lysis buffer (20 mM Tris pH7.5, 150 mM NaCl, 1 mM EDTA, 1mM EGTA, 1% Triton X-100, 2.5 mM sodium pyrophosphate, 1mM  $\beta$ -glycerophosphate, 1 mM Na<sub>3</sub>VO<sub>4</sub>, 1 $\mu$ g /ml Leupeptin, 20 mM N- Ethylmaleimide (Sigma) and protease inhibitor cocktail (Roch Molecular Biochemicals)) for 5 minutes and were scraped into pre-chilled centrifuge tubes. To ensure complete lysis, cell lysate was incubated on ice for 15 minutes and vortexed vigorously every 5 minutes. The lysate was cleared by centrifugation at 14,000 rpm at 4° C for 10 minutes. The protein concentration was determined and approximately 300~400  $\mu$ g of total protein were used for Immunoprecipitation. The lysates were pre-cleared with 50  $\mu$ l of 50 % slurry Protein A Sepharose CL-4B (Amersham Pharmacia Biotech) for 30 min. The pre-cleared supernatant was recovered by centrifugation at 10,000 rpm for 2 minutes. The lysates were incubated with 10  $\mu$ l anti-myc tag (9B11) monoclonal antibody (Cell Signaling Technology Inc.) with gentle agitation at 4° C for 6 hours followed by adding 5  $\mu$ l of rabbit anti-mouse IgG (Sigma) for additional hour. Approximately, 50  $\mu$ l of 50 % slurry Protein A Sepharose CL-4B were added to the immune complex and were incubated for one hour at 4° C with gentle agitation. The Protein A Sepharose CL-4B was recovered by centrifugation at 10,000 rpm at

4° C and washed at least 5 times with ice-cold lysis buffer. The proteins were eluted from the Protein A Sepharose beads by adding 30 µl of 3X SDS sample buffer and boiled for 10 minutes. Proteins (15 µl) were analyzed by western blotting.

### 3.10 CELL CYCLE ANALYSIS

The cell cycle was examined by flow cytometry. HEK-293 cells were seeded at a density of  $1 \times 10^6$  on 60 mm poly-D-lysine-coated plates and grown overnight to 50~70% confluency. Cells were transfected in triplicate with 2 µg wild-type or mutant  $\beta$ -catenin, trypsinized at different time points and counted. Approximately  $1 \times 10^6$  cells were washed twice with PBS and fixed by dropping in 1 ml 70% ethanol while slowly vortexing the cell suspension. The cells were incubated in the dark at -20°C overnight. The fixed cells were pelleted by centrifugation at 5,000 rpm for 5 minutes and resuspended in 1 ml PBS containing 0.2 mg/ml propidium iodide (Sigma) and 0.15 µg/ml RNase and incubated at 37°C for 30 minutes in the dark. Cells were analysed by a fluorescent-activated cell sorter (FACS, Coulter). The distribution of cells within the cell cycle was analyzed using MultiCycle software.

The apoptotic cells were present as a Sub-G1 peak due to the fact that apoptosis induces DNA fragmentation. The small fragments of DNA can be eluted during PBS washing steps. Thus, after staining with a quantitative DNA-binding dye, cells that have lost DNA will take up less stain and will appear to the left of the G1 peak. To visualize apoptotic morphology, HEK-293 cells were washed with PBS and fixed in 1 ml ice-cold 70% ethanol for 20 minutes. The fixed cells were washed with PBS and stained with 0.1 % ethidium bromide in PBS for 5 minutes. The stained cells were washed twice with PBS and visualized under fluorescence microscope.

### 3.11 CASPASE-3 ACTIVITY

Caspase-3 activity was determined fluorometrically. HEK-293 cells were seeded at a density of  $1 \times 10^6$  on 60 mm poly-D-lysine-coated plates and grown overnight to 50~70% confluency. Afterward, cells were transfected in triplicate with 2  $\mu$ g WT or mutant  $\beta$ -catenin for 48 hours. Apoptosis was induced with 100  $\mu$ M ALLN or 500 STS (Sigma) for 20 hours. Cells were trypsinized, counted and approximately  $3 \times 10^6$  cells were washed twice with PBS and suspended in 300  $\mu$ l of lysis buffer (50 mM HEPES, pH 7.4; 100 mM NaCl; 0.1% CHAPS; 10 mM DTT; 1 mM EDTA and 10 % Glycerol). Cell suspension was passed through a 24 gauge needle 10 times to ensure complete lysis. Cell lysate was cleared by centrifugation at 14,000 rpm for 10 minutes at 4° C. The supernatant was recovered and the total protein concentration was determined by Lowry assay. Total protein was assayed in triplicate for caspase-3 activity as followed: 50  $\mu$ g of total protein was mixed with 10.36  $\mu$ M Ac-DEVD-AMC (Enzyme System Products) in a NUNC™ 96-well plate (Fisher Scientific). The total reaction volume (100  $\mu$ l) included assay buffer (50 mM HEPES, pH 7.4; 100 mM NaCl; 0.1 % CHAPS; 10 mM DTT; 1 mM EDTA and 10 % glycerol). The liberation rate of AMC was determined fluorometrically by Cytofluor® plate reader (Applied Biosystems). The emission at 460 nm after excitation at 380 nm was measured every minute for 30 minutes. The concentration of the liberated AMC was calculated by referencing to a fluorescence standard curve of free AMC.

To construct fluorescence standard curve, serial dilutions of AMC were prepared (0,10,15,20,25,30,35,40,50,60,80 and 100  $\mu$ M) in 100  $\mu$ l assay buffer. The AMC fluorometric emission was determined at 460 nm after excitation at 380 nm.



## 4 CHAPTER 4: RESULTS

### 4.1 ANALYSIS OF THE TRANSACTIVATION POTENTIAL OF WT AND MUTANT $\beta$ -CATENIN IN REPORTER ASSAYS

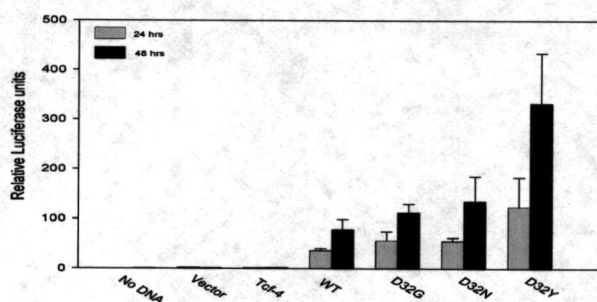
To test the hypothesis that substitution mutations at codon 32 of h $\beta$ -catenin lead to accumulation of transcriptionally active  $\beta$ -catenin in the absence of Wnt signaling stimuli, the transcriptional activation of WT or codon 32 mutant  $\beta$ -catenin was analyzed in reporter assays. In this experiment, HEK-293 cells were co-transfected in triplicate with  $\beta$ -catenin reporter plasmid (TOPFlash), WT or mutant  $\beta$ -catenin, and hTcf-4 expression plasmids as described under material and methods. After 24 and 48 hours, floating and attached cells were harvested and the luciferase reporter gene activity by the various  $\beta$ -catenin constructs was determined after normalization to  $\beta$ -galactosidase activity.

The results are presented in Figure 10. As early as 24 hours, the exogenous WT  $\beta$ -catenin already led to saturation of  $\beta$ -catenin degradation machinery resulting in > 100-fold significant increase in the luciferase activity in both floating and attached cells ( $P = 0.0007$  and  $P = 0.017$ ,  $n=3$  for floating and attached cells respectively compared to non-transfected cells). The same trend of significant transactivation compared to non-transfected cells was seen at 24 hours with D32G, D32N and D32Y  $\beta$ -catenin, however there were no significant differences between the transactivation by WT and mutant  $\beta$ -catenin at this time point (see Figure 10A, compare gray bars). However, at 48 hours, the luciferase activities of the mutants markedly increased compared to the wild type. There was a statistically significant increase in the luciferase activity in the attached cells, 3-fold, 4-fold and 5-fold for D32G, D32N and D32Y respectively relative to the WT ( $P$  values = 0.000006, 0.0028 and 0.0007 respectively,  $n=3$ ). Adding 30 mM LiCl, a potent inhibitor of

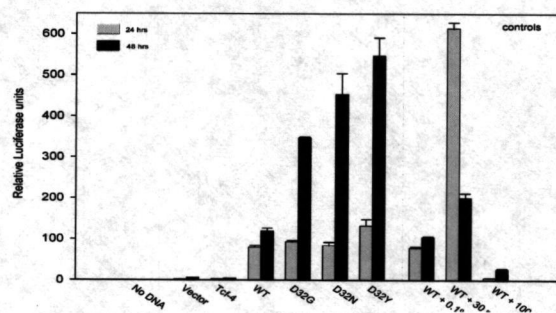
GSK-3 $\beta$  (199), to WT-transfected cells led to significant 7-fold and 2-fold induction in the luciferase activity at 24 and 48 hours respectively. However adding 100  $\mu$ M ALLN, a proteasome inhibitor, to WT-transfected cells led to decreased transcriptional activity, to basal levels (Figure 10B).

To determine whether the luciferase activities of various  $\beta$ -catenin cDNAs were correlated to the protein level, 20  $\mu$ g of each cell lysate at 48 hours was examined by Western blotting with anti- $\beta$ -catenin monoclonal antibodies (Transduction Labs). Densitometric analysis showed strong correlation between the reporter gene activities and  $\beta$ -catenin accumulation. Approximately 2-fold increase in the WT and up to 7-fold increase for D32G, D32N and D32Y was seen compared to non-transfected cells (Figure 10C, lanes 8, 9 and 10). The LiCl-treated cells showed up to 8-fold increase in  $\beta$ -catenin protein levels. In spite of their low transcriptional activity, cells treated with ALLN had substantial accumulation of  $\beta$ -catenin, which was characterized by the appearance of higher molecular weight poly ubiquitinated forms of  $\beta$ -catenin (Figure 10C, arrow in 6). Dimethyl Sulfoxide (DMSO), which was used to dissolve ALLN, did not alter the transactivations or protein accumulation (Figure 10B and 10C, lane 7).

## A) Floating cells



## B) Attached cells



## C) Western blots

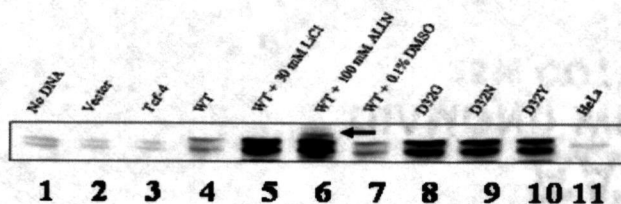


Figure 10: Transactivation potential of  $\beta$ -catenin in HEK-293 cells.

A) Reporter activity in floating cells or B) attached cells was measured after normalizing to  $\beta$ -galactosidase activity. C) HEK-293 cells were transfected with indicated  $\beta$ -catenin cDNA and the attached cells were harvested at 48 hours. Subsequently, cell lysates were analyzed by Western blotting with anti- $\beta$ -catenin antibody. As a control,  $\beta$ -catenin protein was induced as followed: cells were

transfected with WT  $\beta$ -catenin and treated with either 100  $\mu$ M ALLN, or 30 mM LiCl to inhibit the proteasome and GSK-3 $\beta$  activity, respectively.

#### 4.2 ANALYSIS OF THE PHOSPHORYLATION STATUS OF WT AND MUTANT $\beta$ -CATENIN BY WESTERN BLOTTING

To investigate the phosphorylation status of  $\beta$ -catenin, four different antibodies were used. Each antibody recognizes  $\beta$ -catenin when it has a specific phosphorylation status. As mentioned above, anti- $\beta$ -catenin antibody, which recognizes the total  $\beta$ -catenin, showed gross accumulation of mutated  $\beta$ -catenin protein (Figure 10C, lanes 8, 9 and 10). To test whether the accumulated  $\beta$ -catenin was phosphorylated at the critical residues adjacent to Asp-32 (Ser-33, Ser-37 and Thr-41), Western blot with anti-p $\beta$ -catenin-33/37/41 antibody was conducted. Results are shown in Figure 11. Surprisingly, both D32G and D32N  $\beta$ -catenin were strongly phosphorylated (Figure 11A, lanes 8 and 9). Densitometric analysis showed 5-fold and 3-fold induction of p $\beta$ -catenin in D32G and D32N respectively compared to WT and D32Y  $\beta$ -catenin. The signal was very weak for WT  $\beta$ -catenin, which implies a rapid turnover of WT p $\beta$ -catenin under normal circumstances. In contrast, the accumulated D32Y  $\beta$ -catenin was poorly phosphorylated, presumably because the bulky side-chain interferes with adjacent Ser-33.

Although LiCl reportedly is a strong inhibitor of  $\beta$ -catenin phosphorylation (165), HEK-293 cells transfected with WT  $\beta$ -catenin and treated with 30 mM LiCl for 20 hours showed a signal for phosphorylated  $\beta$ -catenin (Figure 11A, lane 5). This was accompanied by reduction in the reporter activity after 48 hours compared to that at 24 hours (Figure 10B). These observations imply that, as cells started to deplete LiCl, GSK-3 $\beta$  rapidly phosphorylates WT  $\beta$ -catenin in a manner that saturates the ubiquitination and degradation machinery. In addition, the p $\beta$ -catenin in cells treated with LiCl lack the higher molecular weight bands, which indicates

that the accumulated p $\beta$ -catenin is saturating the ubiquitination machinery and when p $\beta$ -catenin is ubiquitinated, it is highly instable.

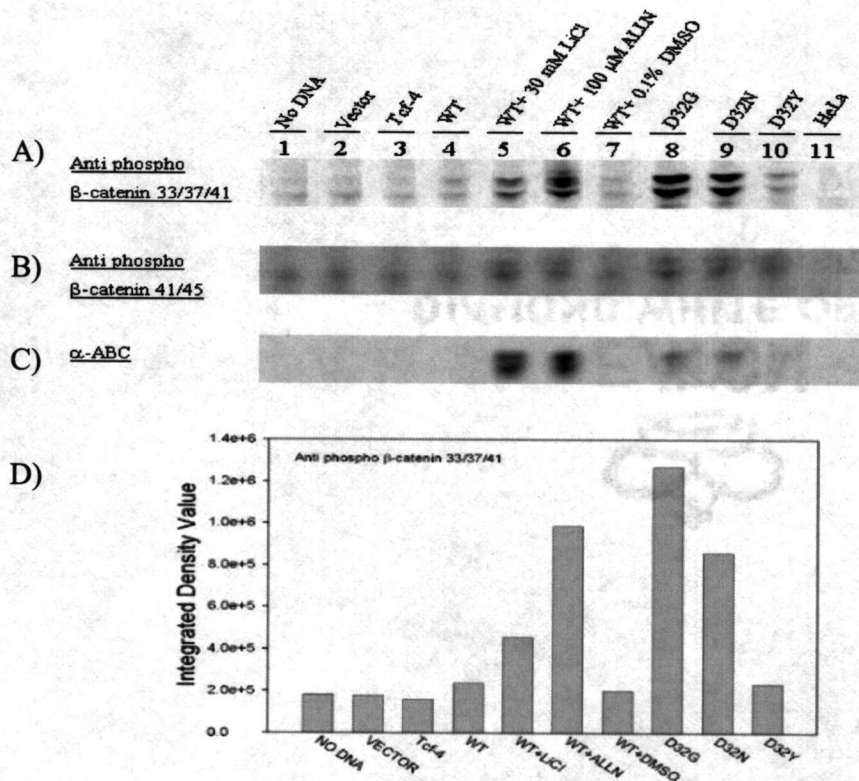


Figure 11: Phosphorylation status of  $\beta$ -catenin.

HEK-293 cells were transfected with WT or mutant  $\beta$ -catenin for 48 hours, and 20  $\mu$ g of total cell lysates were assayed for p $\beta$ -catenin with different  $\beta$ -catenin phospho-specific antibodies. A) Anti-p $\beta$ -catenin-33/37/41; B) Anti-p $\beta$ -catenin-41/45; C)  $\alpha$ ABC (anti-de-phospho- $\beta$ -catenin-37/41). D) Densitometric analysis of blot A.

Next, the phosphorylation status of  $\beta$ -catenin was investigated at slightly more distant from codon 32, namely, Thr-41 and Ser-45. For this purpose, Western blot with anti-p $\beta$ -catenin-41/45 was performed. This antibody is highly specific to

$\beta$ -catenin when it is phosphorylated at either Thr-41 or Ser-45. Results showed that both Thr-41 and Ser-45 residues were phosphorylated to the same extent in all mutant  $\beta$ -catenins (Figure 11B, lanes 8, 9 and 10). In addition, it is noteworthy that LiCl and ALLN did not affect the phosphorylation status of  $\beta$ -catenin at Thr-41 and Ser-45 (Figure 11B, lanes 5 and 6). This observation is in agreement with the new finding that Ser-45 is not a direct substrate for GSK-3 $\beta$ , thus inhibition by LiCl of GSK-3 $\beta$  should have no or minimal effect on Ser-45 phosphorylation.

The dephosphorylation condition of  $\beta$ -catenin was studied next by immunoblotting with  $\alpha$ ABC antibody. This antibody is very specific to  $\beta$ -catenin when it is not phosphorylated at both Thr-41 and Ser-37 (166). As shown in Figure 11C, weak bands were observed for D32G and D32N which indicate minimal dephosphorylation (lanes 8 and 9). However, this antibody could not detect D32Y (lane 10), which, with previous observation that D32Y is not phosphorylated at Ser-37, implies that D32Y is permanently phosphorylated at Thr-41 and is not accessible for dephosphorylation (Figure 11C, lanes 8, 9 and 10). Surprisingly, cells transfected with WT  $\beta$ -catenin and treated with ALLN showed a strong signal that lacks the higher molecular weight bands (Figure 11C, lane 6). This observation suggested that  $\beta$ -catenin is dephosphorylated before ubiquitination or de-ubiquitinated and de-phosphorylated simultaneously. In addition, D32G, D32N and D32Y mutations seem to interfere to different extents with dephosphorylation and de-ubiquitination events resulting in less or no dephosphorylation.

It has been shown that  $\beta$ -catenin is significantly phosphorylated by GSK-3 $\beta$  in the presence of Axin *in vitro* (163). Therefore, to confirm that D32G and D32N but not D32Y are susceptible to phosphorylation by GSK-3 $\beta$ , an *in vitro* kinase assay of GST-GSK-3 $\beta$  was conducted using various GST- $\beta$ -catenin recombinant proteins as substrates. For this experiment, recombinant GST- $\beta$ -catenin, GST-GSK-3 $\beta$  and GST-rAxin were purified from *E.coli* by Glutathione S-transferase (GST) gene fusion system. The kinase reactions were conducted in the presence



and absence of 200  $\mu$ M ATP and analyzed by Western blotting with anti-p $\beta$ -catenin-33/37/41 antibody. The results are shown in Figure 12. Both WT and mutant  $\beta$ -catenin D32G and D32N were susceptible to phosphorylation in the presence of ATP. However, phosphorylation was attenuated in D32Y (3-fold reduction) and  $\Delta$ 45  $\beta$ -catenin (5-fold reduction) compared to the WT  $\beta$ -catenin. The marked reduction in the phosphorylation of  $\Delta$ 45  $\beta$ -catenin is in agreement with recent findings that priming of codon 45 of  $\beta$ -catenin is required for subsequent phosphorylation of  $\beta$ -catenin by GSK-3 $\beta$  *in vivo* (161).

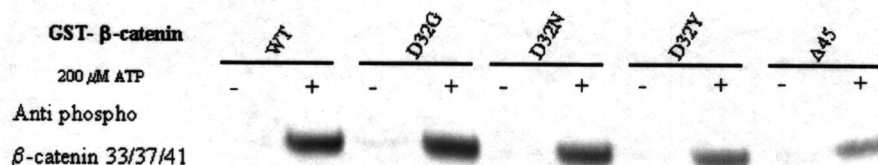


Figure 12: *In vitro* phosphorylation of  $\beta$ -catenin by GSK-3 $\beta$ .

GST- $\beta$ -catenin, GST-rAxin and GST-GSK-3 $\beta$  recombinant proteins were purified by Glutathione S-transferase gene fusion system. The *in vitro* phosphorylation assay of  $\beta$ -catenin was conducted as described under material and methods. The kinase reaction mixture was analyzed by Immunoblotting with anti-p $\beta$ -catenin-33/37/41.

#### 4.3 THE UBIQUITINATION STATUS OF WT AND MUTANT $\beta$ -CATENIN

After establishing that D32G and D32N are susceptible to phosphorylation, the next hypothesis was that the ubiquitination of these two mutants was abrogated. It is well established that phosphorylation of  $\beta$ -catenin is a preceding and obligatory step to ubiquitination. Once  $\beta$ -catenin is phosphorylated, it is quickly ubiquitinated and degraded by proteasome. One of the hallmarks of  $\beta$ -catenin ubiquitination is the appearance of slower migrating bands after Western blot

analysis in the presence of proteasome inhibitors such as ALLN (6). These bands represent the poly-ubiquitinated  $\beta$ -catenin.

Thus, HEK-293 cells were co-transfected in triplicate with 0.5  $\mu$ g of WT or mutant  $\beta$ -catenin plasmid DNA, 0.5  $\mu$ g of TOPFlash and 0.5  $\mu$ g of Tcf-4. Twenty hours prior to harvesting, cells were treated with 100  $\mu$ M ALLN and harvested 48 hours later. The transactivation by various  $\beta$ -catenins was confirmed by the reporter gene assay (Figure 13A). Subsequently, total protein concentration was determined and 20  $\mu$ g of total protein were analyzed by Western blotting with anti  $\beta$ -catenin monoclonal antibody. In the presence of the proteasome inhibitor ALLN, only WT  $\beta$ -catenin showed higher molecular weight bands (see Figure 11A, lane 6 and Figure 13B, lane 5 arrow). However, the ubiquitinated  $\beta$ -catenin band was absent in D32G and D32N, although they were strongly phosphorylated. These observations suggest that all codon 32 mutants  $\beta$ -catenin were not ubiquitinated, regardless of their phosphorylation status.

In addition, ALLN strongly induced the phosphorylation of WT  $\beta$ -catenin (Figure 13C and D, compare lanes 4 and 5), but not of any of the mutants (Figure 13C and D, lanes 6 to 11). Furthermore, the accumulated  $\beta$ -catenin underwent significant dephosphorylation in WT, D32G and D32N (Figure 12D, lanes 4 to 9). However, in agreement with the previous results, an apparent dephosphorylation occurred in D32Y, perhaps due to the presence of low endogenous  $\beta$ -catenin in these cells (Figure 13D, lanes 10 and 11). This suggested the need to distinguish exogenous from endogenous  $\beta$ -catenin.



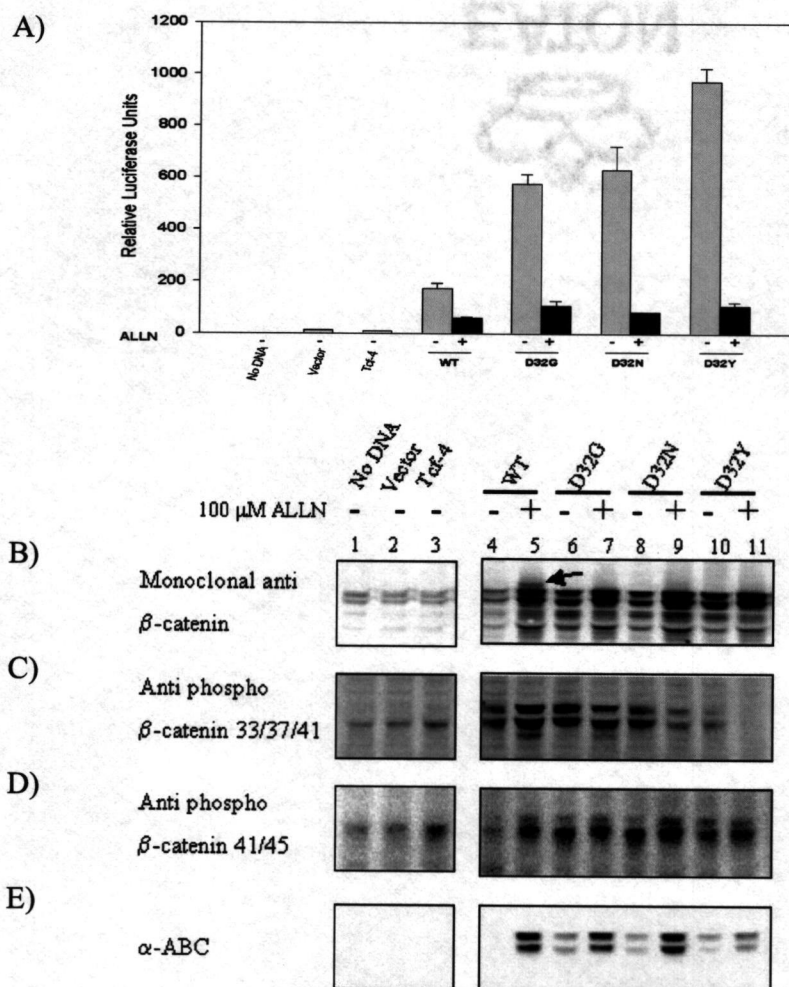


Figure 13: Effects of ALLN on  $\beta$ -catenin transactivation and stability. Sub-confluent HEK-293 cells were co-transfected with 0.5  $\mu$ g of WT or mutant  $\beta$ -catenin, 0.5  $\mu$ g TOPFlash and 0.5  $\mu$ g hTcf-4 for 48 hours. ALLN (100  $\mu$ M) was used to induce  $\beta$ -catenin accumulation for 20 hours. A) Luciferase reporter gene activity by various  $\beta$ -catenin in the presence and absence of ALLN after normalizing to  $\beta$ -galactosidase. Total protein (20  $\mu$ g) was analyzed by Western blotting and probed with the indicated antibodies in panels B, C, D and E.

#### 4.4 ANALYSIS OF THE UBIQUITINATION STATUS OF EXOGENOUS WT AND MUTANT $\beta$ -CATENIN BY WESTERN BLOTTING.

To rule out the possible involvement of endogenous  $\beta$ -catenin in the phosphorylation and ubiquitination assays and to further confirm that various mutant  $\beta$ -catenin are not ubiquitinated, ALLN was tested against exogenous  $\beta$ -catenin. If mutant  $\beta$ -catenin is not ubiquitinated, then ALLN should have no effect on protein levels. For this experiment, HEK-293 cells were transfected with 2  $\mu$ g of either WT or mutant  $\beta$ -catenin. Ten hours prior to harvesting, cells were subjected to 50  $\mu$ M ALLN. At 48 hours, cells were harvested and 20  $\mu$ g protein was assayed by Western blotting with anti- $\beta$ -catenin antibody, which recognizes total  $\beta$ -catenin (exogenous and endogenous) and with anti-myc tag antibody, which recognized only the transfected  $\beta$ -catenin. Results are shown in Figure 14A and B. ALLN treatment resulted in  $\sim$ 10 times induction in exogenous WT  $\beta$ -catenin. However, mutant  $\beta$ -catenin which already  $\sim$  50-fold higher than the WT, responded no further to ALLN. These results further imply that D32G, D32N and D32Y are not ubiquitinated. Discrete higher molecular weight band were only seen for WT, after ALLN treatment.

#### 4.5 IMMUNOPRECIPITATION OF EXOGENOUS WT AND MUTANT $\beta$ -CATENIN

To test whether the slower migrating bands observed after ALLN treatment were exclusively due to  $\beta$ -catenin ubiquitination, HEK-293 cells were transfected with 2  $\mu$ g WT or mutant  $\beta$ -catenin. Twenty hours prior to harvesting, cells were treated with 100  $\mu$ M ALLN and harvested after 48 hours from the start of transfection. Approximately 300  $\mu$ g protein were used for immunoprecipitation with anti-myc tag antibody. The immunoprecipitated  $\beta$ -catenin was analysed by

Western blotting and detected with either anti-myc tag (Cell signaling technology) or anti-ubiquitin body (PharMingen). As illustrated in Figure 15, using anti-myc antibody only WT  $\beta$ -catenin was characterized with the higher molecular weight band (left panel, 1<sup>st</sup> lane). This band was not present in mutants (left panel, lanes 3,4 and 5). Further analysis of the immunoprecipitated  $\beta$ -catenin with anti-ubiquitin antibody showed no ubiquitination for D32Y (Figure 15, right panel, lane 4) and 2-fold reduced ubiquitination for D32NG and D32N compared to WT (arrow). These results confirmed that the slower migrating band in previous blots represents poly ubiquitinated exogenous  $\beta$ -catenin.

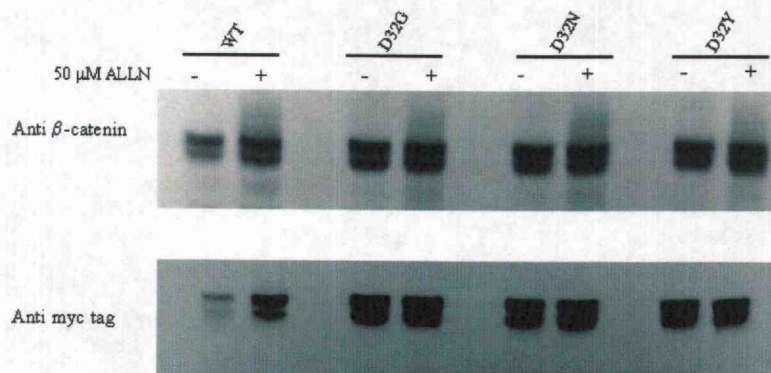


Figure 14: Effects of ALLN on total and exogenous  $\beta$ -catenin  
HEK-293 cells were transfected with 2  $\mu$ g of WT or mutant  $\beta$ -catenin; 50  $\mu$ M of ALLN was used to induce mild  $\beta$ -catenin accumulation for 10 hours. Cells were harvested after 48 hours and total protein concentration was determined by Lowry assay. 20  $\mu$ g of total protein was analyzed with Western blotting and probed with A) anti- $\beta$ -catenin antibody or B) anti-myc tag antibody.



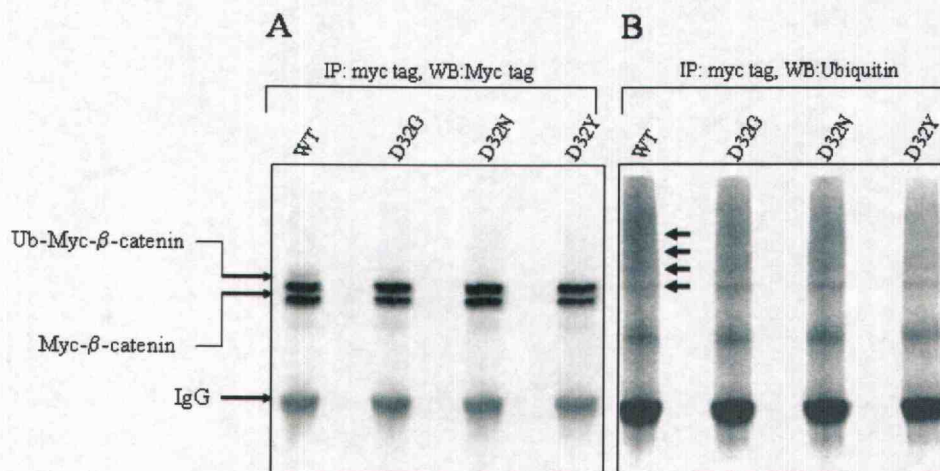


Figure 15: Immunoprecipitation of  $\beta$ -catenin

$\beta$ -catenin was immunoprecipitated from 300  $\mu$ g of total protein from HEK-cells transfected with WT or mutant  $\beta$ -catenin and treated with 100  $\mu$ M ALLN 10 hours prior harvesting. The purified  $\beta$ -catenin was detected with A) anti-myc tag antibody or B) anti-ubiquitin antibody. Arrows show positions of ubiquitinated  $\beta$ -catenin bands.

#### 4.6 COMPARISON BETWEEN D32Y, S33Y AND $\Delta$ 45 $\beta$ -CATENIN TRANSACTIVATION AND PROTEIN ACCUMULATION

Having established that D32Y  $\beta$ -catenin is not phosphorylated or ubiquitinated, the transactivation potential was compared to S33Y and  $\Delta$ 45  $\beta$ -catenin, which are well-characterized mutants (5) HEK-293 cells were co-transfected in triplicate with 0.5  $\mu$ g WT or mutant  $\beta$ -catenin (D32G, D32N, D32Y, S33Y and  $\Delta$ 45), 0.5  $\mu$ g TOPFlash and 0.5  $\mu$ g hTcf-4 plasmid DNA. As a control, cells were treated with 100  $\mu$ M ALLN 20 hours prior to harvesting, and harvested 48 hours from transfection.

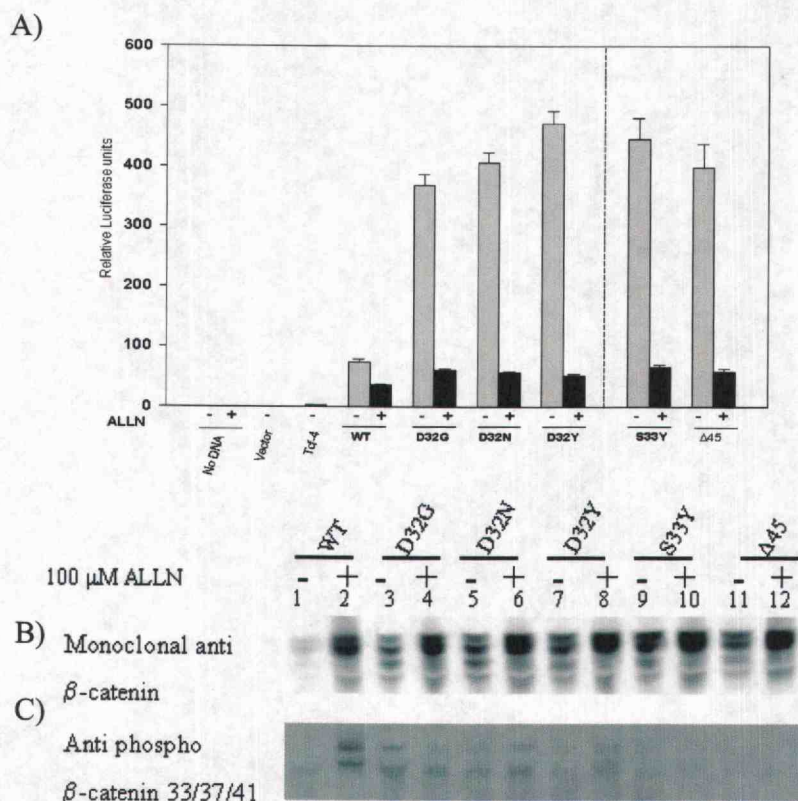


Figure 16: D32Y, S33Y and  $\Delta$ 45  $\beta$ -catenin are functionally equivalent in reporter assays. HEK-293 cells were co-transfected with 0.5  $\mu$ g of various  $\beta$ -catenin, 0.5  $\mu$ g TOPFlash and 0.5  $\mu$ g of hTcf-4. Cells were treated with 100  $\mu$ M ALLN 20 hours before harvesting to inhibit proteasome activity. Cells were harvested after 48 hours of transfection. A) The luciferase reporter gene activity by various  $\beta$ -catenins. B) 20  $\mu$ g of total protein was analyzed by Western blotting with anti- $\beta$ -catenin C) The same lysates were analyzed with anti-p $\beta$ -catenin-33/37/41.

As shown in Figure 16A, the transactivation potential of codon 32 mutant  $\beta$ -catenins were comparable to that of S33Y and  $\Delta$ 45  $\beta$ -catenin (compare gray bars in Figure 16A). However, ALLN suppressed all  $\beta$ -catenin reporter activities to basal levels, regardless of mutation type. Additionally, the same trend of protein accumulation was observed with both S33Y and  $\Delta$ 45  $\beta$ -catenin compared to D32Y

$\beta$ -catenin (Figure 16B, lanes 7 to 12). Moreover, the phosphorylation pattern of D32Y was comparable to S33Y (Figure 16C, compare lane 7 to 9 and lane 8 to 10), however, phosphorylation of  $\Delta 45$   $\beta$ -catenin was completely absent even, in the presence of ALLN (Figure 16C, lanes 11 and 12.)

#### 4.7 THE EFFECTS OF THE PROTEASOMES INHIBITOR ALLN ON $\beta$ -CATENIN TRANSACTIVATION.

It was intriguing that the proteasomes inhibitor ALLN dramatically suppressed the transcriptional activity independent of  $\beta$ -catenin phosphorylation and ubiquitination status. Additionally, it has been reported that proteasomes inhibitors induced caspase-dependent apoptosis in human cells (200, 201). On the other hand, it has been shown that  $\beta$ -catenin was proteolytically processed during apoptosis and the resultant proteolytic fragments lacked the transactivation capability. Published data have shown that  $\beta$ -catenin can be cleaved by caspase-3 at two C-terminal sites and three N-terminal sites. Interestingly, one of the putative caspase-3 recognition sites is localized at codon 32, the exact position where many mutations occur in CRC (179). Based on these observations, the hypothesis was tested that the WT and codon 32 mutant  $\beta$ -catenin is fully and partially proteolytically degraded, respectively upon ALLN-induced apoptosis and that the truncated fragment (armadillo region) competes with full-length  $\beta$ -catenin for binding Tcf-4.

To test this hypothesis, HEK-293 cells were transfected with 0.5  $\mu$ g WT or mutant  $\beta$ -catenin for 48 hours and treated with 100  $\mu$ M ALLN overnight. At the time of harvesting, cells were fixed and stained with the DNA-binding fluorochrome (ethidium bromide) to detect apoptotic morphology. Fluorometric microscopy analysis of stained cells showed condensed chromatin and fragmented nuclei. In addition, the remaining attached cells were characterized by shrunken

and rounded cell bodies under light microscopy, indicating apoptosis (Figure 17).

Next, caspase-3 activation was detected by Western blotting with anti-poly (ADP-ribose) polymerase (PARP) antibody (BD Biosciences). PARP, which is involved in the base excision repair machinery (BER), is a downstream substrate of active caspase-3 (202). During apoptosis, caspase-3 inactivates PARP by cleaving it into 86 kDa and 24 kDa fragments. As shown in Figure 18, caspase-3 was capable of processing PARP in all samples. The caspase-3 dependent cleavage of PARP also was seen, but to less extent, with 500 nM STS, which is a relatively non-selective kinase inhibitor that induces apoptosis in HEK-293 (203). These results suggested that ALLN is a strong inducer of caspase-3-dependent apoptosis at 100  $\mu$ M concentration. In addition, these results ruled out the possibility that  $\beta$ -catenin proteolytic fragment between codon 1 and codon 83, which harbor mutated motif (T<sub>29</sub>Q<sub>30</sub>F<sub>31</sub>X<sub>32</sub>) could inhibit caspase-3 activity.

Subsequent experiments tested whether the ALLN-dependent decline of  $\beta$ -catenin transactivation (Figure 16) was due to caspase-3 activation. In this instance, HEK-293 cells were co-transfected with 0.5 $\mu$ g of WT or D32Y  $\beta$ -catenin, TOPFlash and hTcf-4. Twenty hours before harvesting, cells were treated with 100  $\mu$ M ALLN or co-treated with ALLN and 40  $\mu$ M Z-VAD-FMK (Enzyme system products), which is a potent inhibitor of caspase-3. At the time of harvesting, HEK-293 cells co-treated with ALLN and Z-VAD-FMK exhibited normal morphology and fewer floating cells. In addition, the apoptosis morphology associated with ALLN treatment was abrogated when Z-VAD-FMK was included in the assay (Figure 17). However, the luciferase reporter gene activity was drastically lowered in ALLN treated cells and inhibition of caspase-3 did not restore the reporter gene activity (Figure 20).

To ensure complete inhibition of caspase-3 by Z-VAD-FMK, the same cell lysates from the previous experiment were used for Western blotting with anti-PARP antibody. Results from this experiment are shown in Figure 20. Although ALLN strongly induced apoptosis (lanes 3 and 8), adding Z-VAD-FMK effectively



inhibited PARP cleavage (lanes 4 and 9). These results imply that ALLN strongly inhibits  $\beta$ -catenin transactivation potential by a mechanism other than caspase-3 dependent degradation of  $\beta$ -catenin.

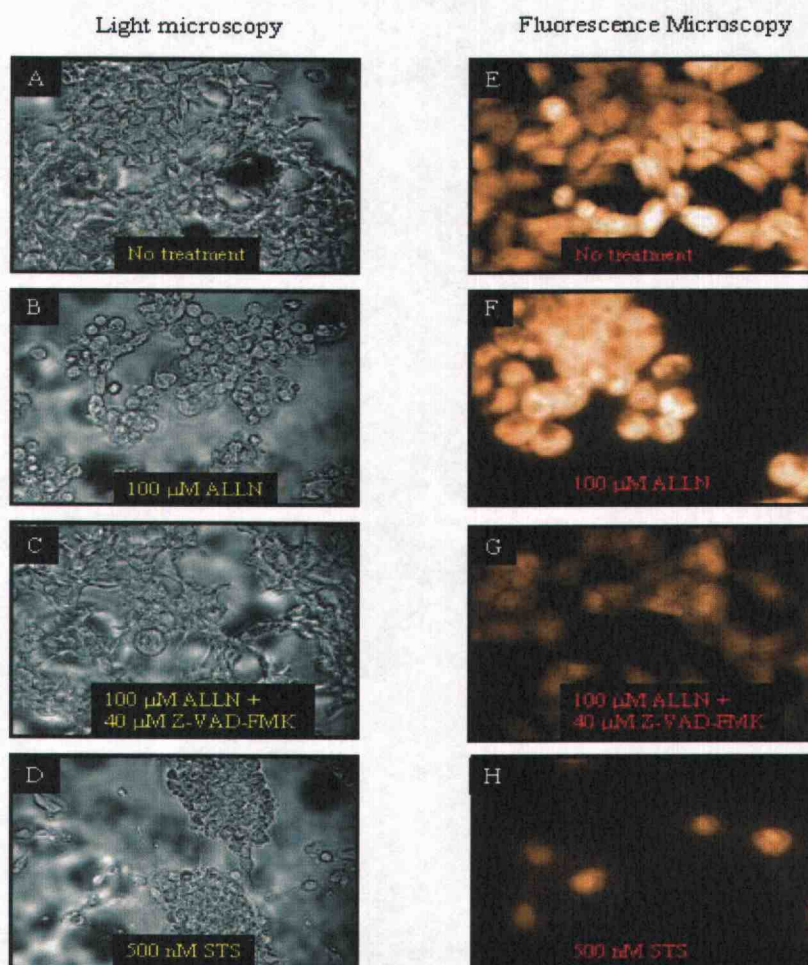


Figure 17: Apoptotic morphology of HEK-293 cells treated with ALLN or STS. HEK-293 cells were transfected with appropriate  $\beta$ -catenin and treated 100  $\mu$ M ALLN, 500 nM STS or 100  $\mu$ M ALLN plus 40  $\mu$ M Z-VAD-FMK. The cells morphology was examined under light microscopy (left panel). Apoptotic cells were detected under fluorescence microscopy after staining with ethidium bromide (right panel).



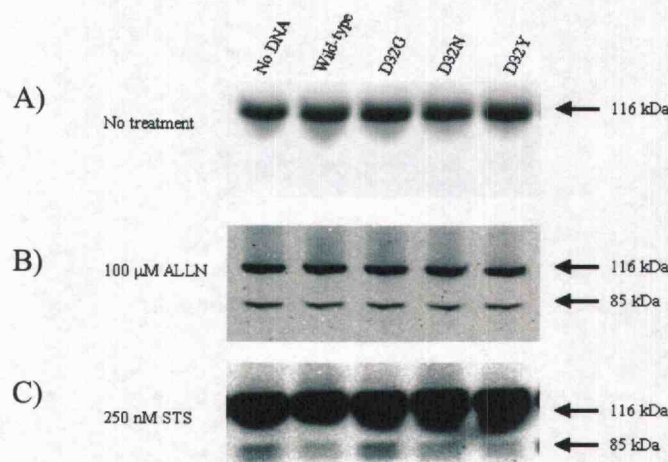


Figure 18: ALLN induces apoptosis in HEK-293 cells.

The cleavage of PARP was assayed by Western blotting with anti-PARP in HEK-293 cells transfected with various  $\beta$ -catenin constructs and treated with either 100  $\mu$ M ALLN or 250 nM STS. A) PARP was active in cells only transfected with various  $\beta$ -catenin cDNA. B) ALLN strongly induced PARP cleavage. C) STS, which is a common apoptosis inducer, modestly induced apoptosis at 250 nM concentration.

#### 4.8 ANALYSIS OF THE EFFECTS OF OVER-EXPRESSION OF $\beta$ -CATENIN ON CELL CYCLE AND APOPTOSIS.

It has been reported that over-expression of  $\beta$ -catenin in MDCK cells altered the cell cycle and stimulated cell proliferation (204). In addition, it has been shown that constitutive  $\beta$ -catenin signaling inhibited apoptosis (175). Consequently, experiments next tested the effect of constitutive expression of WT and mutant  $\beta$ -catenin on apoptosis and cell cycle in HEK-293 cell line.

To determine the effect of over-expression of  $\beta$ -catenin on HEK-293 cell cycle parameters, HEK-293 cells were transfected at 50 % confluency with 2  $\mu$ g WT or mutant  $\beta$ -catenin. The changes in cell cycle were monitored by flow cytometry at 6, 12, 24, 48 and 72 hours. Representative results are shown in Figure

21. The transfected HEK-293 displayed normal cell cycle pattern up-to 72 hours (Figure 21, left panel). In addition, Western blot analysis with antibodies to c-jun (and cyclin D1, not shown), which are target genes of  $\beta$ -catenin involved in cell cycle regulation, showed no changes in protein levels under these circumstances (Figure 22)

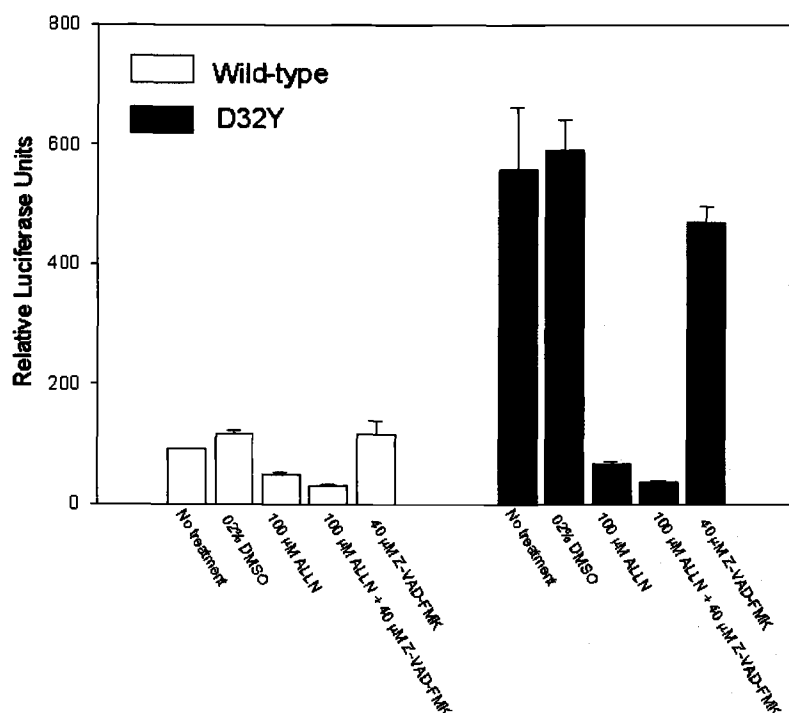


Figure 19: ALLN decreases the transactivation capacity of  $\beta$ -catenin. HEK-293 cells were transfected with WT or D32Y  $\beta$ -catenin and treated with either 100  $\mu$ M ALLN, 40  $\mu$ M Z-VAD-FMK or both for 20 hours. Subsequently, the luciferase reporter activity was determined after normalizing to  $\beta$ -galactosidase activity. Results are expressed as mean  $\pm$  SD, n=3.

Further experiments tested the effect of over-expression of  $\beta$ -catenin on apoptosis in HEK-293 cells. It has been reported elsewhere that HEK-293 cells responded to 250 nM STS treatment and 70 % of the HEK -293 cell population underwent apoptosis over 24 hours incubation time (203) it was shown above that transfecting HEK-293 cell with WT or mutant  $\beta$ -catenin did not hinder caspase-3-dependent PARP cleavage (Figure 18 and Figure 20). Thus, next experiments sought to further explore the effect of over-expression of various  $\beta$ -catenins on HEK-293 cell cycle parameters and apoptosis rate with a more sensitive method.

Apoptosis was induced in transfected HEK-293 cells with 250 nM STS for 24 hours and cells were collected after 72 hours of transfection. Cells were analyzed for apoptosis by flow cytometry using the Sub-G1 peak method for three independent treatments, as described under material and methods. Results are illustrated in Figure 21 (right panel) and Figure 23. STS induced apoptosis, which was preceded by accumulation of cells in the G2/M phase of the cell division cycle (Figure 21, right panel), however, the number of apoptotic cells was reduced by 2-fold in cells transfected with WT or mutant  $\beta$ -catenin compared to control non-transfected cells (Figure 23). There were no statistical differences seen, however, among various  $\beta$ -catenin.

Because over-expression of  $\beta$ -catenin showed modest anti-apoptotic effects in HEK-293 cells, the possible anti-apoptotic effects of  $\beta$ -catenin over-expression on caspase-3 activity were studied. For this purpose, HEK-293 cells were transfected with WT or mutant  $\beta$ -catenin for 48 hours. Twenty-four hours prior to harvesting, apoptosis was induced by 100  $\mu$ M ALLN. Cells were collected and caspase-3 activity was determined fluorometrically as described under material and methods. Caspase-3 activity was reduced in response to  $\beta$ -catenin over-expression compared to non transfected cells (Figure 24).

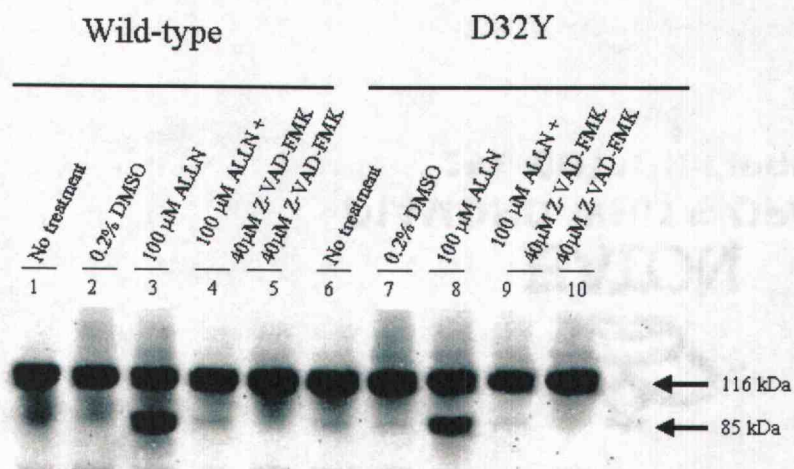


Figure 20: Inhibition of caspase-3 by Z-VAD-FMK.

To confirm the inhibitory effect of Z-VAD-FMK on caspase-3, HEK-293 cells were transfected with either WT or D32Y  $\beta$ -catenin. Twenty hours before harvesting, cells were treated with 100  $\mu$ M ALLN to induce apoptosis or co-treated with 100  $\mu$ M ALLN plus 40  $\mu$ M Z-VAD-FMK to inhibit caspase -3 activity. Inhibition of caspase-3 activity was confirmed by Western blot with anti-PARP.



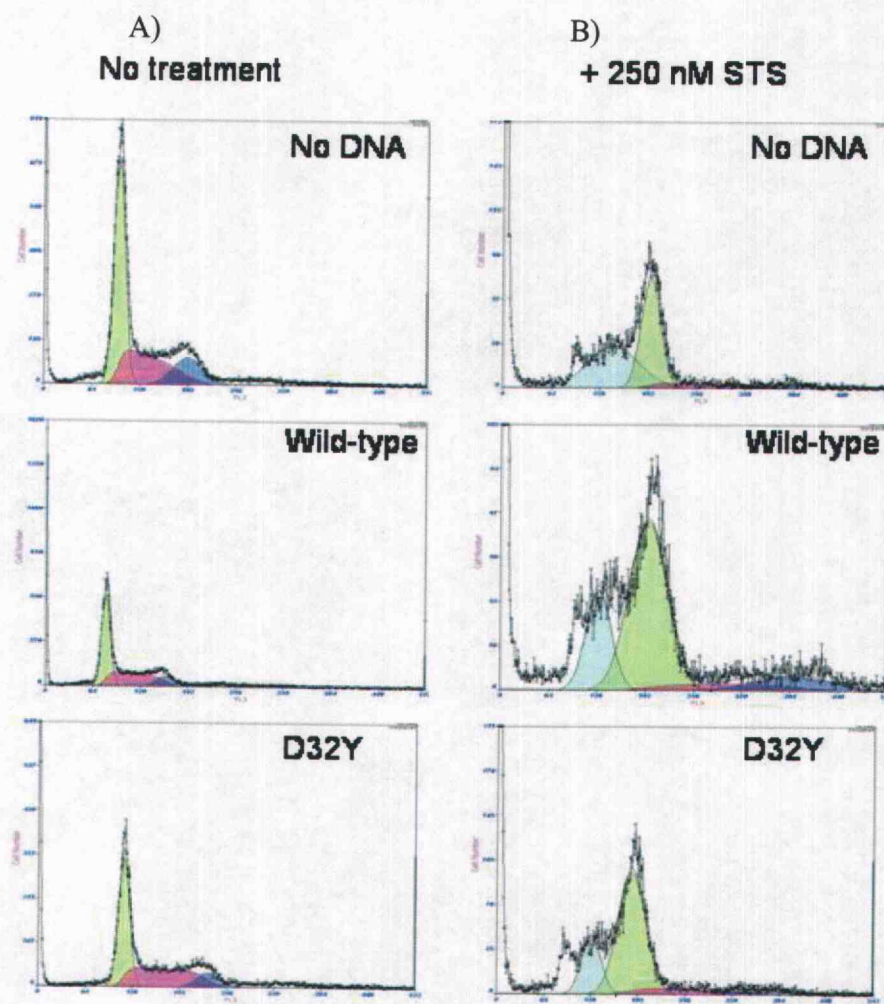


Figure 21: Effect of constitutive  $\beta$ -catenin over-expression on cell cycle kinetics and apoptosis.

HEK-293 cells over-expressing different  $\beta$ -catenins were analyzed for their cell cycle and anti-apoptotic potential. A) Cell cycle analysis by flow cytometry of HEK-293 cells over-expressing indicated  $\beta$ -catenin. B) Repeat of (A) but with STS, an apoptosis-inducing agent.

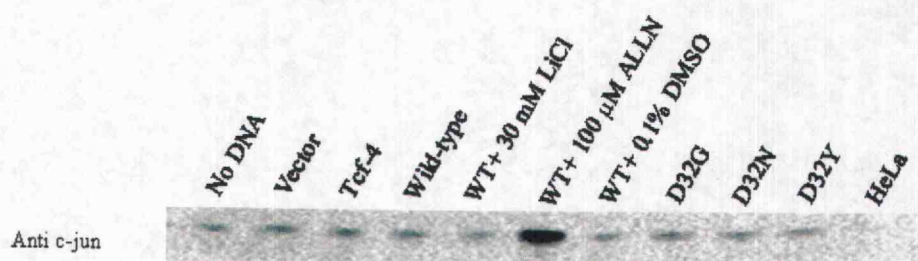


Figure 22: Effects of  $\beta$ -catenin over-expression on c-jun activation. HEK-293 cell overexpressing various  $\beta$ -catenin were analyzed for their level of c-jun protein, which is upregulated by active Wnt signaling in many cancer cell lines. Twenty  $\mu$ g of total protein lysate were analyzed by Western blotting with anti-c-jun antibody.

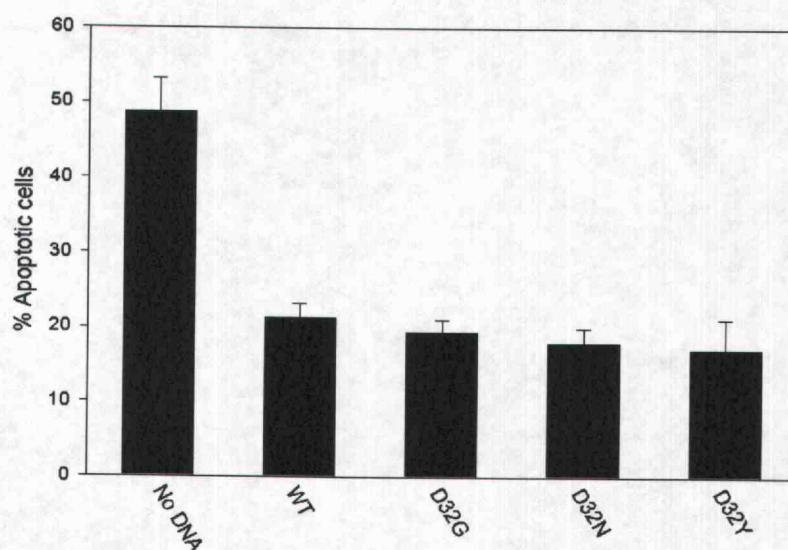


Figure 23: Anti-apoptosis effect of various  $\beta$ -catenin in HEK-293 cells. Apoptosis was induced in HEK-293-transfected with WT or mutant  $\beta$ -catenin by 250 nM STS for 24 hours. Cells were collected and apoptotic cell population was determined by Sub-G1 peak method (FACS analysis) for three independent treatments. Subsequently, the percentage of apoptotic cells was calculated in reference to total number of cells analyzed. Results are presented as mean  $\pm$  SD.

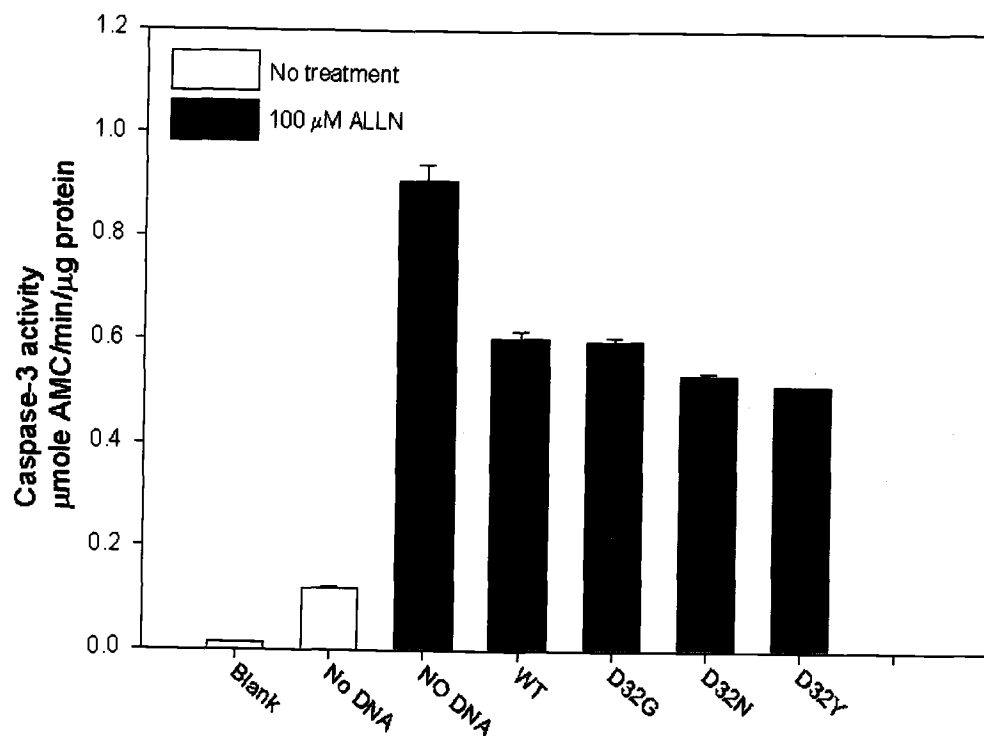


Figure 24: Anti-caspase-3 effects of  $\beta$ -catenins over-expression. Apoptosis was induced in HEK-293 cells, which expressed high levels of various  $\beta$ -catenins. The caspase-3 activity was assessed by measuring the liberation of AMC. Results were normalized to fluorometric standard curve and presented as mean  $\pm$  SD.

## 5 CHAPTER 5: DISCUSSION

It is well-reported in the literature that the majority of mutations in human colon tumors occur in *APC*. In contrast,  $\beta$ -catenin mutations are quite rare in HCRC, and when they occur, they tend to substitute or delete Ser-45 (Figure 6). In contrast, mutations from rodent colon tumors occur predominantly in  $\beta$ -catenin. Surprisingly, the pattern of mutations in the carcinogen-induced rat and mice tumors is different from that observed in human tumors (Figure 8). Previously published study from this laboratory has demonstrated that post-initiation exposure to phytochemicals such as chlorophyllin could shift the spectrum of  $\beta$ -catenin mutations in carcinogen-induced rat tumors. Most of the mutations observed clustered around Ser-33, particularly at Asp-32 (Figure 25) (9). The obvious difference in the distribution of  $\beta$ -catenin mutation in human and animal colon tumors is intriguing. Because of the complexity and diversity of human diet compared to experimental animal diet, which is usually restricted, one might argue that the doses and types of carcinogens used in several experimental studies are irrelevant to humans. It could be that the carcinogens or their metabolic intermediates that are responsible for  $\beta$ -catenin mutations in animals are neutralized by other components of human diet. Another explanation could be that these unusual mutations do indeed occur in human colon, however, they are insufficient to alter  $\beta$ -catenin transcriptional potential. Thus, although some cells harbor these mutations, they exhibit normal  $\beta$ -catenin-mediated signaling and therefore, do not transform into malignant derivatives. The present investigation has shown that substitution mutations at codon 32 of  $\beta$ -catenin are sufficient to stabilize  $\beta$ -catenin. Furthermore, the stabilized  $\beta$ -catenin was transcriptionally active and mimicked the action of mutated  $\beta$ -catenin at Ser-33 or Ser-45.



Figure 25:  $\beta$ -catenin mutation spectrum in carcinogen-induced rat colon tumors.  $\beta$ -catenin mutation spectrum in carcinogen-induced rat colon tumors tends to cluster around codon 33. Note that codon 32 is the most frequent site for substitution mutations. Adapted and modifies after Blum *et al* (9).

In the absence of Wnt stimulation,  $\beta$ -catenin forms a multiprotein complex with APC, Axin, CKI and GSK-3 $\beta$ . In this complex, GSK-3 $\beta$  and CKI are suggested to phosphorylate  $\beta$ -catenin at multiple Serine and Threonine residues at the amino-terminal region of  $\beta$ -catenin, namely Ser-45 by CKI followed by Thr-41, Ser-37 and Ser-33 consecutively by GSK-3 $\beta$ , thereby marking  $\beta$ -catenin for degradation by the ubiquitination-proteosome pathway (136).

This thesis has shown that substitution mutations at Asp-32, which is not a direct target for phosphorylation by GSK-3 $\beta$  or CKI, are sufficient to interfere with proteasome-mediated degradation of  $\beta$ -catenin in HEK-293 cells. Furthermore, the present study has demonstrated that the phosphorylation status of codon 32 mutant  $\beta$ -catenin is influenced by the type of mutation that substitutes Asp-32. Tyrosine, which harbors a bulky aromatic side chain, abolished  $\beta$ -catenin phosphorylation. It

is likely that the bulky side chain of the Tyrosine altered the accessibility of Serine and Threonine residues to GSK-3 $\beta$ . Another possibility could be that introducing Tyrosine at codon 32 might alter the protein conformation in a manner that hinders its availability to phosphorylation. On the contrary, both Asparagine, which harbor a positively charged side chain, and Glycine, which has a small (hydrogen atom) side chain caused accumulation and stabilization of the phosphorylated form of  $\beta$ -catenin *in vivo*.

Results from this study have further shown, for the first time, that partially phosphorylated  $\beta$ -catenin is transcriptionally active. This conclusion is based on the observation that both D32G and D32N  $\beta$ -catenin were highly phosphorylated. These findings are contrary to data reported by Sadot and colleagues, which showed that phosphorylated  $\beta$ -catenin at Ser-33 and Ser-37 is transcriptionally inactive (165). Among the differences that might explain this inconsistency is the disparity in the phosphorylation pattern of  $\beta$ -catenin. The antibody used to detect phosphorylated  $\beta$ -catenin by Sadot group was specific for  $\beta$ -catenin when it is phosphorylated at both Ser-33 and Ser-37. Conversely, the antibody used in the present experiments is specific for  $\beta$ -catenin when it is phosphorylated at Ser-33, Ser-37 or Thr-41. Therefore, it raises a question about simultaneous phosphorylation at more than one site at the any time. It is predicted that the phosphorylation alteration, if it occurred, might affect Ser-33 since it is in close proximity to the mutation site on codon 32. Therefore, the probability of  $\beta$ -catenin phosphorylation is high at both Ser-37 and Thr-41. This suggested that codon 32 mutant  $\beta$ -catenin is partially phosphorylated. This also implies that the complete phosphorylation of N-terminal  $\beta$ -catenin is mandatory to inhibit  $\beta$ -catenin signaling activity. Another consideration might be the structural changes of  $\beta$ -catenin due to mutations at codon 32. These mutations might alter the optimal conformational architecture of  $\beta$ -catenin and therefore change its biological activity.

It has been suggested that the de-phosphorylated form of  $\beta$ -catenin is elevated in response to Wnt-1 and LiCl stimulation (166, 205). In addition, it has been proposed that the dephosphorylation of  $\beta$ -catenin occurs rapidly by a rate comparable to its phosphorylation by GSK-3 $\beta$  (165). However, the exact mechanism of  $\beta$ -catenin dephosphorylation is yet to be elucidated. Results from this laboratory provided some insights. The de-phosphorylated form of  $\beta$ -catenin underwent marked elevation in response to LiCl treatment. In addition, the accumulated  $\beta$ -catenin resulting from extended ALLN treatment showed an increase, to lesser extent, of the relative amount of the dephosphorylated  $\beta$ -catenin. ALLN is a proteasomes inhibitor, thereby inducing the accumulation of phosphorylated/ubiquitinated form of  $\beta$ -catenin (6, 125). The level of  $\beta$ -catenin dephosphorylation observed after ALLN treatment in these experiments was slightly higher than that reported before (205). One major variant is the concentration and incubation time of ALLN. In this investigation, a 10-fold higher concentration (100  $\mu$ M of ALLN) and 3-times longer treatment (20 hours) was used than in prior studies. However, the appearance of the dephosphorylated  $\beta$ -catenin after prolonged ALLN treatment might indicate a direct induction of the  $\beta$ -catenin dephosphorylation machinery in response to ALLN treatment, or in response to the accumulation of phosphorylated  $\beta$ -catenin. Support for this conception came from the observation that treatment of cells transfected with D32G or D32N  $\beta$ -catenin, which were accessible to phosphorylation, resulted in induction in the dephosphorylation of  $\beta$ -catenin (Figure 13E, compare lane 6 to 7 and lane 8 to 9). In contrast, D32Y  $\beta$ -catenin, which was not available for phosphorylation by GSK-3 $\beta$ , showed less dephosphorylation in response to ALLN treatment (Figure 13E, compare lane 10 to 11).

Results from this thesis have reported a successful GSK-3 $\beta$ -dependent phosphorylation of  $\beta$ -catenin *in vitro*. However, the degree of phosphorylation was mutation-type dependent. Whereas D32G and D32N  $\beta$ -catenin were

phosphorylated to the same extent as the WT, a marked attenuation in D32Y and  $\Delta 45$   $\beta$ -catenin phosphorylation occurred *in vitro*. These results further show the impaired phosphorylation of D32Y  $\beta$ -catenin, and re-emphasize the significant role of Ser-45 for  $\beta$ -catenin phosphorylation *in vitro*. Additional support came from three published studies. The first study has shown that GSK-3 $\beta$  can phosphorylate WT  $\beta$ -catenin in the presence of Axin *in vitro* (163). The second study has recently demonstrated that substitution mutations at Ser-33, Ser-37 and their surroundings have abolished recognition of  $\beta$ -catenin by  $\beta$ -TrCp *in vitro*. The same study suggested that Ser-45 is a priming substrate for CKI $\alpha$  (113). The third study has reported that the pre-phosphorylation of Ser-45 of  $\beta$ -catenin by CKI $\epsilon$  enhances the affinity of GSK-3 $\beta$  towards Thr-41, Ser-37 and Ser-33.

Since  $\beta$ -catenin phosphorylation at its GSK-3 $\beta$  region is followed by rapid ubiquitination and proteasome-dependent degradation under normal circumstances (6), this thesis investigated the possible ubiquitination of D32G and D32N  $\beta$ -catenin. Evidence is presented that codon 32 mutant  $\beta$ -catenin, phosphorylated or non-phosphorylated, was unable to acquire ubiquitination. One explanation is that substitution mutations at codon 32 disrupt the  $\beta$ -TrCp recognition motif within GSK-3 $\beta$  region of  $\beta$ -catenin. Sequence analysis has shown that  $\beta$ -catenin harbors an I $\kappa$ B $\alpha$ -like six-amino acid conserved sequence (Asp-Ser-Gly-Ile-His-Ser). Phosphorylation of the two Serine residues (33 and 37) within this sequence triggers the phosphorylation-dependent recognition of  $\beta$ -catenin by  $\beta$ -TrCp and subsequent ubiquitination (113, 167). Additionally, the same trend of phosphorylated  $\beta$ -catenin accumulation was seen in ts20 CHO-cell line, which harbors a specific temperature-sensitive mutation in the E1 ubiquitin conjugation enzyme. When shifted to the restrictive temperature, these cells failed to ubiquitinate  $\beta$ -catenin, even though it was highly phosphorylated. These data support the notion that D32G and D32N interfere with  $\beta$ -TrCp-dependent ubiquitination rather than  $\beta$ -catenin phosphorylation.

A dramatic reduction was noted of Tcf-mediated transcription by WT or mutant  $\beta$ -catenin upon ALLN treatment. In addition, pilot studies (data not shown) suggested that even 25  $\mu$ M of ALLN for 10 hours was sufficient to inhibit the TOPFlash-based transactivation of WT as well as D32N, and  $\Delta$ 45  $\beta$ -catenin. These results contrast with reports by Staal *et al.* They have used 10  $\mu$ M ALLN concentration and shorter incubation time (6 hours) to show that ALLN suppresses the Tcf-mediated transcriptional activity of WT  $\beta$ -catenin but not its mutant counterpart S33Y  $\beta$ -catenin (205). On the contrary, the ALLN concentration and incubation time used in the present investigation were slightly different, and were primarily based on published data, in which HEK-293 cells were treated with 100  $\mu$ M ALLN (206). Although the other reports did not discuss any cytotoxic effects of ALLN treatment at 100  $\mu$ M on HEK cells, one of the major observations associated with ALLN treatment was the induction of apoptosis in the present work.

Several studies have reported that proteasome inhibitors such as ALLN can induce caspase-3-dependent apoptosis in HEK-293 cells (207). On the other hand, it has been shown that  $\beta$ -catenin is cleaved by caspase-3 during apoptosis (179). Therefore, one hypothesis was that the core region of  $\beta$ -catenin (entire Arm-repeat region), which results from caspase-3 dependent degradation of  $\beta$ -catenin, could compete with full-length  $\beta$ -catenin for Tcf-4 binding. Results from these experiments have shown that inhibition of ALLN-induced caspase-3 activation by caspase-3-like specific tetrapeptide inhibitor (Z-DEVD-fmk) did not restore the transactivation potential of  $\beta$ -catenin. Furthermore, it has been reported that apoptotic cells harbor high LEF-1-mediated transactivation when transfected with WT or mutant  $\beta$ -catenin (180). This observation rules out the possibility that the suppression of  $\beta$ -catenin transactivation upon ALLN-induced apoptosis is an artifact of apoptosis. Consequently, it seems that ALLN suppresses  $\beta$ -catenin transactivation by a mechanism independent of apoptosis. Additionally, the exact

ALLN-dependent suppression of  $\beta$ -catenin transactivation is still not clear, however, it is possible that ALLN affects not only  $\beta$ -catenin but also Tcf-4 or other proteins involved in TCF-controlled transcription. Another explanation could be that the prolonged ALLN treatment allows for other side events to occur. For example, one possible event is the build-up of transcriptionally inactive endogenous WT  $\beta$ -catenin which is known to bind Tcf-4 but can not form ternary structure with DNA, as reported by Sadot *et al.*(165), the latter could compete with exogenous  $\beta$ -catenin for Tcf-4 binding. Interestingly, blocking proteasome activity in HCT-116 cells resulted in marked increase in the phosphorylated  $\beta$ -catenin. HCT-116 cells harbor heterozygous mutation in  $\beta$  catenin (165). Thus, based on the observation that ALLN was unable to enhance the phosphorylation of mutant  $\beta$ -catenin, it can be assumed that the induction in the phosphorylated  $\beta$ -catenin in HCT-116 cells is due to the wild-type allele. Therefore, a substantial reduction might be expected in  $\beta$ -catenin-mediated transactivation, upon prolonged ALLN treatment of HCT-116 cells. Support for this hypothesis came from the observation that the phytochemical curcumin was capable to induce apoptosis and suppress  $\beta$ -catenin transactivation in HCT-116 cells. Surprisingly, inhibition of caspase-3 with Z-DEVD-fmk was unable to block the curcumin-induced decrease in the  $\beta$ -catenin transactivation. The author of this work explained this phenomenon by irreversible alteration in other functional components of the  $\beta$ -catenin transactivation complex (208).

Previous study has suggested that over-expression of exogenous WT  $\beta$ -catenin induces apoptosis independent of its transcription activity and does not involve cell cycle regulators such as p53 and cyclin D1 (180). Although cyclin D1 expression was not affected by over-expression of  $\beta$ -catenin (up to 72 hours) in the present study, results have shown no sign of apoptosis or cell cycle alteration in response to WT or mutant  $\beta$ -catenin over-expression in HEK-293 cells. One clarification might be the cell type. Whereas Kim *et al* used normal fibroblasts and carcinoma cell

lines; HEK-293 cell line was used in this thesis work. The latter cells originated from primary human embryonal kidney and are characterized by tight control over  $\beta$ -catenin/Tcf-4 signaling. In fact, 72 hours post transfection, cells were 100% confluent and exhibited the normal monolayer morphology. In addition, it seems that these cells also exert tight control over Wnt signaling target genes. Among genes tested for over-expression were *c-jun* (Figure 22) and *cyclin D1* (not shown). The endogenous protein level of both were hardly detected, however, the relative amount of c-jun protein increased upon ALLN treatment. This result is in agreement with the well-defined proteasomal-mediated degradation of c-jun (209). Furthermore, evidence is shown that over-expression of  $\beta$ -catenin by transient transfection had modest anti-apoptotic effects in HEK-293 cells. It has been reported that Wnt-1-mediated constitutive up-regulation of  $\beta$ -catenin inhibits chemotherapeutic agent-induced apoptosis. This inhibition was dependent on  $\beta$ -catenin mediated transactivation (175). Although the level of  $\beta$ -catenin/Tcf-4 signaling by transient transfection of mutant  $\beta$ -catenin was far greater than Wnt-1 dependent transactivation (205), results from this thesis showed modest survival stimulation upon STS treatment. This difference may be due to both cell type and apoptotic stimuli. Recent studies have demonstrated that  $\beta$ -catenin is cleaved by caspase-3 during STS and anoikis-induced apoptosis, and that cleaved  $\beta$ -catenin reduced its transactivation potential. Although codon 32 mutant  $\beta$ -catenin harbors mutations at one of the putative caspase-3 recognition sites, it is unlikely that the cleaved product of  $\beta$ -catenin could inhibit caspase-3-dependent apoptosis. This conclusion is based on the observation that the percentage of apoptotic cells as well as caspase-3 activity was equivalent in cells transfected with either WT or codon 32 mutant  $\beta$ -catenin (Figures 23 and 24).

## 6 CHAPTER 6: CONCLUSIONS

In summary, the collective work in this thesis has shown that the widely held principle that accumulated  $\beta$ -catenin is a consequence of mutations at Serine and Threonine residues of  $\beta$ -catenin is not completely true. The signaling function of WT or mutant  $\beta$ -catenin was directly analyzed in a gene reporter assay by co-transfection of a LEF/TCF-member with a reporter plasmid containing a TCF-dependent promoter. Results from this assay have shown marked increase in the transactivation potential of  $\beta$ -catenin. Further analysis by Western blotting confirmed  $\beta$ -catenin accumulation. In addition, thesis results have shown that the degree of phosphorylation of mutant  $\beta$ -catenin is determined by the type of mutation at codon 32. Furthermore, the proteasomes-dependent degradation of mutant  $\beta$ -catenin was impaired due to insufficient phosphorylation and ubiquitination. Interestingly, the proteasome inhibitor, ALLN, was sufficient to completely suppress  $\beta$ -catenin mediated transactivation. Results from these experiments have revealed that the amount of  $\beta$ -catenin is not the only determinant of its transactivation capacity.

Finally, future studies should be conducted to investigate the effect of chemotherapeutic agents such as proteasome inhibitors and Sodium Butyrate on  $\beta$ -catenin translocation in normal and colorectal cell lines. Recent data described the discovery of a novel protein "HAKAI" ("destruction" in Japanese), an E3 ubiquitin ligase that facilitates the dynamic recycling of Adherin adhesion complexes. In epithelial cells, activation of the tyrosine kinase *Src* leads to the tyrosine phosphorylation of  $\beta$ -catenin and E-cadherin, followed by HAKAI-mediated ubiquitination and endocytosis of the E-cadherin complex (155). These findings suggest a new hypothetical avenue of down regulation of cytosolic  $\beta$ -catenin. It is well established that E-cadherin sequesters the cytoplasmic pool of  $\beta$ -catenin, and



thus, limits the relative amount of free cytosolic  $\beta$ -catenin (210). However, mutations in APC or  $\beta$ -catenin itself may lead to accumulation of  $\beta$ -catenin that exceeds the capacity of E-cadherin binding. Thus, by developing a mechanism that induces E-cadherin expression, and thereby increases  $\beta$ -catenin sequestration at cell-cell junction,  $\beta$ -catenin that escapes phosphorylation/ubiquitylation because of mutations within its phosphorylation sites can be tyrosine-phosphorylated and subsequently endocytosed and degraded by an alternative mechanism.

## REFERENCES

1. Cancer Facts & Figures 2003: The American Cancer Society.
2. Hanahan, D. and Weinberg, R. A. The hallmarks of cancer. *Cell*, 100: 57-70, 2000.
3. Fearon, E. R. Cancer progression. *Curr Biol*, 9: R873-875, 1999.
4. Fearnhead, N. S., Britton, M. P., and Bodmer, W. F. The ABC of APC. *Hum. Mol. Genet.*, 10: 721-733, 2001.
5. Morin, P. J., Sparks, A. B., Korinek, V., Barker, N., Clevers, H., Vogelstein, B., and Kinzler, K. W. Activation of  $\beta$ -catenin-Tcf signaling in colon cancer by mutations in  $\beta$ -catenin or APC. *Science*, 275: 1787-1790, 1997.
6. Aberle, H., Bauer, A., Stappert, J., Kispert, A., and Kemler, R.  $\beta$ -catenin is a target for the ubiquitin-proteasome pathway. *Embo J*, 16: 3797-3804, 1997.
7. Polakis, P. Wnt signaling and cancer. *Genes Dev*, 14: 1837-1851, 2000.
8. Bingham, S. A. Diet and colorectal cancer prevention. *Biochem Soc Trans*, 28: 12-16, 2000.
9. Blum, C. A., Xu, M., Orner, G. A., Fong, A. T., Bailey, G. S., Stoner, G. D., Horio, D. T., and Dashwood, R. H.  $\beta$ -Catenin mutation in rat colon tumors initiated by 1,2-dimethylhydrazine and 2-amino-3-methylimidazo[4,5-f]quinoline, and the effect of post-initiation treatment with chlorophyllin and indole-3-carbinol. *Carcinogenesis*, 22: 315-320, 2001.
10. Burt, R. W. Colon cancer screening. *Gastroenterology*, 119: 837-853, 2000.
11. Dashwood, R. H. Early detection and prevention of colorectal cancer (review). *Oncol Rep*, 6: 277-281, 1999.

12. Marchand, L. L. Combined influence of genetic and dietary factors on colorectal cancer incidence in Japanese Americans. *J Natl Cancer Inst Monogr* 101-105, 1999.
13. Rozen, P., Fireman, Z., Figer, A., Legum, C., Ron, E., and Lynch, H. T. Family history of colorectal cancer as a marker of potential malignancy within a screening program. *Cancer*, 60: 248-254, 1987.
14. Giovannucci, E. and Willett, W. C. Dietary factors and risk of colon cancer. *Ann Med*, 26: 443-452, 1994.
15. Kadlubar, F., Kaderlik, R. K., Mulder, G. J., Lin, D., Butler, M. A., Teitel, C. H., Minchin, R. F., Ilett, K. F., Friesen, M. D., Bartsch, H., and et al. Metabolic activation and DNA adduct detection of PhIP in dogs, rats, and humans in relation to urinary bladder and colon carcinogenesis. *Princess Takamatsu Symp*, 23: 207-213, 1995.
16. Gertig, D. M. and Hunter, D. J. Genes and environment in the etiology of colorectal cancer. *Semin Cancer Biol*, 8: 285-298, 1998.
17. Sachse, C., Smith, G., Wilkie, M. J. V., Barrett, J. H., Waxman, R., Sullivan, F., Forman, D., Bishop, D. T., and Wolf, C. R. A pharmacogenetic study to investigate the role of dietary carcinogens in the etiology of colorectal cancer. *Carcinogenesis*, 23: 1839-1850, 2002.
18. Potter, J. D. Colorectal cancer: molecules and populations. *J Natl Cancer Inst*, 91: 916-932, 1999.
19. Nagao, M. and Sugimura, T. Carcinogenic factors in food with relevance to colon cancer development. *Mutat Res*, 290: 43-51, 1993.
20. Dashwood, W. M., Orner, G. A., and Dashwood, R. H. Inhibition of  $\beta$ -catenin/Tcf activity by white tea, green tea, and epigallocatechin-3-gallate (EGCG): minor contribution of H(2)O(2) at physiologically relevant EGCG concentrations. *Biochem Biophys Res Commun*, 296: 584-588, 2002.

21. Orner, G. A., Dashwood, W. M., Blum, C. A., Diaz, G. D., Li, Q., Al-Fageeh, M., Tebbutt, N., Heath, J. K., Ernst, M., and Dashwood, R. H. Response of Apc(min) and A33 ( $\Delta N$   $\beta$ -cat) mutant mice to treatment with tea, sulindac, and 2-amino-1-methyl-6-phenylimidazo[4,5-*b*]pyridine (PhIP). *Mutat Res*, 506-507: 121-127, 2002.
22. Calvisi, D. F., Factor, V. M., Loi, R., and Thorgeirsson, S. S. Activation of  $\beta$ -catenin during hepatocarcinogenesis in transgenic mouse models: relationship to phenotype and tumor grade. *Cancer Res*, 61: 2085-2091, 2001.
23. Ogawa, K., Yamada, Y., Kishibe, K., Ishizaki, K., and Tokusashi, Y.  $\beta$ -catenin mutations are frequent in hepatocellular carcinomas but absent in adenomas induced by diethylnitrosamine in B6C3F1 mice. *Cancer Res*, 59: 1830-1833, 1999.
24. Samowitz, W. S., Powers, M. D., Spirio, L. N., Nollet, F., van Roy, F., and Slattery, M. L.  $\beta$ -catenin mutations are more frequent in small colorectal adenomas than in larger adenomas and invasive carcinomas. *Cancer Res*, 59: 1442-1444, 1999.
25. Takahashi, M., Nakatsugi, S., Sugimura, T., and Wakabayashi, K. Frequent mutations of the  $\beta$ -catenin gene in mouse colon tumors induced by azoxymethane. *Carcinogenesis*, 21: 1117-1120, 2000.
26. Tsujiuchi, T., Tsutsumi, M., Sasaki, Y., Takahama, M., and Konishi, Y. Different frequencies and patterns of  $\beta$ -catenin mutations in hepatocellular carcinomas induced by N-nitrosodiethylamine and a choline-deficient L-amino acid-defined diet in rats. *Cancer Res*, 59: 3904-3907, 1999.
27. Tsukamoto, T., Tanaka, H., Fukami, H., Inoue, M., Takahashi, M., Wakabayashi, K., and Tatematsu, M. More frequent  $\beta$ -catenin gene mutations in adenomas than in aberrant crypt foci or adenocarcinomas in the large intestines of 2-amino-1-methyl-6-phenylimidazo[4,5-*b*]pyridine (PhIP)-treated rats. *Jpn J Cancer Res*, 91: 792-796, 2000.
28. Dashwood, R. H., Suzui, M., Nakagama, H., Sugimura, T., and Nagao, M. High frequency of  $\beta$ -catenin (*ctnnb1*) mutations in the colon tumors induced by two heterocyclic amines in the F344 rat. *Cancer Res*, 58: 1127-1129, 1998.

29. Fodde, R., Smits, R., and Clevers, H. APC, signal transduction and genetic instability in colorectal cancer. *Nat Rev Cancer*, 1: 55-67, 2001.
30. Fearon, E. R. and Vogelstein, B. A genetic model for colorectal tumorigenesis. *Cell*, 61: 759-767, 1990.
31. Vogelstein, B. and Kinzler, K. W. The multistep nature of cancer. *Trends Genet*, 9: 138-141, 1993.
32. Vogelstein, B., Fearon, E. R., Kern, S. E., Hamilton, S. R., Preisinger, A. C., Nakamura, Y., and White, R. Allelotype of colorectal carcinomas. *Science*, 244: 207-211, 1989.
33. Kinzler, K. W. and Vogelstein, B. Cancer-susceptibility genes. Gatekeepers and caretakers. *Nature*, 386: 761, 763, 1997.
34. Vogelstein, B., Fearon, E. R., Hamilton, S. R., Kern, S. E., Preisinger, A. C., Leppert, M., Nakamura, Y., White, R., Smits, A. M., and Bos, J. L. Genetic alterations during colorectal-tumor development. *N Engl J Med*, 319: 525-532, 1988.
35. Jass, J. R., Young, J., and Leggett, B. A. Evolution of colorectal cancer: change of pace and change of direction. *J Gastroenterol Hepatol*, 17: 17-26, 2002.
36. Smith, G., Carey, F. A., Beattie, J., Wilkie, M. J., Lightfoot, T. J., Coxhead, J., Garner, R. C., Steele, R. J., and Wolf, C. R. Mutations in APC, Kirsten-ras, and p53--alternative genetic pathways to colorectal cancer. *Proc Natl Acad Sci U S A*, 99: 9433-9438, 2002.
37. Lengauer, C., Kinzler, K. W., and Vogelstein, B. Genetic instabilities in human cancers. *Nature*, 396: 643-649, 1998.
38. Kinzler, K. W. and Vogelstein, B. Landscaping the cancer terrain. *Science*, 280: 1036-1037, 1998.
39. Lindblom, A. Different mechanisms in the tumorigenesis of proximal and distal colon cancers. *Curr Opin Oncol*, 13: 63-69, 2001.

40. Rodrigues, N. R., Rowan, A., Smith, M. E., Kerr, I. B., Bodmer, W. F., Gannon, J. V., and Lane, D. P. p53 mutations in colorectal cancer. *Proc Natl Acad Sci U S A*, 87: 7555-7559, 1990.
41. Mitchell, R. J., Farrington, S. M., Dunlop, M. G., and Campbell, H. Mismatch Repair Genes hMLH1 and hMSH2 and Colorectal Cancer: A HuGE Review. *Am J Epidemiol*, 156: 885-902, 2002.
42. Kinzler, K. W. and Vogelstein, B. Lessons from hereditary colorectal cancer. *Cell*, 87: 159-170, 1996.
43. Ichii, S., Horii, A., Nakatsuru, S., Furuyama, J., Utsunomiya, J., and Nakamura, Y. Inactivation of both APC alleles in an early stage of colon adenomas in a patient with familial adenomatous polyposis (FAP). *Hum Mol Genet*, 1: 387-390, 1992.
44. Levy, D. B., Smith, K. J., Beazer-Barclay, Y., Hamilton, S. R., Vogelstein, B., and Kinzler, K. W. Inactivation of both APC alleles in human and mouse tumors. *Cancer Res*, 54: 5953-5958, 1994.
45. Groden, J., Thliveris, A., Samowitz, W., Carlson, M., Gelbert, L., Albertsen, H., Joslyn, G., Stevens, J., Spirio, L., Robertson, M., and et al. Identification and characterization of the familial adenomatous polyposis coli gene. *Cell*, 66: 589-600, 1991.
46. Laurent-Puig, P., Beroud, C., and Soussi, T. APC gene: database of germline and somatic mutations in human tumors and cell lines. *Nucleic Acids Res*, 26: 269-270, 1998.
47. Nakamura, Y. The role of the adenomatous polyposis coli (APC) gene in human cancers. *Adv Cancer Res*, 62: 65-87, 1993.
48. Kohoutova, M., Stekrova, J., Jirasek, V., and Kapras, J. APC germline mutations identified in Czech patients with familial adenomatous polyposis. *Hum Mutat*, 19: 460-461, 2002.
49. Jen, J., Powell, S. M., Papadopoulos, N., Smith, K. J., Hamilton, S. R., Vogelstein, B., and Kinzler, K. W. Molecular determinants of dysplasia in colorectal lesions. *Cancer Res*, 54: 5523-5526, 1994.

50. Yan, H., Dobbie, Z., Gruber, S. B., Markowitz, S., Romans, K., Giardiello, F. M., Kinzler, K. W., and Vogelstein, B. Small changes in expression affect predisposition to tumorigenesis. *Nat Genet*, 30: 25-26, 2002.
51. Hayakumo, T., Azuma, T., Nakajima, M., Yasuda, K., Cho, E., Mukai, H., Mizuma, Y., Ashihara, T., Mizuno, S., Hirano, S., and et al. [Prevalence of K-ras gene mutations in human colorectal cancers. *Nippon Shokakibyo Gakkai Zasshi*, 88: 1539-1544, 1991.
52. Bos, J. L., Fearon, E. R., Hamilton, S. R., Verlaan-de Vries, M., van Boom, J. H., van der Eb, A. J., and Vogelstein, B. Prevalence of ras gene mutations in human colorectal cancers. *Nature*, 327: 293-297, 1987.
53. Baker, S., Preisinger, A., Jessup, J., Paraskeva, C., Markowitz, S., Willson, J., Hamilton, S., and Vogelstein, B. p53 gene mutations occur in combination with 17p allelic deletions as late events in colorectal tumorigenesis. *Cancer Res*, 50: 7717-7722, 1990.
54. Smith, A. J., Stern, H. S., Penner, M., Hay, K., Mitri, A., Bapat, B. V., and Gallinger, S. Somatic APC and K-ras codon 12 mutations in aberrant crypt foci from human colons. *Cancer Res*, 54: 5527-5530, 1994.
55. Thiagalingam, S., Lengauer, C., Leach, F. S., Schutte, M., Hahn, S. A., Overhauser, J., Willson, J. K., Markowitz, S., Hamilton, S. R., Kern, S. E., Kinzler, K. W., and Vogelstein, B. Evaluation of candidate tumour suppressor genes on chromosome 18 in colorectal cancers. *Nat Genet*, 13: 343-346, 1996.
56. Mehlen, P., Rabizadeh, S., Snipas, S. J., Assa-Munt, N., Salvesen, G. S., and Bredesen, D. E. The DCC gene product induces apoptosis by a mechanism requiring receptor proteolysis. *Nature*, 395: 801-804, 1998.
57. Leach, F. S., Nicolaides, N. C., Papadopoulos, N., Liu, B., Jen, J., Parsons, R., Peltomaki, P., Sistonen, P., Aaltonen, L. A., Nystrom-Lahti, M., and et al. Mutations of a mutS homolog in hereditary nonpolyposis colorectal cancer. *Cell*, 75: 1215-1225, 1993.
58. Papadopoulos, N., Nicolaides, N. C., Wei, Y. F., Ruben, S. M., Carter, K. C., Rosen, C. A., Haseltine, W. A., Fleischmann, R. D., Fraser, C. M., Adams, M. D., and et al. Mutation of a mutL homolog in hereditary colon cancer. *Science*, 263: 1625-1629, 1994.

59. Peltomaki, P. and de la Chapelle, A. Mutations predisposing to hereditary nonpolyposis colorectal cancer. *Adv Cancer Res*, 71: 93-119, 1997.
60. Nannery, W. M., Barone, J. G., and Abouchdid, C. Familial polyposis coli & Gardner's syndrome. *N J Med*, 87: 731-733, 1990.
61. Spirio, L., Olschwang, S., Groden, J., Robertson, M., Samowitz, W., Joslyn, G., Gelbert, L., Thliveris, A., Carlson, M., Otterud, B., and et al. Alleles of the APC gene: an attenuated form of familial polyposis. *Cell*, 75: 951-957, 1993.
62. Pedemonte, S., Sciallero, S., Gismondi, V., Stagnaro, P., Biticchi, R., Haeouaine, A., Bonelli, L., Nicolo, G., Groden, J., Bruzzi, P., Aste, H., and Varesco, L. Novel germline APC variants in patients with multiple adenomas. *Genes Chromosomes Cancer*, 22: 257-267, 1998.
63. Lynch, H. T., Smyrk, T. C., Watson, P., Lanspa, S. J., Lynch, J. F., Lynch, P. M., Cavalieri, R. J., and Boland, C. R. Genetics, natural history, tumor spectrum, and pathology of hereditary nonpolyposis colorectal cancer: an updated review. *Gastroenterology*, 104: 1535-1549, 1993.
64. Vasen, H. F., Wijnen, J. T., Menko, F. H., Kleibeuker, J. H., Taal, B. G., Griffioen, G., Nagengast, F. M., Meijers-Heijboer, E. H., Bertario, L., Varesco, L., Bisgaard, M. L., Mohr, J., Fodde, R., and Khan, P. M. Cancer risk in families with hereditary nonpolyposis colorectal cancer diagnosed by mutation analysis. *Gastroenterology*, 110: 1020-1027, 1996.
65. Fuchs, C. S., Giovannucci, E. L., Colditz, G. A., Hunter, D. J., Speizer, F. E., and Willett, W. C. A prospective study of family history and the risk of colorectal cancer. *N Engl J Med*, 331: 1669-1674, 1994.
66. Bosman, F. T. The hamartoma-adenoma-carcinoma sequence. *J Pathol*, 188: 1-2, 1999.
67. Kruschewski, M., Noske, A., Haier, J., Runkel, N., Anagnostopoulos, Y., and Buhr, H. J. Is reduced expression of mismatch repair genes MLH1 and MSH2 in patients with sporadic colorectal cancer related to their prognosis? *Clin Exp Metastasis*, 19: 71-77, 2002.
68. Terdiman, J. P. Genomic events in the adenoma to carcinoma sequence. *Semin Gastrointest Dis*, 11: 194-206, 2000.



69. Jubb, A. M., Bell, S. M., and Quirke, P. Methylation and colorectal cancer. *J Pathol*, 195: 111-134, 2001.
70. Menigatti, M., Di Gregorio, C., Borghi, F., Sala, E., Scarselli, A., Pedroni, M., Foroni, M., Benatti, P., Roncucci, L., Ponz de Leon, M., and Percesepe, A. Methylation pattern of different regions of the MLH1 promoter and silencing of gene expression in hereditary and sporadic colorectal cancer. *Genes Chromosomes Cancer*, 31: 357-361, 2001.
71. Aaltonen, L. A., Peltomaki, P., Leach, F. S., Sistonen, P., Pylkkanen, L., Mecklin, J. P., Jarvinen, H., Powell, S. M., Jen, J., Hamilton, S. R., and et al. Clues to the pathogenesis of familial colorectal cancer. *Science*, 260: 812-816, 1993.
72. Massa, M. J., Iniesta, P., Gonzalez-Quevedo, R., de Juan, C., Caldes, T., Sanchez-Pernaute, A., Cerdan, J., Torres, A. J., Balibrea, J. L., and Benito, M. Differential prognosis of replication error phenotype and loss of heterozygosity in sporadic colorectal cancer. *Eur J Cancer*, 35: 1676-1682, 1999.
73. Smalley, M. J. and Dale, T. C. Wnt signalling in mammalian development and cancer. *Cancer Metastasis Rev*, 18: 215-230, 1999.
74. Ramakrishna, N. R. and Brown, A. M. Wingless, the Drosophila homolog of the proto-oncogene Wnt-1, can transform mouse mammary epithelial cells. *Dev Suppl* 95-103, 1993.
75. Parr, B. A. and McMahon, A. P. Dorsalizing signal Wnt-7a required for normal polarity of D-V and A-P axes of mouse limb. *Nature*, 374: 350-353, 1995.
76. Yang, Y. and Niswander, L. Interaction between the signaling molecules WNT7a and SHH during vertebrate limb development: dorsal signals regulate anteroposterior patterning. *Cell*, 80: 939-947, 1995.
77. Wodarz, A. and Nusse, R. Mechanisms of Wnt signaling in development. *Annu. Rev. Cell Dev. Biol.*, 14: 59-88, 1998.
78. Sokol, S., Christian, J. L., Moon, R. T., and Melton, D. A. Injected Wnt RNA induces a complete body axis in *Xenopus* embryos. *Cell*, 67: 741-752, 1991.

79. Zeng, L., Fagotto, F., Zhang, T., Hsu, W., Vasicek, T. J., Perry, W. L., 3rd, Lee, J. J., Tilghman, S. M., Gumbiner, B. M., and Costantini, F. The mouse Fused locus encodes Axin, an inhibitor of the Wnt signaling pathway that regulates embryonic axis formation. *Cell*, 90: 181-192, 1997.
80. Lee, F. S., Lane, T. F., Kuo, A., Shackleford, G. M., and Leder, P. Insertional mutagenesis identifies a member of the Wnt gene family as a candidate oncogene in the mammary epithelium of int-2/Fgf-3 transgenic mice. *Proc Natl Acad Sci U S A*, 92: 2268-2272, 1995.
81. Bradbury, J. M., Niemeyer, C. C., Dale, T. C., and Edwards, P. A. Alterations of the growth characteristics of the fibroblast cell line C3H 10T1/2 by members of the Wnt gene family. *Oncogene*, 9: 2597-2603, 1994.
82. Shimizu, H., Julius, M. A., Giarre, M., Zheng, Z., Brown, A. M., and Kitajewski, J. Transformation by Wnt family proteins correlates with regulation of  $\beta$ -catenin. *Cell Growth Differ*, 8: 1349-1358, 1997.
83. Holcombe, R. F., Marsh, J. L., Waterman, M. L., Lin, F., Milovanovic, T., and Truong, T. Expression of Wnt ligands and Frizzled receptors in colonic mucosa and in colon carcinoma. *Mol Pathol*, 55: 220-226, 2002.
84. Holmen, S. L., Salic, A., Zylstra, C. R., Kirschner, M. W., and Williams, B. O. A novel set of Wnt-Frizzled fusion proteins identifies receptor components that activate  $\beta$ -catenin-dependent signaling. *J Biol Chem*, 277: 34727-34735, 2002.
85. Terasaki, H., Saitoh, T., Shiokawa, K., and Katoh, M. Frizzled-10, up-regulated in primary colorectal cancer, is a positive regulator of the WNT -  $\beta$ -catenin - TCF signaling pathway. *Int J Mol Med*, 9: 107-112, 2002.
86. Jonkers, J., Korswagen, H. C., Acton, D., Breuer, M., and Berns, A. Activation of a novel proto-oncogene, *Frat1*, contributes to progression of mouse T-cell lymphomas. *Embo J*, 16: 441-450, 1997.
87. Saitoh, T., Moriwaki, J., Koike, J., Takagi, A., Miwa, T., Shiokawa, K., and Katoh, M. Molecular cloning and characterization of FRAT2, encoding a positive regulator of the WNT signaling pathway. *Biochem Biophys Res Commun*, 281: 815-820, 2001.

88. Yost, C., Farr, G. H., 3rd, Pierce, S. B., Ferkey, D. M., Chen, M. M., and Kimelman, D. GBP, an inhibitor of GSK-3, is implicated in *Xenopus* development and oncogenesis. *Cell*, 93: 1031-1041, 1998.
89. Li, L., Yuan, H., Weaver, C. D., Mao, J., Farr, G. H., 3rd, Sussman, D. J., Jonkers, J., Kimelman, D., and Wu, D. Axin and Frat1 interact with dvl and GSK, bridging Dvl to GSK in Wnt-mediated regulation of LEF-1. *Embo J*, 18: 4233-4240, 1999.
90. Franca-Koh, J., Yeo, M., Fraser, E., Young, N., and Dale, T. C. The Regulation of Glycogen Synthase Kinase-3 Nuclear Export by Frat/GBP. *J Biol Chem*, 277: 43844-43848, 2002.
91. Saitoh, T., Mine, T., and Katoh, M. Molecular cloning and expression of proto-oncogene FRAT1 in human cancer. *Int J Oncol*, 20: 785-789, 2002.
92. Noordermeer, J., Klingensmith, J., Perrimon, N., and Nusse, R. dishevelled and armadillo act in the wingless signalling pathway in *Drosophila*. *Nature*, 367: 80-83, 1994.
93. Willert, K., Brink, M., Wodarz, A., Varmus, H., and Nusse, R. Casein kinase 2 associates with and phosphorylates dishevelled. *Embo J*, 16: 3089-3096, 1997.
94. Peters, J. M., McKay, R. M., McKay, J. P., and Graff, J. M. Casein kinase I transduces Wnt signals. *Nature*, 401: 345-350, 1999.
95. Seeling, J. M., Miller, J. R., Gil, R., Moon, R. T., White, R., and Virshup, D. M. Regulation of  $\beta$ -catenin signaling by the B56 subunit of protein phosphatase 2A. *Science*, 283: 2089-2091, 1999.
96. Ikeda, S., Kishida, M., Matsuura, Y., Usui, H., and Kikuchi, A. GSK-3 $\beta$ -dependent phosphorylation of adenomatous polyposis coli gene product can be modulated by  $\beta$ -catenin and protein phosphatase 2A complexed with Axin. *Oncogene*, 19: 537-545, 2000.
97. Ratcliffe, M. J., Itoh, K., and Sokol, S. Y. A positive role for the PP2A catalytic subunit in Wnt signal transduction. *J Biol Chem*, 275: 35680-35683, 2000.

98. Ruediger, R., Pham, H. T., and Walter, G. Alterations in protein phosphatase 2A subunit interaction in human carcinomas of the lung and colon with mutations in the A $\beta$  subunit gene. *Oncogene*, 20: 1892-1899, 2001.
99. Ruediger, R., Pham, H. T., and Walter, G. Disruption of protein phosphatase 2A subunit interaction in human cancers with mutations in the A $\alpha$  subunit gene. *Oncogene*, 20: 10-15, 2001.
100. Embi, N., Rylatt, D. B., and Cohen, P. Glycogen synthase kinase-3 from rabbit skeletal muscle. Separation from cyclic-AMP-dependent protein kinase and phosphorylase kinase. *Eur J Biochem*, 107: 519-527, 1980.
101. Frame, S. and Cohen, P. GSK3 takes centre stage more than 20 years after its discovery. *Biochem J*, 359: 1-16, 2001.
102. Plyte, S. E., Hughes, K., Nikolakaki, E., Pulverer, B. J., and Woodgett, J. R. Glycogen synthase kinase-3: functions in oncogenesis and development. *Biochim Biophys Acta*, 1114: 147-162, 1992.
103. Ding, V. W., Chen, R. H., and McCormick, F. Differential regulation of glycogen synthase kinase 3 $\beta$  by insulin and Wnt signaling. *J Biol Chem*, 275: 32475-32481, 2000.
104. Hedgepeth, C. M., Deardorff, M. A., Rankin, K., and Klein, P. S. Regulation of glycogen synthase kinase 3 $\beta$  and downstream Wnt signaling by Axin. *Mol Cell Biol*, 19: 7147-7157, 1999.
105. Hagen, T. and Vidal-Puig, A. Characterisation of the phosphorylation of  $\beta$ -catenin at the GSK-3 priming site Ser45. *Biochem Biophys Res Commun*, 294: 324-328, 2002.
106. Ruel, L., Stambolic, V., Ali, A., Manoukian, A. S., and Woodgett, J. R. Regulation of the protein kinase activity of Shaggy(Zeste-white3) by components of the wingless pathway in *Drosophila* cells and embryos. *J Biol Chem*, 274: 21790-21796, 1999.

107. Thomas, G. M., Frame, S., Goedert, M., Nathke, I., Polakis, P., and Cohen, P. A GSK3-binding peptide from FRAT1 selectively inhibits the GSK3-catalysed phosphorylation of axin and  $\beta$ -catenin. *FEBS Lett*, 458: 247-251, 1999.
108. Vincan, E., Leet, C. S., Reyes, N. I., Dilley, R. J., Thomas, R. J., and Phillips, W. A. Sodium butyrate-induced differentiation of human LIM2537 colon cancer cells decreases GSK-3 $\beta$  activity and increases levels of both membrane-bound and Apc/axin/GSK-3 $\beta$  complex-associated pools of  $\beta$ -catenin. *Oncol Res*, 12: 193-201, 2000.
109. Rubinfeld, B., Souza, B., Albert, I., Muller, O., Chamberlain, S. H., Masiarz, F. R., Munemitsu, S., and Polakis, P. Association of the APC gene product with beta-catenin. *Science*, 262: 1731-1734, 1993.
110. Neufeld, K. L., Zhang, F., Cullen, B. R., and White, R. L. APC-mediated downregulation of  $\beta$ -catenin activity involves nuclear sequestration and nuclear export. *EMBO Rep*, 1: 519-523, 2000.
111. Chan, S. K. and Struhl, G. Evidence that Armadillo transduces wingless by mediating nuclear export or cytosolic activation of Pangolin. *Cell*, 111: 265-280, 2002.
112. Hsu, W., Zeng, L., and Costantini, F. Identification of a domain of Axin that binds to the serine/threonine protein phosphatase 2A and a self-binding domain. *J Biol Chem*, 274: 3439-3445, 1999.
113. Amit, S., Hatzubai, A., Birman, Y., Andersen, J. S., Ben-Shushan, E., Mann, M., Ben-Neriah, Y., and Alkalay, I. Axin-mediated CKI phosphorylation of  $\beta$ -catenin at Ser 45: a molecular switch for the Wnt pathway. *Genes Dev*, 16: 1066-1076, 2002.
114. Mai, M., Qian, C., Yokomizo, A., Smith, D. I., and Liu, W. Cloning of the human homolog of conductin (AXIN2), a gene mapping to chromosome 17q23-q24. *Genomics*, 55: 341-344, 1999.

115. Liu, W., Dong, X., Mai, M., Seelan, R. S., Taniguchi, K., Krishnadath, K. K., Halling, K. C., Cunningham, J. M., Boardman, L. A., Qian, C., Christensen, E., Schmidt, S. S., Roche, P. C., Smith, D. I., and Thibodeau, S. N. Mutations in AXIN2 cause colorectal cancer with defective mismatch repair by activating  $\beta$ -catenin/TCF signalling. *Nat Genet*, 26: 146-147, 2000.
116. Sakanaka, C., Leong, P., Xu, L., Harrison, S. D., and Williams, L. T. Casein kinase I $\epsilon$  in the wnt pathway: regulation of  $\beta$ -catenin function. *Proc Natl Acad Sci U S A*, 96: 12548-12552, 1999.
117. Sakanaka, C., Sun, T. Q., and Williams, L. T. New steps in the Wnt/ $\beta$ -catenin signal transduction pathway. *Recent Prog Horm Res*, 55: 225-236, 2000.
118. Lickert, H., Bauer, A., Kemler, R., and Stappert, J. Casein kinase II phosphorylation of E-cadherin increases E-cadherin/ $\beta$ -catenin interaction and strengthens cell-cell adhesion. *J Biol Chem*, 275: 5090-5095, 2000.
119. Kishida, M., Hino, S., Michiue, T., Yamamoto, H., Kishida, S., Fukui, A., Asashima, M., and Kikuchi, A. Synergistic activation of the Wnt signaling pathway by Dvl and casein kinase I $\epsilon$ . *J Biol Chem*, 276: 33147-33155, 2001.
120. Rubinfeld, B., Tice, D. A., and Polakis, P. Axin-dependent phosphorylation of the adenomatous polyposis coli protein mediated by casein kinase I $\epsilon$ . *J Biol Chem*, 276: 39037-39045, 2001.
121. Liu, C., Li, Y., Semenov, M., Han, C., Baeg, G. H., Tan, Y., Zhang, Z., Lin, X., and He, X. Control of beta-catenin phosphorylation/degradation by a dual-kinase mechanism. *Cell*, 108: 837-847, 2002.
122. Sakanaka, C. Phosphorylation and Regulation of beta-Catenin by Casein Kinase Iepsilon. *J Biochem (Tokyo)*, 132: 697-703, 2002.
123. Schwarz-Romond, T., Asbrand, C., Bakkers, J., Kuhl, M., Schaeffer, H. J., Huelsken, J., Behrens, J., Hammerschmidt, M., and Birchmeier, W. The ankyrin repeat protein Diversin recruits Casein kinase I $\epsilon$  to the  $\beta$ -catenin degradation complex and acts in both canonical Wnt and Wnt/JNK signaling. *Genes Dev*, 16: 2073-2084, 2002.

124. Marikawa, Y. and Elinson, R. P.  $\beta$ -TrCP is a negative regulator of Wnt/ $\beta$ -catenin signaling pathway and dorsal axis formation in *Xenopus* embryos. *Mech Dev*, 77: 75-80, 1998.
125. Orford, K., Crockett, C., Jensen, J. P., Weissman, A. M., and Byers, S. W. Serine phosphorylation-regulated ubiquitination and degradation of  $\beta$ -catenin. *J Biol Chem*, 272: 24735-24738, 1997.
126. Molenaar, M., van de Wetering, M., Oosterwegel, M., Peterson-Maduro, J., Godsave, S., Korinek, V., Roose, J., Destree, O., and Clevers, H. XTcf-3 transcription factor mediates  $\beta$ -catenin-induced axis formation in *Xenopus* embryos. *Cell*, 86: 391-399, 1996.
127. Liu, C., Kato, Y., Zhang, Z., Do, V. M., Yankner, B. A., and He, X.  $\beta$ -Trcp couples  $\beta$ -catenin phosphorylation-degradation and regulates *Xenopus* axis formation. *Proc Natl Acad Sci U S A*, 96: 6273-6278, 1999.
128. Bafico, A., Liu, G., Yaniv, A., Gazit, A., and Aaronson, S. A. Novel mechanism of Wnt signalling inhibition mediated by Dickkopf-1 interaction with LRP6/Arrow. *Nat Cell Biol*, 3: 683-686, 2001.
129. Wallingford, J. B., Rowning, B. A., Vogeli, K. M., Rothbacher, U., Fraser, S. E., and Harland, R. M. Dishevelled controls cell polarity during *Xenopus* gastrulation. *Nature*, 405: 81-85, 2000.
130. Willert, K., Logan, C. Y., Arora, A., Fish, M., and Nusse, R. A *Drosophila* Axin homolog, Daxin, inhibits Wnt signaling. *Development*, 126: 4165-4173, 1999.
131. He, X., Saint-Jeannet, J. P., Woodgett, J. R., Varmus, H. E., and Dawid, I. B. Glycogen synthase kinase-3 and dorsoventral patterning in *Xenopus* embryos. *Nature*, 374: 617-622, 1995.
132. Rubinfeld, B., Albert, I., Porfiri, E., Fiol, C., Munemitsu, S., and Polakis, P. Binding of GSK3 $\beta$  to the APC- $\beta$ -catenin complex and regulation of complex assembly. *Science*, 272: 1023-1026, 1996.

133. Hart, M., Concordet, J. P., Lassot, I., Albert, I., del los Santos, R., Durand, H., Perret, C., Rubinfeld, B., Margottin, F., Benarous, R., and Polakis, P. The F-box protein  $\beta$ -Trop associates with phosphorylated  $\beta$ -catenin and regulates its activity in the cell. *Curr Biol*, 9: 207-210, 1999.
134. Behrens, J., von Kries, J. P., Kuhl, M., Bruhn, L., Wedlich, D., Grosschedl, R., and Birchmeier, W. Functional interaction of  $\beta$ -catenin with the transcription factor LEF-1. *Nature*, 382: 638-642, 1996.
135. Mann, B., Gelos, M., Siedow, A., Hanski, M. L., Gratchev, A., Ilyas, M., Bodmer, W. F., Moyer, M. P., Riecken, E. O., Buhr, H. J., and Hanski, C. Target genes of  $\beta$ -catenin-T cell-factor/lymphoid-enhancer-factor signaling in human colorectal carcinomas. *Proc Natl Acad Sci U S A*, 96: 1603-1608, 1999.
136. Huelsken, J. and Behrens, J. The Wnt signalling pathway. *J Cell Sci*, 115: 3977-3978, 2002.
137. McCrea, P. D., Turck, C. W., and Gumbiner, B. A homolog of the armadillo protein in *Drosophila* (plakoglobin) associated with E-cadherin. *Science*, 254: 1359-1361, 1991.
138. Willert, K. and Nusse, R.  $\beta$ -catenin: a key mediator of Wnt signaling. *Curr Opin Genet Dev*, 8: 95-102, 1998.
139. Nollet, F., Berx, G., Molemans, F., and van Roy, F. Genomic organization of the human  $\beta$ catenin gene (*CTNNB1*). *Genomics*, 32: 413-424, 1996.
140. Kraus, C., Liehr, T., Hulsken, J., Behrens, J., Birchmeier, W., Grzeschik, K. H., and Ballhausen, W. G. Localization of the human  $\beta$ -catenin gene (*CTNNB1*) to 3p21: a region implicated in tumor development. *Genomics*, 23: 272-274, 1994.
141. Li, Q., Dixon, B. M., Al-Fageeh, M., Blum, C. A., and Dashwood, R. H. Sequencing of the rat  $\beta$ -catenin gene (*Ctnnb1*) and mutational analysis of liver tumors induced by 2-amino-3-methylimidazo[4,5-f]quinoline. *Gene*, 283: 255-262, 2002.
142. Huber, A. H., Nelson, W. J., and Weis, W. I. Three-dimensional structure of the armadillo repeat region of  $\beta$ -catenin. *Cell*, 90: 871-882, 1997.



143. Overduin, M., Harvey, T. S., Bagby, S., Tong, K. I., Yau, P., Takeichi, M., and Ikura, M. Solution structure of the epithelial cadherin domain responsible for selective cell adhesion. *Science*, 267: 386-389, 1995.
144. Ivanov, D. B., Philippova, M. P., and Tkachuk, V. A. Structure and functions of classical cadherins. *Biochemistry (Mosc)*, 66: 1174-1186, 2001.
145. Aberle, H., Butz, S., Stappert, J., Weissig, H., Kemler, R., and Hoschuetzky, H. Assembly of the cadherin-catenin complex in vitro with recombinant proteins. *J Cell Sci*, 107 (Pt 12): 3655-3663, 1994.
146. Nollet, F., Berx, G., and van Roy, F. The role of the E-cadherin/catenin adhesion complex in the development and progression of cancer. *Mol Cell Biol Res Commun*, 2: 77-85, 1999.
147. Cox, R. T., Kirkpatrick, C., and Peifer, M. Armadillo is required for adherens junction assembly, cell polarity, and morphogenesis during *Drosophila* embryogenesis. *J Cell Biol*, 134: 133-148, 1996.
148. Huber, A. H. and Weis, W. I. The structure of the beta-catenin/E-cadherin complex and the molecular basis of diverse ligand recognition by beta-catenin. *Cell*, 105: 391-402, 2001.
149. Roura, S., Miravet, S., Piedra, J., Garcia de Herreros, A., and Dunach, M. Regulation of E-cadherin/Catenin association by tyrosine phosphorylation. *J Biol Chem*, 274: 36734-36740, 1999.
150. Pokutta, S. and Weis, W. I. Structure of the dimerization and  $\beta$ -catenin-binding region of  $\alpha$ -catenin. *Mol Cell*, 5: 533-543, 2000.
151. Ireton, R. C., Davis, M. A., van Hengel, J., Mariner, D. J., Barnes, K., Thoreson, M. A., Anastasiadis, P. Z., Matrisian, L., Bundy, L. M., Sealy, L., Gilbert, B., van Roy, F., and Reynolds, A. B. A novel role for p120 catenin in E-cadherin function. *J Cell Biol*, 159: 465-476, 2002.
152. Takeichi, M. Cadherins in cancer: implications for invasion and metastasis. *Curr Opin Cell Biol*, 5: 806-811, 1993.

153. Kawanishi, J., Kato, J., Sasaki, K., Fujii, S., Watanabe, N., and Niitsu, Y. Loss of E-cadherin-dependent cell-cell adhesion due to mutation of the beta-catenin gene in a human cancer cell line, HSC-39. *Mol Cell Biol*, 15: 1175-1181, 1995.
154. Perrimon, N. The genetic basis of patterned baldness in *Drosophila*. *Cell*, 76: 781-784, 1994.
155. Fujita, Y., Krause, G., Scheffner, M., Zechner, D., Leddy, H. E., Behrens, J., Sommer, T., and Birchmeier, W. Hakai, a c-Cbl-like protein, ubiquitinates and induces endocytosis of the E-cadherin complex. *Nat Cell Biol*, 4: 222-231, 2002.
156. Hamaguchi, M., Matsuyoshi, N., Ohnishi, Y., Gotoh, B., Takeichi, M., and Nagai, Y. p60v-src causes tyrosine phosphorylation and inactivation of the N-cadherin-catenin cell adhesion system. *Embo J*, 12: 307-314, 1993.
157. Hecht, A., Litterst, C. M., Huber, O., and Kemler, R. Functional characterization of multiple transactivating elements in  $\beta$ -catenin, some of which interact with the TATA-binding protein in vitro. *J Biol Chem*, 274: 18017-18025, 1999.
158. Piedra, J., Martinez, D., Castano, J., Miravet, S., Dunach, M., and de Herreros, A. G. Regulation of  $\beta$ -catenin structure and activity by tyrosine phosphorylation. *J Biol Chem*, 276: 20436-20443, 2001.
159. Kim, K. and Lee, K. Y. Tyrosine phosphorylation translocates  $\beta$ -catenin from cell-->cell interface to the cytoplasm, but does not significantly enhance the LEF-1-dependent transactivating function. *Cell Biol Int*, 25: 421-427, 2001.
160. Yost, C., Torres, M., Miller, J. R., Huang, E., Kimelman, D., and Moon, R. T. The axis-inducing activity, stability, and subcellular distribution of  $\beta$ -catenin is regulated in *Xenopus* embryos by glycogen synthase kinase 3. *Genes Dev*, 10: 1443-1454, 1996.
161. Liu, C., Li, Y., Semenov, M., Han, C., Baeg, G. H., Tan, Y., Zhang, Z., Lin, X., and He, X. Control of  $\beta$ -catenin phosphorylation/degradation by a dual-kinase mechanism. *Cell*, 108: 837-847, 2002.

162. Sakanaka, C. Phosphorylation and Regulation of  $\beta$ -Catenin by Casein Kinase I $\epsilon$ . *J Biochem (Tokyo)*, 132: 697-703, 2002.
163. Ikeda, S., Kishida, S., Yamamoto, H., Murai, H., Koyama, S., and Kikuchi, A. Axin, a negative regulator of the Wnt signaling pathway, forms a complex with GSK-3 $\beta$  and  $\beta$ -catenin and promotes GSK-3 $\beta$ -dependent phosphorylation of  $\beta$ -catenin. *Embo J*, 17: 1371-1384, 1998.
164. Ikeda, S., Kishida, M., Matsuura, Y., Usui, H., and Kikuchi, A. GSK-3 $\beta$ -dependent phosphorylation of adenomatous polyposis coli gene product can be modulated by  $\beta$ -catenin and protein phosphatase 2A complexed with Axin. *Oncogene*, 19: 537-545, 2000.
165. Sadot, E., Conacci-Sorrell, M., Zhurinsky, J., Shnizer, D., Lando, Z., Zharhary, D., Kam, Z., Ben-Ze'ev, A., and Geiger, B. Regulation of S33/S37 phosphorylated  $\beta$ -catenin in normal and transformed cells. *J Cell Sci*, 115: 2771-2780, 2002.
166. van Noort, M., Meeldijk, J., van der Zee, R., Destree, O., and Clevers, H. Wnt signaling controls the phosphorylation status of  $\beta$ -catenin. *J Biol Chem*, 277: 17901-17905, 2002.
167. Winston, J. T., Strack, P., Beer-Romero, P., Chu, C. Y., Elledge, S. J., and Harper, J. W. The SCF $\beta$ -TRCP-ubiquitin ligase complex associates specifically with phosphorylated destruction motifs in I $\kappa$ B $\alpha$  and  $\beta$ -catenin and stimulates I $\kappa$ B $\alpha$  ubiquitination in vitro. *Genes Dev*, 13: 270-283, 1999.
168. Liu, C., Kato, Y., Zhang, Z., Do, V. M., Yankner, B. A., and He, X.  $\beta$ -Trcp couples  $\beta$ -catenin phosphorylation-degradation and regulates *Xenopus* axis formation. *Proc Natl Acad Sci U S A*, 96: 6273-6278, 1999.
169. Taya, S., Yamamoto, T., Kanai-Azuma, M., Wood, S. A., and Kaibuchi, K. The deubiquitinating enzyme Fam interacts with and stabilizes  $\beta$ -catenin. *Genes Cells*, 4: 757-767, 1999.
170. Fagotto, F., Gluck, U., and Gumbiner, B. M. Nuclear localization signal-independent and importin/karyopherin-independent nuclear import of  $\beta$ -catenin. *Curr Biol*, 8: 181-190, 1998.

171. Henderson, B. R. Nuclear-cytoplasmic shuttling of APC regulates  $\beta$ -catenin subcellular localization and turnover. *Nat Cell Biol*, 2: 653-660, 2000.
172. Brantjes, H., Roose, J., van De Wetering, M., and Clevers, H. All Tcf HMG box transcription factors interact with Groucho-related co-repressors. *Nucleic Acids Res*, 29: 1410-1419, 2001.
173. Hecht, A. and Kemler, R. Curbing the nuclear activities of  $\beta$ -catenin. Control over Wnt target gene expression. *EMBO Rep*, 1: 24-28, 2000.
174. Earnshaw, W. C., Martins, L. M., and Kaufmann, S. H. Mammalian caspases: structure, activation, substrates, and functions during apoptosis. *Annu Rev Biochem*, 68: 383-424, 1999.
175. Chen, S., Guttridge, D. C., You, Z., Zhang, Z., Fribley, A., Mayo, M. W., Kitajewski, J., and Wang, C. Y. Wnt-1 signaling inhibits apoptosis by activating  $\beta$ -catenin/T cell factor-mediated transcription. *J Cell Biol*, 152: 87-96, 2001.
176. Brancolini, C., Lazarevic, D., Rodriguez, J., and Schneider, C. Dismantling cell-cell contacts during apoptosis is coupled to a caspase-dependent proteolytic cleavage of  $\beta$ -catenin. *J Cell Biol*, 139: 759-771, 1997.
177. Herren, B., Levkau, B., Raines, E. W., and Ross, R. Cleavage of  $\beta$ -catenin and plakoglobin and shedding of VE-cadherin during endothelial apoptosis: evidence for a role for caspases and metalloproteinases. *Mol Biol Cell*, 9: 1589-1601, 1998.
178. Fukuda, K. Apoptosis-associated cleavage of  $\beta$ -catenin in human colon cancer and rat hepatoma cells. *Int J Biochem Cell Biol*, 31: 519-529, 1999.
179. Steinhusen, U., Badock, V., Bauer, A., Behrens, J., Wittman-Liebold, B., Dorken, B., and Bommert, K. Apoptosis-induced cleavage of  $\beta$ -catenin by caspase-3 results in proteolytic fragments with reduced transactivation potential. *J Biol Chem*, 275: 16345-16353, 2000.
180. Kim, K., Pang, K. M., Evans, M., and Hay, E. D. Overexpression of  $\beta$ -catenin induces apoptosis independent of its transactivation function with LEF-1 or the involvement of major G1 cell cycle regulators. *Mol Biol Cell*, 11: 3509-3523, 2000.

181. Chen, S., Guttridge, D. C., You, Z., Zhang, Z., Fribley, A., Mayo, M. W., Kitajewski, J., and Wang, C. Y. Wnt-1 signaling inhibits apoptosis by activating beta-catenin/T cell factor-mediated transcription. *J Cell Biol*, 152: 87-96, 2001.
182. Wong, N. A. and Pignatelli, M.  $\beta$ -catenin--a linchpin in colorectal carcinogenesis? *Am J Pathol*, 160: 389-401, 2002.
183. Bienz, M. and Clevers, H. Linking colorectal cancer to Wnt signaling. *Cell*, 103: 311-320, 2000.
184. Kakiuchi, H., Watanabe, M., Ushijima, T., Toyota, M., Imai, K., Weisburger, J. H., Sugimura, T., and Nagao, M. Specific 5'-GGGA-3'-->5'-GGA-3' mutation of the APC gene in rat colon tumors induced by 2-amino-1-methyl-6-phenylimidazo[4,5-*b*]pyridine. *Proc Natl Acad Sci U S A*, 92: 910-914, 1995.
185. Toyota, M., Ushijima, T., Kakiuchi, H., Canzian, F., Watanabe, M., Imai, K., Sugimura, T., and Nagao, M. Genetic alterations in rat colon tumors induced by heterocyclic amines. *Cancer*, 77: 1593-1597, 1996.
186. Suzui, M., Ushijima, T., Dashwood, R. H., Yoshimi, N., Sugimura, T., Mori, H., and Nagao, M. Frequent mutations of the rat  $\beta$ -catenin gene in colon cancers induced by methylazoxymethanol acetate plus 1-hydroxyanthraquinone. *Mol Carcinog*, 24: 232-237, 1999.
187. de La Coste, A., Romagnolo, B., Billuart, P., Renard, C. A., Buendia, M. A., Soubrane, O., Fabre, M., Chelly, J., Beldjord, C., Kahn, A., and Perret, C. Somatic mutations of the  $\beta$ -catenin gene are frequent in mouse and human hepatocellular carcinomas. *Proc Natl Acad Sci U S A*, 95: 8847-8851, 1998.
188. Suzui, M., Ushijima, T., Dashwood, R. H., Yoshimi, N., Sugimura, T., Mori, H., and Nagao, M. Frequent mutations of the rat beta-catenin gene in colon cancers induced by methylazoxymethanol acetate plus 1-hydroxyanthraquinone. *Mol Carcinog*, 24: 232-237, 1999.
189. Takahashi, M., Nakatsugi, S., Sugimura, T., and Wakabayashi, K. Frequent mutations of the beta-catenin gene in mouse colon tumors induced by azoxymethane. *Carcinogenesis*, 21: 1117-1120, 2000.

190. Takahashi, M., Mutoh, M., Kawamori, T., Sugimura, T., and Wakabayashi, K. Altered expression of beta-catenin, inducible nitric oxide synthase and cyclooxygenase-2 in azoxymethane-induced rat colon carcinogenesis. *Carcinogenesis*, 21: 1319-1327, 2000.
191. Yamada, Y., Yoshimi, N., Hirose, Y., Kawabata, K., Matsunaga, K., Shimizu, M., Hara, A., and Mori, H. Frequent  $\beta$ -catenin gene mutations and accumulations of the protein in the putative preneoplastic lesions lacking macroscopic aberrant crypt foci appearance, in rat colon carcinogenesis. *Cancer Res*, 60: 3323-3327, 2000.
192. Pulling, L. C., Klinge, D. M., and Belinsky, S. A. p16INK4a and  $\beta$ -catenin alterations in rat liver tumors induced by NNK. *Carcinogenesis*, 22: 461-466, 2001.
193. Suzui, M., Sugie, S., Mori, H., Okuno, M., Tanaka, T., and Moriwaki, H. Different mutation status of the  $\beta$ -catenin gene in carcinogen-induced colon, brain, and oral tumors in rats. *Mol Carcinog*, 32: 206-212, 2001.
194. Ubagai, T., Ochiai, M., Kawamori, T., Imai, H., Sugimura, T., Nagao, M., and Nakagama, H. Efficient induction of rat large intestinal tumors with a new spectrum of mutations by intermittent administration of 2-amino-1-methyl-6-phenylimidazo[4,5-*b*]pyridine in combination with a high fat diet. *Carcinogenesis*, 23: 197-200, 2002.
195. Ho, S. N., Hunt, H. D., Horton, R. M., Pullen, J. K., and Pease, L. R. Site-directed mutagenesis by overlap extension using the polymerase chain reaction. *Gene*, 77: 51-59, 1989.
196. Aiyar, A., Xiang, Y., and Leis, J. Site-directed mutagenesis using overlap extension PCR. *Methods Mol Biol*, 57: 177-191, 1996.
197. Porfiri, E., Rubinfeld, B., Albert, I., Hovanes, K., Waterman, M., and Polakis, P. Induction of a  $\beta$ -catenin-LEF-1 complex by wnt-1 and transforming mutants of  $\beta$ -catenin. *Oncogene*, 15: 2833-2839, 1997.
198. Lowry, O. H., N. J. Rosebrough, A.L. Farr and R. J. Randall Protein measurement with the Folin-Phenol reagents. *J. Biol. Chem.*, 193: 265-275, 1951.

199. Stambolic, V., Ruel, L., and Woodgett, J. R. Lithium inhibits glycogen synthase kinase-3 activity and mimics wingless signalling in intact cells. *Curr Biol*, 6: 1664-1668, 1996.
200. Zhu, D. M. and Uckun, F. M. Calpain inhibitor II induces caspase-dependent apoptosis in human acute lymphoblastic leukemia and non-Hodgkin's lymphoma cells as well as some solid tumor cells. *Clin Cancer Res*, 6: 2456-2463, 2000.
201. Atencio, I. A., Ramachandra, M., Shabram, P., and Demers, G. W. Calpain inhibitor 1 activates p53-dependent apoptosis in tumor cell lines. *Cell Growth Differ*, 11: 247-253, 2000.
202. Dantzer, F., Schreiber, V., Niedergang, C., Trucco, C., Flatter, E., De La Rubia, G., Oliver, J., Rolli, V., Menissier-de Murcia, J., and de Murcia, G. Involvement of poly(ADP-ribose) polymerase in base excision repair. *Biochimie*, 81: 69-75, 1999.
203. Perkins, D., Pereira, E. F., Gober, M., Yarowsky, P. J., and Aurelian, L. The herpes simplex virus type 2 R1 protein kinase (ICP10 PK) blocks apoptosis in hippocampal neurons, involving activation of the MEK/MAPK survival pathway. *J Virol*, 76: 1435-1449, 2002.
204. Orford, K., Orford, C. C., and Byers, S. W. Exogenous expression of  $\beta$ -catenin regulates contact inhibition, anchorage-independent growth, anoikis, and radiation-induced cell cycle arrest. *J Cell Biol*, 146: 855-868, 1999.
205. Staal, F. J., Noort Mv, M., Strous, G. J., and Clevers, H. C. Wnt signals are transmitted through N-terminally dephosphorylated  $\beta$ -catenin. *EMBO Rep*, 3: 63-68, 2002.
206. Musial, A. and Eissa, N. T. Inducible Nitric-oxide Synthase Is Regulated by the Proteasome Degradation Pathway. *J. Biol. Chem.*, 276: 24268-24273, 2001.
207. Tenev, T., Marani, M., McNeish, I., and Lemoine, N. R. Pro-caspase-3 overexpression sensitises ovarian cancer cells to proteasome inhibitors. *Cell Death Differ*, 8: 256-264, 2001.

208. Jaiswal, A. S., Marlow, B. P., Gupta, N., and Narayan, S.  $\beta$ -catenin-mediated transactivation and cell-cell adhesion pathways are important in curcumin (diferuylmethane)-induced growth arrest and apoptosis in colon cancer cells. *Oncogene*, 21: 8414-8427, 2002.
209. Fuchs, S. Y., Xie, B., Adler, V., Fried, V. A., Davis, R. J., and Ronai, Z. e. c-Jun NH2-terminal Kinases Target the Ubiquitination of Their Associated Transcription Factors. *J. Biol. Chem.*, 272: 32163-32168, 1997.
210. Stockinger, A., Eger, A., Wolf, J., Beug, H., and Foisner, R. E-cadherin regulates cell growth by modulating proliferation-dependent  $\beta$ -catenin transcriptional activity. *J Cell Biol*, 154: 1185-1196, 2001.